Summer 8-15-2015

Essential Roles of Stat3 in Zebrafish Development

Yinzi Liu
Washington University in St. Louis

WASHINGTON UNIVERSITY IN ST. LOUIS

Division of Biology and Biomedical Sciences
Developmental, Regenerative and Stem Cell Biology

Dissertation Examination Committee:
Lilianna Solnica-Krezel, Chair
S. Kerry Kornfeld, Co-Chair
Christina A. Gurnett
Stephen L. Johnson
Craig Micchelli

Essential Roles of Stat3 in Zebrafish Development

by
Yinzi Liu

A dissertation presented to the
Graduate School of Arts & Sciences
of Washington University in
partial fulfillment of the
requirements for the degree
of Doctor of Philosophy

August 2015
St. Louis, Missouri

Table of Contents

List of Figures

List of Tables

List of Abbreviations

AP	anteroposterior
BCR	blastocoel roof
BMP	bone morphogenetic protein
boz	*bozozok*
C&E	convergence and extension
CE	convergent extension
dn	dominant negative
dpf	day(s) postfertilization
DV	dorsoventral
ECM	extracellular matrix
EMT	epithelial-to-mesenchymal transition
FAK	focal adhesion kinase
FGF	fibroblast growth factor
FN	fibronectin
Fz	Frizzled
GPCR	G protein-coupled receptor
HIES	Hyper IgE syndrome
hpf	hour(s) postfertilization
IBD	inflammatory bowel disease
IL	interleukin
Jak	Janus kinase
kny	*knypek*
LM	laminin
LMT	low melting temperature

LR	left-right
MAPK	mitogen-activated protein kinase
MBT	mid-blastrula transition
MMP	matrix metalloproteinase
mpf	minute(s) postfertilization
MZ	maternal zygotic
PCP	planar cell polarity
PDGF	platelet-derived growth factor
PI3K	phosphoinositide 3-kinase
PPP	prechordal plate progenitor
Rok2	Rho kinase 2
SDCM	spinning disk confocal microscope
slb	*silberblick*
snh	*snailhouse*
SOCS	suppressor of cytokine signaling
spt	*spadetail*
sqt	*squint*
Stat	Signal transducer and activator of transcription
TAD	transactivation domain
TGFβ	transforming growth factor β
TLR	Toll-like receptor
TNF	tumor necrosis factor
tri	*trilobite*
YSL	yolk syncytial layer
chd	*chordin*

szl	*sizzled*
gsc	*goosecoid*
S1P	sphingosine-1-phosphate
MO	morpholino
TALEN	transcriptional activator like-effector nuclease
WISH	whole-mount *in situ* hybridization

Acknowledgments

This thesis is the result of the guidance and support from my advisor and committee, as well as inspiration and encouragement from many remarkable individuals.

First and foremost, I offer my sincerest gratitude to my advisor, Dr. Lilianna Solnica-Krezel, who has supported me with her knowledge and patience, and by showing me what a great scientist, person, and leader should look like. She's no doubt the best scientist I've ever seen. "Human computer" is one way to describe her – she literally remembers almost every zebrafish paper. Somehow she manages to "sort" and "store" this large amount of information, "synthesize" her own critical interpretation, and can easily "locate" any piece of data anytime after she blinks a few times (maybe that's the trick, like mouse double clicking). She sets up high standard for herself and her science, which has greatly influenced and will continue to influence me. Whenever I make a conclusion based on the evidence I collect or get ready to submit an application and the like, I ask myself "would Lila frown at this" and interrogate my experimental design, my writing and many other things by applying the "Lila standards". She's also absolutely a great leader of her lab and the Department of Developmental Biology, driven, creative, supportive, inspiring, and caring for everybody around her. I have always looked up to her and seen her as my role model. I feel lucky to have Lila as my mentor and I thank her for teaching me science, critical thinking skills, and most importantly for showing me how to become a mature and professional person of integrity and high standards which include those on food and snacks – I was definitely fed very well during my years in the LSK lab.

I would also like to thank my committee for their guidance through the years. Thank you to Drs. Kerry Kornfeld, Steve Johnson, Craig Micchelli, Christina Gurnett, and my former chair

Raphael Kopan. They not only showed their support with scientific ideas and critiques but also with encouragement. Dr. Jim Skeath is also the best program director I could ever imagine.

I thank all the LSK lab members, present and past. Over the years they've become family. Thank you Diane for all the inspiring discussions, for sharing your office with me sometimes, for the massage, and for the wonderful food George prepare. Thank you Isa for guiding me to join this lab. Thank you Jade for being my Asian twin and awesome friend. Thank you Anna for being the best lab manager/cat lover/snack buddy. Thank you Margot, Ryan, Jimann and Jiakun for discussion. Thank you Steve and John for keeping my fish happy, especially those maternal zygotic princes and princesses. Most importantly, thank you Terin for being my best friend and sister. A big thank you to everybody in the lab supporting me over the years.

I could not have become who I am today without some awesome individuals. I'd like to thank Vera, Emel, Cynthia, Terin, Joe and many others for being my best friends in life, supporting me through my difficult times, running together, exploring great restaurants and performances in St. Louis, debating over business and political issues, and feeding me with delicious food and baked goods. We share each other's happiness and sorrow and encourage each other to chase our dreams. Many wonderful things would never have happened without their encouragement.

I'm also grateful for a few other things and organizations outside the lab. I will miss my time at BALSA and my BALSA colleagues/friends. Joining BALSA and becoming a leader opened a new door for my graduate school life. I have learned so much from my BALSA experience and made many friends who share the same interests and career goals with me. I'd like to thank my case partners for helping me grow in so many different ways. I also thank the

"Ether Ensemble" piano-string quintet members for playing music with me. I would always remember the wonderful time we spend together practicing and performing. Maybe one day we can get together again and officially begin our wedding music business for real.

Finally, I want to express my love and gratitude to my parents, who are the ultimate source of my energy and strengths. Their unconditional love and support are the biggest reason I am who I am today. I can't imagine how difficult it has been for them to not be able to see their only child for years. But they trust and support me the whole time. I also thank my animal friends – "Qiuqiu" the hamster, the "Bird" parakeet family, and Genie the kitteh, who has been supporting me throughout my thesis writing by being the sweetest kitty.

Yinzi Liu

Washington University in St. Louis

August 2015

Dedicated to my parents and my beloved animals

for their constant support and unconditional love.

I love you all dearly.

ABSTRACT OF THE DISSERTATION

Essential Roles of Stat3 in Zebrafish Development

by

Yinzi Liu

Doctor of Philosophy in Biology and Biomedical Sciences

Developmental, Regenerative and Stem Cell Biology

Washington University in St. Louis, 2015

Professor Lilianna Solnica-Krezel, Chair

Professor S. Kerry Kornfeld, Co-Chair

Vertebrate gastrulation is a fundamental morphogenetic process during which germ layers are formed, patterned and shaped into a body plan with organ rudiments. Among the conserved gastrulation movements, convergence and extension (C&E) occur concurrently to narrow the germ layers mediolaterally and elongate them along the anteroposterior embryonic axis. C&E are largely driven by cell migration and cell intercalation, while cell proliferation has been considered dispensable and even incompatible with gastrulation movements and morphogenesis. Signal transducer and activator of transcription 3 (Stat3) has been implicated by antisense morpholino loss-of-function study in regulation of zebrafish C&E movements in part by promoting non cell-autonomously convergence movements and the Wnt/Planar Cell Polarity (Wnt/PCP) signaling-dependent mediolateral (ML) cell polarity that underlies polarized gastrulation cell behaviors. In this thesis work, I showed that TALEN-based genetic disruption of both maternal and zygotic *stat3* function led to proliferation and axis extension defects without affecting convergence movement or planar cell polarity. Rather, my studies posit an alternative model of Stat3 function during early embryogenesis, whereby Stat3 promotes extension of

embryonic tissues via Cdc25a-dependent cell proliferation. These results clarify the role of Stat3 function in gastrulation and providing evidence that cell proliferation plays a small but significant role in tissue extension during gastrulation. Despite decreased early cell proliferation and extension movements during gastrulation, *stat3*–deficient zebrafish mutants complete gastrulation, contrasting the severe C&E defects induced by *stat3* morpholino. I therefore used *stat3* morpholino as a tool and uncovered several novel regulators of C&E by gene expression profiling. Among those, Fam132a, a conserved secreted peptide, regulates morphogenesis of the prechordal and chorda axial mesoderm likely in a Wnt/PCP-independent manner. In particular, Fam132a modulates the collective anterior migration of the prechordal plate progenitors by limiting cell contact, required for their effective directed migration. Together, my work has established a conserved role of Stat3 in regulation of cell proliferation, and uncovered novel regulators of zebrafish gastrulation. In addition, *stat3*-deficient juveniles develop scoliosis and excessive inflammation phenotypes, affording a genetic model of *STAT3*-associated human diseases.

Chapter 1

Introduction

Cell divisions, fate specification, and cell movements are key processes that transform a fertilized egg into an embryo with a basic animal body plan. In this thesis, we use zebrafish as a model to study functions of Signal transducer and activator of transcription (Stat3) signaling in each of those key events during animal development.

1.1 Key Events during Embryogenesis

1.1.1 Cell Divisions

Zebrafish embryogenesis is a rapid process driven by cell proliferation, fate specification and cell movements. During the first three hours of development, zebrafish embryos undergo rapid and synchronous cell divisions every 15 minutes (Kimmel et al., 1995). A typical cell cycle consists of DNA synthesis (S), mitosis (M) and two gap phases (G1 and G2) (Morgan, 2007). By contrast, during the cleavage stage of zebrafish and amphibian embryogenesis, cells alternate between S and M phases without any gap phases (Bouldin and Kimelman, 2014). After mid-blastula transition (MBT, 512-cell stage, 2.75 hours postfertilization (hpf)), cell cycles slow down and become asynchronous with the acquisition of a G2 phase (Dalle Nogare et al., 2009). MBT marks the beginning of zygotic transcription despite of a few genes that may be transcribed

before MBT (Harvey et al., 2013). During gastrulation, cell divisions occur only very infrequently (Kane et al., 1992; Kimmel et al., 1994; Warga and Kimmel, 1990).

Previous studies have established a conserved role of Cdc25a in cell proliferation during embryogenesis in various organisms. Cdc25a, one of the Cdc25 phosphatases, is a key regulator of G1-S and G2-M transitions in the eukaryotic cell cycle (Boutros et al., 2007). Before zygotic transcription turns on at MBT, all developmental processes including cell division are enabled by maternal gene products (Harvey et al., 2013). Evidence from *Drosophila* and *Xenopus* indicates that the rapid pre-MBT mitotic entry is propelled by Cdc25a translated from maternal RNAs through activation of Cyclin B/Cdk1 complexes (Bouldin and Kimelman, 2014; Edgar and Datar, 1996; Kim et al., 1999; Tsai et al., 2014). Around MBT, while periodic degradation of maternal Cdc25a is essential for cell cycle lengthening (Dalle Nogare et al., 2009; Edgar and Datar, 1996; Shimuta et al., 2002), dynamic Cdc25a activity continues to be continuously required for cell divisions during development, as cells arrest in G2 in the *Drosophila string*/*cdc25* mutant (Edgar and O'Farrell, 1990) and in zebrafish *standstill*/*cdc25a* mutant (Verduzco et al., 2012). Likewise, depletion of mouse *Cdc25a* leads to embryonic death during gastrulation (Lee et al., 2009). In zebrafish, although *cdc25a* mutant embryos are able to complete gastrulation and organogenesis possibly due to functional redundancy of its homolog *cdc25d*, embryos display short and curved body shape at 1 day postfertilization (dpf) (Verduzco et al., 2012). How Cdc25a is transcriptionally activated in these early embryos remains poorly understood. During tumorigenesis, Cdc25a is thought to work as an oncogene. Indeed, CDC25 is often overexpressed in various human cancers, in which it drives abnormal cell proliferation downstream of multiple signaling pathways including Stat3 (Barre et al., 2005; Boutros et al., 2007).

1.1.2 Axis Specification, Germ Layer Induction and Patterning

Contemporaneous with the early cell proliferation are inductive events that specify embryonic axis, and establish and pattern germ layers. The embryonic shield, a thickening in the dorsal blastoderm that forms at early gastrulation (6 hpf), is considered the equivalent of the Spemann-Mangold gastrula organizer in zebrafish (Schier and Talbot, 2001; Shih and Fraser, 1996). The organizer, which largely gives rise to the prechordal plate (anterior axial mesoderm) and the notochord (posterior axial mesoderm, chordamesoderm), plays a fundamental and non cell-autonomous role in cell fate specification and regulation of gastrulation movements (Schier, 2001). A key early step in the gastrula organizer formation is the nuclear accumulation of maternal β-catenin in the dorsal blastomeres and dorsal yolk syncytial layer (YSL) at midblastula stage (128-cell stage, 2¼ hpf) (Schneider et al., 1996). β-catenin, a key transcriptional effector of canonical Wnt signaling, activates transcription of a Nodal-related gene *squint* (*sqt*), as well as a dorsalizing homeobox gene *bozozok* (*boz*) and secreted protein Chordin (Schier, 2001; Schier and Talbot, 2001; Solnica-Krezel and Driever, 2001). The Nodal-related genes *cyclops* (*cyc*) and *sqt* expressed in the margin/YSL are known to induce mesoderm and endoderm (Feldman et al., 1998). Sqt acts at a long range and can induce mesendoderm cell fate at a distance, while Cyc acts more locally (Chen and Schier, 2001). As a result, germ layers are specified with ectoderm localized predominantly near the animal pole, and mesoderm and endoderm around the margin (Feldman et al., 1998; Kimmel et al., 1990).

β-catenin nuclear localization and *bozozok* expression mark the formation of the teleost equivalent of Nieuwkoop Center in amphibians. As a result, the Spemann-Mangold organizer is established as a source of secreted proteins such as Chordin, Dickkopf1 (Dkk1) and

other molecules, which bind Bone morphogenetic proteins (Bmps) and/or Wnt in the extracellular space and antagonize their ventralizing and posteriorizing activities (reviewed in (Schier, 2001)). Bmp pathway components are essential for ventral cell type formation. Embryos with genetic inactivation of Bmp pathway component genes such as *swirl*/*bmp2b* or with ectopic Bmp antagonists such as Chordin are strongly dorsalized with the expansion of dorsal and anterior tissues at the expense of ventroposterior structure (Kishimoto et al., 1997; Mullins et al., 1996; Nguyen et al., 1998). Opposite to the earlier role of maternal β-catenin/Wnt signaling as described earlier, zygotic Wnt8 and Wnt3a in zebrafish cooperate to establish ventroposterior cell fates (Lekven et al., 2001; Shimizu et al., 2005a). A ventral to dorsal gradient of Bmp/Wnt activity is established and maintained during gastrulation to pattern the dorsoventral (DV) as well as anteroposterior (AP) axes (Hammerschmidt et al., 1996), and cells acquire different fates depending on their various positions in the gastrula. The organizer at the dorsal margin induces dorsal and anterior structures (Saude et al., 2000), while the ventral and lateral margin, or the posterior organizer, induces posterior structures such as blood, pronephros, tail, posterior trunk, and hindbrain. Laterally located cells are presomitic mesoderm and heart progenitors (Agathon et al., 2003; Kimmel et al., 1990; Woo and Fraser, 1997).

1.1.3 Gastrulation

Vertebrate gastrulation, a term derived from the Greek word “gaster” meaning gut or belly, is a fundamental process during early animal development. During this period, series of morphogenetic processes remodel an embryo into three germ layers, ectoderm, mesoderm, and endoderm, as well as AP, DV and left-right (LR) body axes (Leptin, 2005). There are four evolutionarily conserved gastrulation movements, each of which leads to a specific change in tissue shape. In zebrafish, epiboly starts the earliest, and results in thinning and spreading of

embryonic tissues towards the vegetal pole. Later, internalization of the presumptive mesoderm and endoderm cells at the blastula margin creates the multilayered embryos (Solnica-Krezel, 2005).

Concurrently, convergence and extension (C&E), two individual gastrulation movements in zebrafish, narrow the germ layers mediolaterally and elongate them along the AP axis (Roszko et al., 2009; Solnica-Krezel, 2006). Zebrafish C&E movements vary in a spatiotemporal manner, and are mainly achieved by two cellular behaviors: cell intercalation and cell migration (Figure 1.1) (Roszko et al., 2009; Tada and Heisenberg, 2012). Cells in the ventral gastrula region do not undergo C&E, but migrate towards the vegetal pole instead, contributing to epiboly (Myers et al., 2002). Lateral mesodermal cells start from slow dorsal convergence at midgastrulation; then at late gastrulation, they adopt a mediolaterally polarized morphology and migrate collectively and more efficiently toward the dorsal midline (Jessen et al., 2002; Sepich et al., 2000). Paraxial mesoderm undergoes modest C&E via a combination of polarized planar and radial intercalations (Yin et al., 2008), while the posterior axial mesoderm shows modest convergence but much faster extension driven by ML planar intercalation (Glickman et al., 2003; Yin et al., 2008). In Chapter 2, I describe experimental evidence that Stat3-dependent cell proliferation is also required for normal extension of chordamesoderm. At the anteriormost axial mesoderm, prechordal plate progenitor (PPP) cells migrate collectively as a cohesive group toward anterior, contributing to AP axis extension (Montero et al., 2005; Warga and Kimmel, 1990). Chapter 3 explores this particular migration process of PPP cells in detail and its new regulator, a conserved secreted protein, Fam132a.

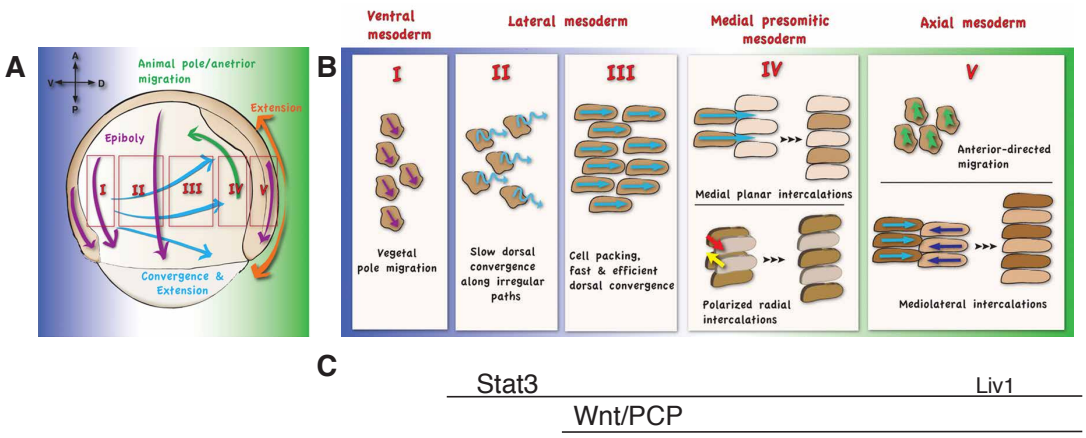

Figure 1.1 Different cell behaviors that contribute to C&E movements along the dorsoventral axis of the zebrafish gastrulae (modified from Roszko et al. 2009). In a zebrafish gastrula (A), C&E movements vary in a spatiotemporal manner, as highlighted in B. Cells in the ventral gastrula region do not undergo C&E, but migrate towards the vegetal pole instead (I). The lateral mesendodermal cells start from slow dorsal convergence (II), then adopt a mediolaterally polarized morphology and migrate fast to the dorsal midline (III). The paraxial mesodermal cells undergo modest C&E via a combination of polarized planar and radial intercalations (IV), while the axial mesoderm shows modest convergence but much faster extension driven by mediolateral intercalations (V). Prechordal plate cells undergo anterior-directed migration. Lateral view; animal to the top, dorsal to the right. (C) The requirements of Stat3 (proposed by morpholino-based studies) and Wnt/PCP for the different cell behaviors involved in C&E. According to the morpholino studies, Stat3 is required as early as the initiation of the slow convergence (B, II) to regulate dorsal convergence of the lateral mesodermal cells non cell-autonomously and the anterior migration of prechordal plate progenitors cell-autonomously. Wnt/PCP pathway is essential for mediolateral cell elongation underlying fast dorsal migration of the lateral domain and mediolateral cell polarization with axial mesoderm. Liv1 was proposed to be a direct target of Stat3 and regulates the anterior migration of prechordal plate cells.

1.2 Cellular and Molecular Mechanisms Underlying C&E Gastrulation Movements

1.2.1 Planar Cell Polarity in C&E

Many molecular pathways have been shown to regulate C&E gastrulation movements. Gpr125, an adhesion G-protein coupled receptor (aGPCR), was proposed to regulate C&E by modulating the composition of Wnt/Planar Cell Polarity (Wnt/PCP) components on cell membranes (Li et al., 2013). In addition, Has2 (Bakkers et al., 2004), Gα12/13 heterotrimeric G proteins (Lin et al., 2005), and prostaglandin signaling (Cha et al., 2006) have also been shown to mediate C&E movements during zebrafish gastrulation.

Wnt/PCP signaling which polarizes cells in the tissue plane is considered one of the major regulators of C&E morphogenetic movements in all vertebrates (Figure 1.2). Cells with Wnt/PCP signaling-mediated planar polarity are elongated along the ML axis, a key cellular mechanism underlying the directed migration and polarized intercalation cell behaviors during C&E (Gray et al., 2011). Core components of the Wnt/PCP pathway initially defined in *Drosophila* include membrane proteins Frizzled, Strabismus/Van Gogh, Flamingo/Starry Night, and cytoplasmic proteins Dishevelled (Dvl), Prickle and Diego (Zallen, 2007). Downstream effectors of Wnt/PCP signaling include Daam1, RhoI and JNK pathway that transduce the polarity signal to cytoskeletal organization and function (Huelsken and Behrens, 2002). Disruption of planar polarity signaling by mutations in the zebrafish Wnt/PCP pathway components such as *trilobite* (*tri*)/*van gogh like 2* (*vangl2*) (Jessen et al., 2002)*, knypek* (*kny*)/*glypican 4* (Topczewski et al., 2001), *silberblick* (*slb*)/*wnt11* (Heisenberg et al., 2000), and *pipetail* (*ppt*)/*wnt5* (Kilian et al., 2003), etc., leads to rounder and randomly oriented cells during

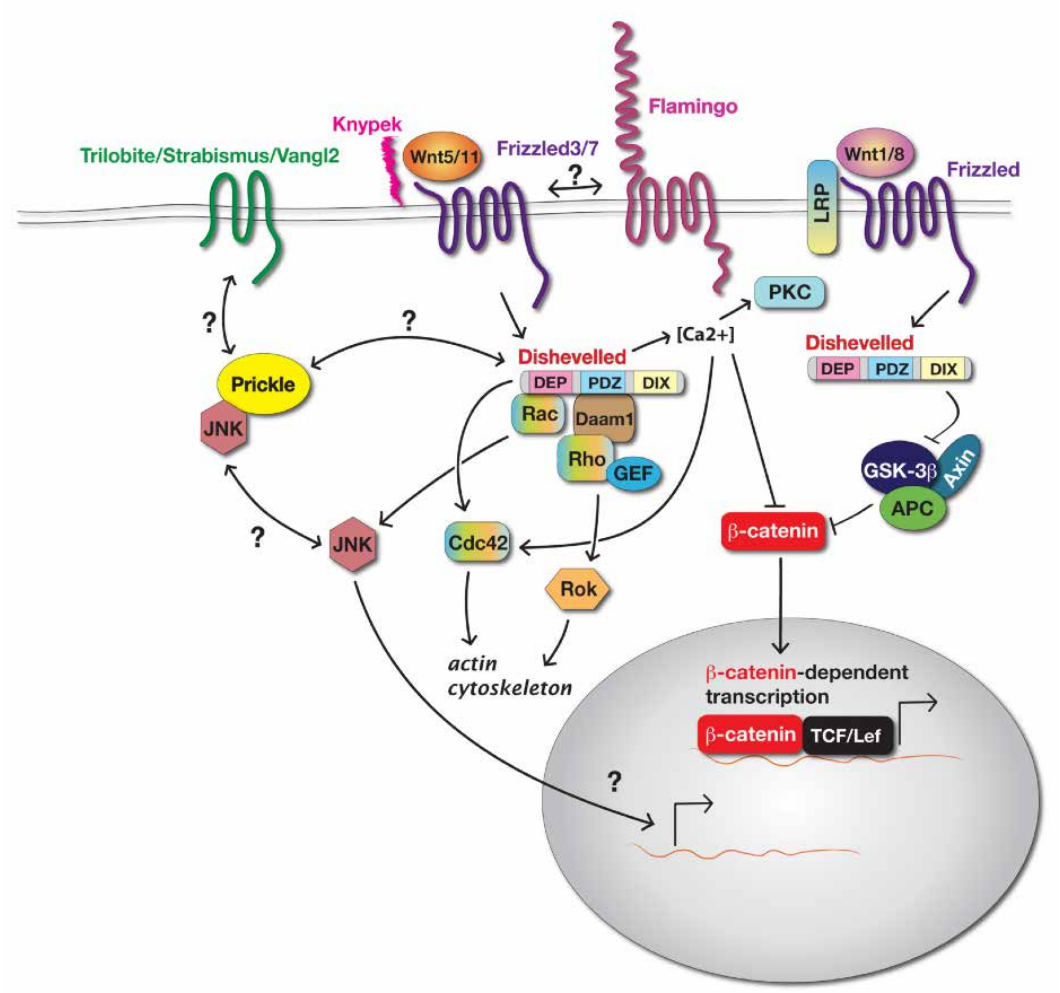

Figure 1.2 Schematic illustration of the canonical Wnt (Wnt/β-catenin) and the non-canonical Wnt/Planar Cell Polarity (Wnt/PCP) signaling pathways in vertebrates (adopted from Roszko et al., 2009).

gastrulation, impaired C&E movements, and as a result a shorter AP axis and a wider notochord and somites at the end of gastrulation. Many of these mutant embryos also show synophthalmia and cyclopia, or partial or complete fusions of eye fields.

1.2.2 Cell Proliferation in C&E

Cell proliferation is generally considered dispensable for morphogenesis during gastrulation, when cell division takes place only at a very low level, particularly in tissues such as the axial mesoderm, which undergoes dynamic cell rearrangement and morphogenesis (Saka and Smith, 2001). Blockage of cell divisions in the zebrafish *emi* mutant at early gastrulation does not affect the completion of gastrulation (Zhang et al., 2008). Experimentally elevating cell proliferation level, on the other hand, results in gastrulation defects as demonstrated by studies in *Ciona*, *Xenopus* and zebrafish (Bouldin et al., 2014; Leise and Mueller, 2004; Ogura et al., 2011). Contrasting this notion is our finding that Stat3/Cdc25a-dependent cell proliferation promotes axis extension during zebrafish gastrulation. Details will be discussed in Chapter 2.

1.2.3 Cell-Cell Adhesion in C&E

More and more evidence demonstrates the fundamental roles of cell-cell adhesion as a driving force during gastrulation. First, cell adhesion is critical for germ layer assembly and separation, as posited by Steinberg's "Differential Adhesion Theory" (Steinberg, 1970, 1975, 2007). Cell adhesion during embryogenesis is mainly mediated by cadherins, which are conserved transmembrane adhesion molecules (Hammerschmidt and Wedlich, 2008; Takeichi, 1988). Cells within different germ layers express different cadherin types and/or levels, and aggregates only form among cells with the same type and level of adhesion molecules both *in vitro* and *in vivo* (Steinberg, 2007). This theory was recently improved by work addressing cell-cortex tensions as differential intercellular adhesion alone is not sufficient to sort different germ layer progenitors.

In fact, both *intro* and *in vivo* experiments showed that aggregate formation and cell sorting of zebrafish progenitors cells correlate with "differential surface tension", which is a result of a combination of actomyosin-dependent cell-cortex tension under the regulation of Nodal/Transforming Growth Factor β (TGFβ) signaling and cadherin-dependent cell adhesion (Krieg et al., 2008). Second, cell adhesion is essential for cell intercalation. Convergence extension (CE) in *Xenopus* is mainly achieved by ML cell intercalation. It has been shown that either too much or too little cell-cell adhesion mediated by C-cadherin impedes ML intercalation during amphibian gastrulation (Lee and Gumbiner, 1995; Zhong et al., 1999). Both morpholino- and mutation-induced loss of zebrafish *cdh1*/*e-cadherin* function led to C&E defects in the axial mesoderm, which undergoes active ML intercalation (Babb and Marrs, 2004; Shimizu et al., 2005b). Third, cell adhesion is the foundation of collective cell migration, such as migration of PPP cells during gastrulation. Collective migration is the coordinated migration of a group of cells during which cells make stable or dynamic contacts, move in a uniform direction at comparable speed, and affect one another while migrating (Theveneau and Mayor, 2013). During collective migration of epithelial sheets, epithelial cells rely on cadherins to form and maintain stable adherens junctions (Nishimura and Takeichi, 2009; Theveneau and Mayor, 2013). Although mesenchymal cells, such as mesodermal cells during gastrulation, do not maintain stable cell contacts, they still require certain levels of cadherins to interact with each other and migrate (Theveneau and Mayor, 2013). In addition, the ventral-to-dorsal Bmp gradient in the zebrafish gastrulae was shown to establish a reverse gradient of cell-cell adhesiveness, specifying different domains of cell behaviors contributing to C&E (Figure 1.1) (Myers et al., 2002; von der Hardt et al., 2007).

Multiple cadherins have been implicated in vertebrate gastrulation. *Xenopus* embryos rely on C-cadherin for ectoderm and mesoderm morphogenesis during gastrulation (Lee and Gumbiner, 1995). In Zebrafish, E-cadherin/Cadherin 1 (Cdh1) has been shown to regulate epiboly, C&E of ectoderm and mesoderm, and the collective migration of PPP cells (Babb and Marrs, 2004; Kane et al., 2005; Montero et al., 2005; Shimizu et al., 2005b). N-cadherin/Cadherin 2 (Cdh2) is also required for C&E of zebrafish mesoderm (Warga and Kane, 2007). Cadherin-dependent cell adhesion is strictly regulated to ensure normal morphogenesis. E-cadherin, for example, has been shown to be regulated at both transcriptional and post-transcriptional levels during collective migration of zebrafish PPP cells. Transcriptionally, E-cadherin level is controlled by its transcriptional repressor Snail (Batlle et al., 2000). Interference with expression or stability of zebrafish Snail1a and Snail1b led to defective anterior migration of this cell group (Blanco et al., 2007; Speirs et al., 2010; Yamashita et al., 2004). Post-transcriptionally, dynamic membrane localization of E-cadherin is essential during collective migration to allow rapid assembly and disassembly of cell junction (Hammerschmidt and Wedlich, 2008). Wnt11 was reported to regulate E-cadherin endocytosis via Rab5c independent of Wnt/PCP signaling during PPP cell migration. In *slb*/*wnt11* zebrafish mutant gastrulae, despite increased and persistent membrane accumulation of E-cadherin, mutant cells appeared less adhesive and failed to migrate anteriorly (Ulrich et al., 2005).

1.2.4 Extracellular Matrix in C&E

The extracellular matrix (ECM) is a collection of various extracellular molecules that are synthesized and secreted by surrounding cells (Rozario and DeSimone, 2010). Studies in the past three decades significantly expanded our understanding of the roles of ECM during embryogenesis. Besides being a passive, structural supporting role, ECM has been shown to

mediate growth factor signaling and generate mechanical signals through cell-matrix interaction, etc. (Rozario and DeSimone, 2010). Indeed, a fibronectin (FN) matrix assembled on the surface of the blastocoel roof (BCR) is essential for the anterior migration of *Xenopus* PPP cells and convergent extension (CE) of chordamesodermal cells (Davidson et al., 2006). Interaction with the FN matrix is likely mediated by integrin signaling, as inhibition of integrin β1 function caused depletion of FN matrix, loss of cell polarity in mesodermal cells, misregulated C-cadherin-dependent cell-cell adhesion, and as a result impaired CE movements (Davidson et al., 2006; Marsden and DeSimone, 2001, 2003). Similar to *Xenopus*, during zebrafish embryogenesis FN and Laminin (LM)-containing matrix is assembled during gastrulation at germ layer interfaces under the regulation of Wnt/PCP signaling, and is also critical for C&E movements of multiple tissues (Davidson et al., 2004; Dohn et al., 2013; Latimer and Jessen, 2010).

The interaction of gastrulating cells with the ECM is predominantly achieved by the binding of ECM components to integrin receptors on the cell surface. Binding of a ligand, such as FN, induces a conformational change in the integrin receptor and subsequent activation of many focal adhesion molecules, including Focal adhesion kinase (FAK). In turn, activated FAK modulates small GTPases to mediate cytoskeletal rearrangements within the cell, also known as the "outside-in signaling". During *Xenopus* gastrulation, FN matrix was reported to regulate C&E through interaction with integrin α5β1 receptor (Davidson et al., 2006). In zebrafish, at least 19 integrin genes have been identified, including nine α subunits and eight β subunits (Jessen, 2015). Mutant studies implicated Integrin α5 in somitogenesis (Koshida et al., 2005). However, little is known about the integrin subunits that function during C&E.

1.3 Stat3 Signaling

1.3.1 JAK/STAT Pathway

The Janus Kinase/Signal Transducer and Activator of Transcription (JAK/STAT) pathway is an essential mediator of cytokine and growth factor signaling. A canonical JAK/STAT pathway entails sequential tyrosine phosphorylations triggered by the ligand-receptor interaction. In particular, binding of cytokines to their receptors results in receptor dimerization, which allows activation of JAKs and the following phosphorylation of receptors by JAKs. Activated receptors are then able to recruit cytosolic STATs through their SH2 domain, leading to phosphorylation and dimerization of STATs. STAT dimers undergo nuclear translocation and activate or suppress transcription of their target genes (Darnell et al., 1994; Levy and Darnell, 2002). Originally identified as regulators of interferon response, JAK/STAT pathways have been implicated in various physiological and pathological processes such as hematopoiesis, adult immune response, and tumorigenesis through their essential functions in cell proliferation and differentiation (Ward et al., 2000).

In mammals there are four members of JAKs (Jak1-3 and Tyk2) as well as seven members of STATs (Stat1-4, Stat5a, Stat5b and Stat6) (Hou et al., 2002). In zebrafish, four Jaks (Jak1, 2a, 2b, 3 and Tyk2) and nine Stats (Stat1.a, 1.b, 1ψ, 2, 3, 4, 5.1, 5.2 and Stat6) have been identified (Liongue et al., 2012). STAT proteins are structurally conserved, as they all contain a DNA-binding domain, a SH3 domain, a SH2 domain, and a transactivation domain (TAD). In particular, the SH2 domain is essential for both tyrosine-phosphorylation and dimerization of STATs (Darnell, 1997).

1.3.2 Stat3 in Animal Development

Stat3 plays numerous essential roles in development, homeostasis and disease. Traditionally, Stat3 is activated by cytokine signals through Gp130 and Jak. Adding to the diversity of Stat3

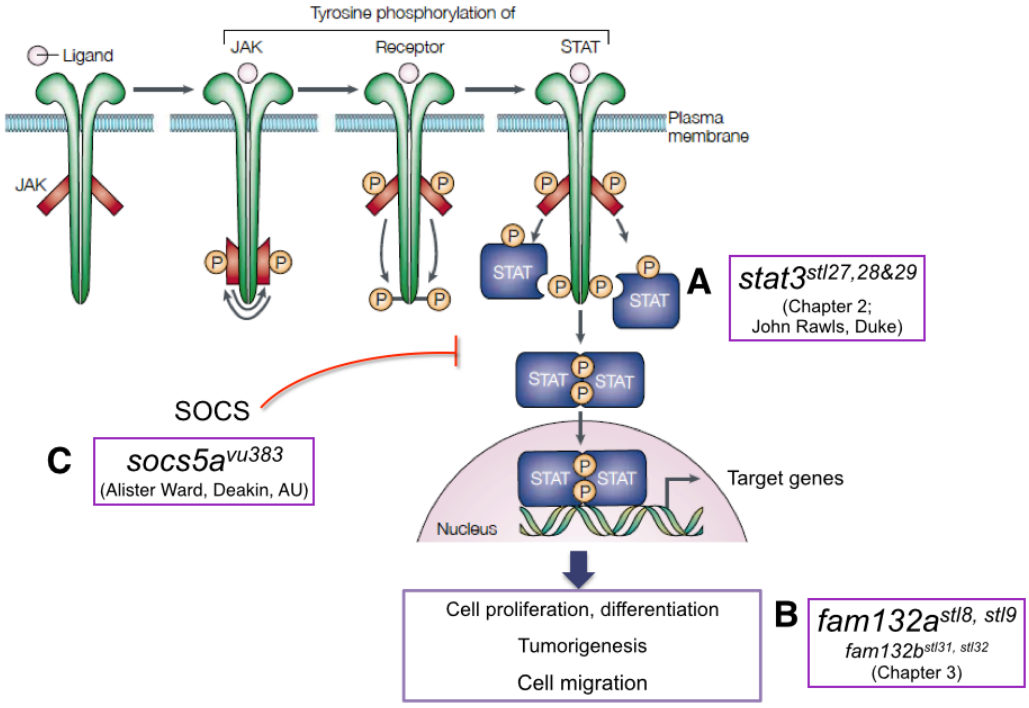

Figure 1.3 Schematic illustration of Stat3 signaling and summary of this thesis work (modified from Levy and Darnell et a., 2002). (A) Chapter 2 describes my studies on Stat3 during zebrafish embryonic as well as late development using zebrafish *stat3* mutant lines I generated (*stl27*, *stl28*, and *stl2*). Characterization of the late phenotypes is in collaboration with Dr. John Rawls at Duke University. (B) Chapter 3 describes an initiative we took using *stat3* morpholino as a tool to identify novel regulators of C&E gastrulation movements, and the functional characterization of Fam132a in the collective migration of the prechordal plate progenitors using the zebrafish *fam132a* mutants I generated. (C) I also identified a zebrafish *socs5a* mutant line. Socs5a is a potential negative regulator of Stat3. In collaboration with Dr. Alister Ward at Deakin University, we are exploring its function in hematopoiesis and liver development.

signaling is the recent findings of additional pathways for Stat3 activation including GPCRs and Toll-like receptors (TLRs) (Yu et al., 2014). As a transcription factor, Stat3 activates or inhibits expression of downstream targets involved in cell proliferation, apoptosis, stem cell maintenance, differentiation, and migration during development (Yu et al., 2014). In *Drosophila*, STAT, the fly homolog of vertebrate Stat3, regulates border cell migration in the developing egg chamber (Beccari et al., 2002; Silver and Montell, 2001) as well as stem cell maintenance through adhesion regulation in the testis stem cell niche (Leatherman and Dinardo, 2010). Among all the murine *Stat* genes, only *Stat3* knockout causes embryonic lethality by early gastrulation (Takeda et al., 1997), indicating a requirement of Stat3 in embryogenesis.

Previous morpholino studies also indicated Stat3 in zebrafish C&E gastrulation movements. Zebrafish Stat3 is activated shortly after MBT via tyrosine-phosphorylation downstream of the maternal Wnt/β-catenin pathway in the dorsal blastomeres and YSL independently of Boz and Sqt, and activated Stat3 is later localized in PPP cells at early segmentation stage (Yamashita et al., 2002). Stat3 was proposed to induce the signals for C&E without affecting cell fate specification. In particular, Stat3 was shown to regulate the dorsal convergence of lateral mesodermal cells non cell-autonomously in part through Wnt/PCP signaling, and the extension of the anterior axial mesodermal cell-autonomously by promoting epithelial-to-mesenchymal transition (EMT) (Miyagi et al., 2004; Yamashita et al., 2002; Yamashita et al., 2004). It was proposed that Stat3 transcriptionally activates Liv1, a zinc transporter essential for Snail nuclear translocation (Yamashita et al., 2004). However, the molecular mechanisms underlying Stat3 regulating lateral mesoderm convergence have not been reported. It also remains unclear what receptor and Jak are involved in Stat3 activation at these early stages.

Stat3 is also involved in organogenesis, as revealed by many studies using conditional *Stat3* knockout (CKO) mice. For example, Stat3 regulates bone homeostasis and promotes bone formation, as deletion of *Stat3* in osteoclasts and osteoblasts individually resulted in decreased bone density and volume due to elevated osteoclastogenesis and reduced bone formation rate, respectively (Itoh et al., 2006b; Zhang et al., 2005). A mouse keratinocyte-specific CKO model and *in vitro* wound-healing assay demonstrated the requirement of Stat3 in skin homeostasis via cell migration regulation (Sano et al., 1999). In addition, Stat3 signaling has been identified by dominant negative and morpholino-interference as an early injury response in zebrafish heart and eye regeneration (Fang et al., 2013; Nelson et al., 2012).

1.3.3 Stat3 in Disease

Abnormal Stat3 activity is found under many disease conditions. In cancerous cells, Stat3 is often constitutively active and promote cancer progression through various mechanisms. Through its transcriptional activities, Stat3 drives excessive cell proliferation through upregulation of many cell cycle-regulators such as c-Myc and Cyclin D, promotes pluripotency of cancer stem cells via c-Myc and Nanog, and potentiates cancer cell metastasis by modulating cytoskeleton and ECM (reviewed in (Carpenter and Lo, 2014; Yu et al., 2014). In addition, non-transcriptional functions of Stat3 in microtubule stability, mitochondria function, and chromatin modulation have also been implicated in cancer, obesity and inflammation (Gao and Bromberg, 2006; Yu et al., 2014).

Stat3 is a key regulator of immune responses. In human, *STAT3* has been associated with Hyper-IgE syndrome (HIES), a primary immunodeficiency (Holland et al., 2007). Autosomal dominant *STAT3* mutations are considered to underlie a variety of symptoms in HIES patients including misregulated Tumor necrosis factor α (TNFα) and other cytokines, recurrent bacterial

infections, elevated IgE, enhanced osteoporosis, and a high penetrance of scoliosis (Holland et al., 2007; Mogensen, 2013; Paulson et al., 2008). Similar symptoms except scoliosis were also reported in a mouse *Stat3* model of HIES (Steward-Tharp et al., 2014). Moreover, disruption of murine *Stat3* in hematopoietic cells causes Crohn's disease-like immunodeficiency (Welte et al., 2003).

1.3.4 Stat3 in Cell Migration

Increasing evidence implicates Stat3 signaling in cell polarity, cell migration and invasiveness (Hou et al., 2002). The *Drosophila* Stat92E signaling is essential for the establishment of planar polarity in the developing eye, where a gradient of Jak/Stat activity regulates ommatidial polarity via an unknown mechanism (Zeidler et al., 1999). Stat92E also plays critical roles in border cell migration (Beccari et al., 2002; Silver and Montell, 2001). In mammals, STAT3 signaling is required in trophoblast invasion (Fitzgerald et al., 2005) and Interleukin-6 (IL-6)-mediated T-cell migration (McLoughlin et al., 2005). Tyrosine-phosphorylated STAT3 potentiates metastasis of various types of cancer cells through, for example, transcriptional activation of genes encoding the Matrix metalloproteinases 1 (MMPs) in bladder cancer cell migration (Groner et al., 2008; Itoh et al., 2006a). Phosphorylated Stat3 also interacts with Focal adhesion kinase (FAK) and Paxillin in focal adhesions to promote cell migration (Silver et al., 2004). Highlighting the transcription-independent roles of Stat3, *in vitro* studies using murine embryonic fibroblasts showed that cytoplasmic, non-tyrosine-phosphorylated Stat3 facilitates cell migration during wound healing by modulating cytoskeleton network through Stathmin and Rho GTPases (Ng et al., 2006; Teng et al., 2009). Through interacting with Stathmin, a microtubule-destabilizing factor, Stat3 suppresses Stathmin function in microtubule depolymerization and in turn promotes cell migration (Ng et al., 2006).

1.3.5 SOCS: Negative Regulator of Stat3 Signaling

Suppressor of cytokine signaling (SOCS) proteins bind to and inhibit the activity of the receptors or JAKs, and thus negatively regulate JAK/STAT pathway. SOCS proteins are usually induced by cytokine stimulation, and inhibit either the same cytokine or different cytokines, known as "negative-feedback loop" and "cross talk", respectively (Croker et al., 2008). There are at least eight members, CIS and SOCS1-7, in the mammalian SOCS family, and 12 in Zebrafish. Among them, SOCS1 and SOCS3 are well-established negative regulators of IL6-mediated STAT3 pathway (Croker et al., 2008; Croker et al., 2003). I identified and recovered a mutant line (*socs5a*$^{vu383)}$ that harbors a nonsense mutation in the *socs5a* gene using Targeting Induced Local Lesions in Genome (TILLING) method (Wienholds et al., 2003). Under a collaboration, this mutant is currently analyzed in the laboratory of Dr. Alister Ward at Deakin University, AU in their studies of Socs4 and Socs5a during zebrafish hematopoiesis and liver development.

1.4 Objectives, Findings and Significance of This Work

Stat3 is a common oncogene in human cancer and an essential regulator of animal embryogenesis. Although much is known about its roles in cancer formation and progression, how it governs early development remains poorly understood. This work has investigated the roles of Stat3 signaling in C&E gastrulation movements during zebrafish development, providing insights into potential universal roles of Stat3 in embryonic development.

Firstly, this study clarifies the role of Stat3 during zebrafish embryogenesis. Previous morpholino-mediated downregulation of zebrafish Stat3 resulted in strong C&E defects, leading to a model whereby Stat3 controlled gastrulation by promoting some unidentified cell non-autonomous convergence signals as well as regulating PCP-dependent ML cell elongation (Yamashita et al., 2002). To elucidate the roles and underlying mechanisms of Stat3 in C&E, I

generated zebrafish *stat3* mutants using Transcription activator-like effector nuclease (TALEN) method. I showed that in the absence of maternal and zygotic Stat3 expression, mutant embryos were able to complete gastrulation with mild extension defects in the axial and paraxial mesoderm and no obvious convergence defects. In addition, *stat3* mutant cells exhibited normal ML alignment and slightly less elongated shape; zygotic *stat3* deficiency does not exacerbate gastrulation defects of Wnt/PCP mutants, arguing against a role of Stat3 in PCP signaling. Unexpectedly, *stat3* deficient embryos throughout early development exhibit defects in cell proliferation, one of the key developmental events overlooked in the morphogenesis of various tissues during gastrulation. I demonstrated that cell proliferation promotes extension of both axial and paraxial mesoderm, as reduction of cell proliferation in early zebrafish embryos by genetic inactivation of *stat3* or chemical manipulations impairs extension morphogenesis. Mechanistically, Cdc25a is transcriptionally downregulated in *stat3* mutant embryos, and restoring Cdc25a expression suppressed both proliferation and morphogenetic defects in *stat3* mutants. Finally, *stat3*-deficient mutant zebrafish exhibit scoliosis, excessive inflammation and abnormal gut morphology before they die during juvenile stages, and may empower genetic investigation of human idiopathic scoliosis and Hyper-IgE Syndrome, and lead to a novel model of inflammatory bowel disease (IBD).

Secondly, my work has led to identification of novel molecules and pathways during zebrafish gastrulation. My studies on *stat3* mutant indicated that *stat3* morpholino-induced severe C&E phenotypes are likely *stat3*-independent, which made *stat3* morpholino a great tool for fishing for novel molecules that are involved in C&E movements. Using a combination of microarray and bioinformatics analyses, I identified six candidate genes that are predicted to encode secreted molecules and/or involved in cell migration, and are downregulated by *stat3*

morpholino. I further showed with gain-of-function studies that two genes, *fam132a* and *cartpt* the functions of which were not characterized in zebrafish or development, are novel molecules that regulate zebrafish C&E movements.

Thirdly, this work has characterized functions of a novel secreted molecule, Fam132a, in the anterior migration of zebrafish PPP cells during gastrulation. Tissue cohesion has been shown to be critical for directionality and the coherent migratory behavior of this group (Dumortier et al., 2012; Tada and Heisenberg, 2012). I demonstrated that overexpression of Fam132a disrupted tissue cohesion and cell contact persistence, and caused loss of tissue integrity and less coherent migration of PPP cells; whereas loss of *fam132a* function partially suppressed the cell contact maintenance and collective migration defects in *slb* mutant embryos. Fam132a affords a new tool to study mechanisms underlying collective migration and invasion of mesenchymal cells.

In addition, my work has led to several collaborations with other laboratories. Zebrafish *socs5a* mutant that I identified is studied by Alister Ward group at Deakin University, AU. Socs5a is a potential negative regulator of Stat3 signaling. The roles of Stat3 in immune response and gut homeostasis are investigated in collaboration with Dr. John Rawls at Duke University.

C&E are fundamental morphogenetic movements during gastrulation. C&E defects are associated with numerous birth defects in human such as spina bifida, and lead to miscarriages in severe cases. Together, my thesis work elucidates the role of Stat3/Cdc25a-dependent cell proliferation in morphogenesis during gastrulation, identifies novel regulators of C&E movements, and leads to better understanding of collective migration of mesenchymal-like cells. Proliferation and collective migration/invasion are also common cellular mechanisms shared by

morphogenesis during development and cancer formation/metastasis. My studies of Stat3 and other molecules in developmental processes will therefore provide mechanistic and therapeutic insights into human cancer.

Chapter 2

Stat3/Cdc25a-Dependent Cell Proliferation Promotes Axis Extension during Zebrafish Gastrulation

Yinzi Liu, Lilianna Solnica-Krezel

Department of Developmental Biology, Washington University School of Medicine in St. Louis, St. Louis, MO 63108, USA

2.1 Summary

Cell proliferation has generally been considered dispensable for anteroposterior extension and mediolateral convergence of embryonic axis during vertebrate gastrulation. Zebrafish signal transducer and activator of transcription 3 (Stat3) was proposed to govern convergence and extension movements in part by promoting Wnt/Planar Cell Polarity (PCP) signaling, a

conserved regulator of cell migration and polarized intercalation underlying vertebrate gastrulation. Here, using a zebrafish *stat3* null mutant and pharmacological tools, we demonstrate that cell proliferation promotes extension of both axial and paraxial mesoderm. We further show Stat3 regulates extension but not convergence of axial and paraxial mesoderm by promoting cell proliferation, in part through transcriptional activation of Cdc25a, without significantly affecting PCP signaling. Restoring Cdc25a expression suppressed proliferation and morphogenetic defects in *stat3* mutants. Finally, *stat3* mutant zebrafish develop scoliosis and excessive inflammation later during development, affording a genetic model of human idiopathic scoliosis and Hyper-IgE Syndrome.

2.2 Introduction

Signal transducer and activator of transcription 3 (STAT3) is an essential mediator of cytokine and growth factor signaling involved in animal development, homeostasis and disease (Darnell et al., 1994; Levy and Darnell, 2002). Typically a transcription factor, STAT3 activates or inhibits expression of downstream targets involved in cell proliferation, apoptosis, stem cell maintenance, differentiation, and migration in normal tissues. Non-transcriptional functions of STAT3 in microtubule, mitochondria, and chromatin regulation have also been reported (Ng et al., 2006; Yu et al., 2014). In cancerous cells, constitutively active STAT3 drives cell proliferation through upregulation of cell cycle-regulators such as c-Myc and Cyclin D, promotes pluripotency of cancer stem cells, and potentiates metastasis by modulating cytoskeleton and extracellular matrix (Carpenter and Lo, 2014; Yu et al., 2014). Underscoring its role in immune responses, autosomal dominant *STAT3* mutations account for numerous symptoms in Hyper-IgE

syndrome (HIES) patients such as misregulated TNFα and scoliosis (Holland et al., 2007; Paulson et al., 2008; Steward-Tharp et al., 2014). Disruption of murine *Stat3* in hematopoietic cells causes Crohn's disease-like immunodeficiency (Welte et al., 2003).

Stat3 is also a key developmental regulator. Firstly, *Drosophila* STAT signaling regulates border cell migration in the developing egg chamber (Silver and Montell, 2001). Secondly, *Stat3* knockout mice die by early gastrulation (Takeda et al., 1997), suggesting some critical but yet undefined roles of Stat3 in embryogenesis. Indeed, morpholino studies in zebrafish unveiled requirement of Stat3 in planar cell polarity (PCP) signaling and gastrulation movements (Miyagi et al., 2004; Yamashita et al., 2002). Later during development, Stat3 promotes bone formation, as deletion of *Stat3* in mouse osteoclasts and osteoblasts resulted in decreased bone density and bone volume (Itoh et al., 2006b; Zhang et al., 2005). Dominant negative and morpholino-interference also implicated zebrafish Stat3 in heart and eye regeneration (Fang et al., 2013; Nelson et al., 2012).

Here we report analyses of zebrafish *stat3* mutants and propose a different mechanism wherein Stat3 regulates gastrulation by promoting cell proliferation. Early zebrafish embryos undergo rapid and synchronous cell divisions (Kimmel et al., 1995) consisting of DNA synthesis (S) and mitosis (M) phases without transcription. After mid-blastula transition (MBT) and activation of the zygotic genome, cell cycles slow down and become asynchronous with the acquisition of a G2 phase (Dalle Nogare et al., 2009). Conserved from fly, amphibian and fish to mammals, Cdc25a phosphatase is a key promoter of cell cycle progression during embryogenesis (Bouldin and Kimelman, 2014; Edgar and Datar, 1996; Kim et al., 1999; Tsai et al., 2014). Through activation of Cyclin B/Cdk1 complexes, Cdc25a synthesized from both maternal and

zygotic RNAs propels mitotic entry. But how Cdc25a is activated in these early events is unclear.

Following MBT is gastrulation, a fundamental morphogenetic process during which cells migrate and rearrange to establish future body plan. Convergence and extension (C&E) are evolutionarily conserved gastrulation movements that narrow the germ layers mediolaterally and lengthen them along the anteroposterior (AP) axis (Keller, 2002). Mainly mediated by Wnt/PCP signaling, cells become mediolaterally elongated and either migrate dorsally (convergence) or engage in polarized intercalations that preferentially separate anterior and posterior neighbors to drive convergent extension movements (Gray et al., 2011; Keller, 2002). Disruption of such polarity in the zebrafish PCP mutants such as *silberblick* (*slb*)/*wnt11* and *trilobite* (*tri*)/*vangl2* leads to rounder and less oriented cells, and consequently a shorter and wider body (Heisenberg et al., 2000; Jessen et al., 2002). Interestingly, disrupted cell elongation, impaired mediolateral cell orientation and defective C&E were also reported in *stat3* morphant, implicating Stat3 as a regulator of PCP signaling during zebrafish gastrulation (Miyagi et al., 2004; Yamashita et al., 2002).

Cell proliferation and gastrulation movements have to be coordinated to achieve proper embryogenesis. Indeed, rapid cell proliferation usually precedes gastrulation to ensure sufficient number of cells, and cell divisions only occur infrequently during gastrulation (Leise and Mueller, 2004). Gastrulating cells divide at the expense of migration by rounding up and abolishing their planar polarized asymmetries (Ciruna et al., 2006), likely because cell division and motility utilize common cytoskeleton machineries. Limiting cell divisions has been shown necessary for C&E of the paraxial mesoderm in *Xenopus* (Leise and Mueller, 2004) and posterior body elongation in zebrafish (Bouldin et al., 2014). Conversely, cell proliferation appears

dispensable for axis elongation during gastrulation, as the zebrafish *emi* mutant in which mitosis ceases from early gastrulation, and embryos where cell proliferation is chemically inhibited during gastrulation, both complete gastrulation featuring elongated bodies (Quesada-Hernandez et al., 2010; Zhang et al., 2008). However, without careful analyses of C&E movements in these embryos, some contribution of cell proliferation to gastrulation cannot be excluded.

Here, we report that Stat3-dependent cell proliferation promotes extension movements during zebrafish gastrulation. Using transcription activator-like effector nuclease (TALEN) method we generated null *stat3* mutations. We found that neither maternal nor zygotic *stat3* functions are essential for the completion of embryogenesis. However, *stat3* mutants die during juvenile stages exhibiting scoliosis and excessive inflammation, thus enabling future studies of development and diseases such as cancer, HIES, and idiopathic scoliosis. Strikingly, rather than typical PCP-based C&E defects, MZ*stat3* gastrulae manifested cell proliferation and transient and mild extension defects in the axial and paraxial mesoderm. As the underlying cellular mechanism, we demonstrate that reduced cell proliferation accounts for extension defects in *stat3* mutant gastrulae. We further show that the evolutionarily conserved Stat3 function of promoting cell cycle progression through transcriptional activation of Cdc25a is required for axis elongation during gastrulation.

2.3 Results

2.3.1 *stat3* Mutants Develop Scoliosis, Excessive Inflammation and Cannot Survive to Adulthood

We generated *stat3* mutant zebrafish using TALEN method (Figure 2.1A, see also Experimental Procedures). The *stl27* and *stl28* alleles contain 7- and 2-base pair deletions in Exon 5, respectively, resulting in frameshift and premature stop codons, encoding proteins predicted to lack almost all the critical functional domains of the Stat3 protein (Figure 2.1B).

Surprisingly, neither zygotic $stat3^{stl27/stl27}$ nor $stat3^{stl28/stl28}$ mutant embryos showed overt gastrulation defects described in the previous morpholino studies (Yamashita et al., 2002), and displayed normal morphology at 1 day post fertilization (dpf). Although $stat3^{stl27/stl27}$ mutant larvae exhibited normal notochord and spinal structures (Figure 2.2), they appeared significantly smaller compared to siblings during later larval stages (Figure 2.1G), and manifested spinal curvatures in all dimensions without any skeletal abnormalities as revealed by Alizarin Red staining and micro-computed tomographic (μCT) imaging (Figures 2.1J, 2.2). Scoliotic mutants could be discerned as early as 19 dpf; they were fragile and lethargic, and progressively died by 1.5 to 2 months of age (Figure 2.1H). μCT analyses revealed a slight reduction in bone mineral density (Figure 2.1K) and nearly 40% reduction in the total bone volume in *stat3* juveniles (Figure 2.1L). Given the roles of Stat3 in immune responses (Holland et al., 2007; Steward-Tharp et al., 2014), we analyzed $stat3^{stl27/stl27}$ animals for markers of inflammation, and observed a significant upregulation of transcripts encoding pro-inflammatory factors Tnfα and

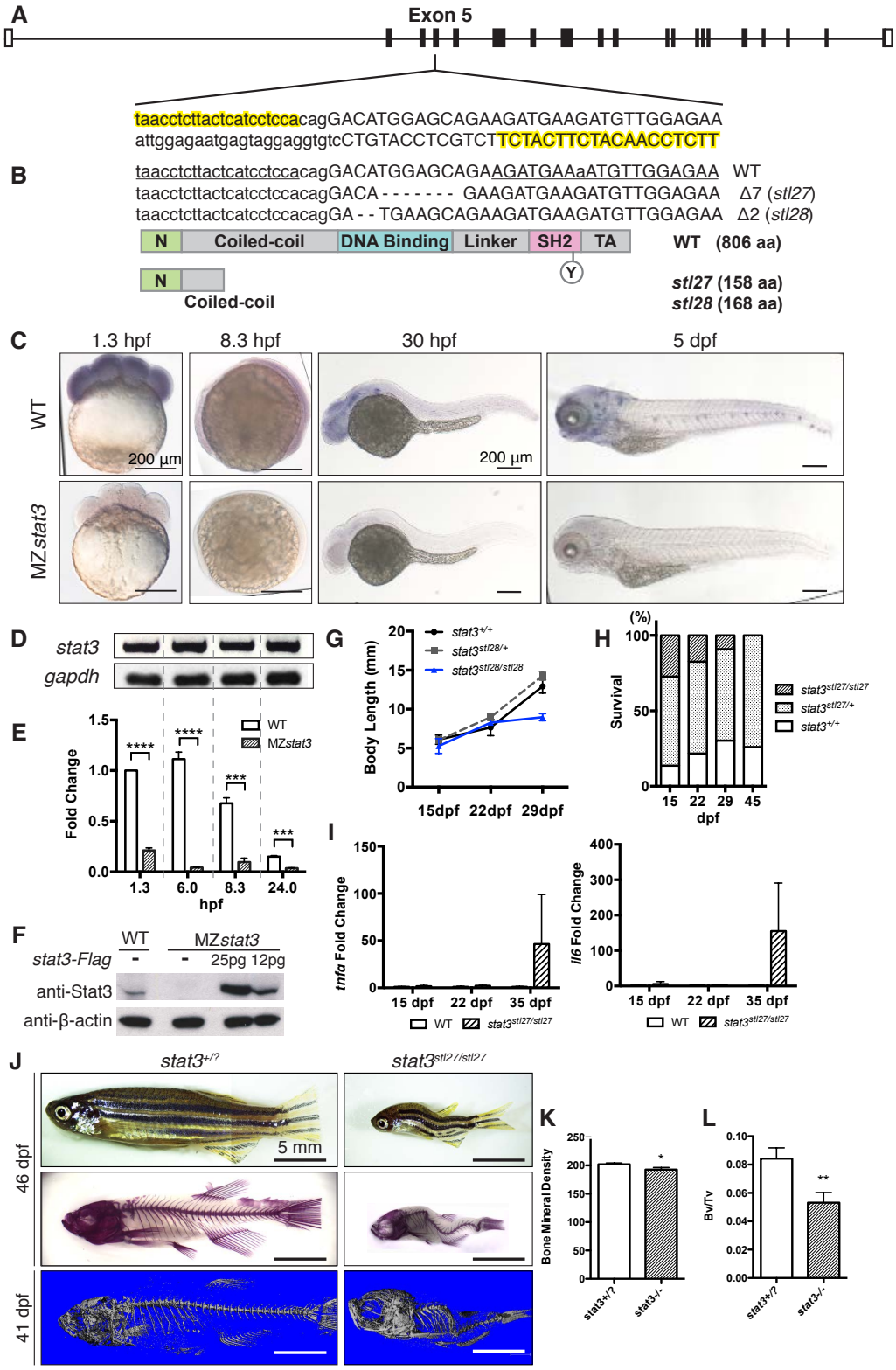

Figure 2.1 Zebrafish *stat3* null mutants generated using TALEN method develop late-onset scoliosis and cannot survive to adulthood.

(A) Design of TALEN pair targeting zebrafish *stat3* gene.

(B) Sequence alignments and illustration of encoded proteins of *stl27* and *stl28* alleles.

(C) Expression patterns of *stat3* transcripts detected by WISH in WT and MZ*stat3* embryos (lateral view).

(D) RT-PCR showing *stat3* expression levels in WT embryos at 1.3, 6, 8.3 and 24 hpf. *gapdh* was used as an internal control.

(E) qRT-PCR showing *stat3* transcript levels in WT and MZ*stat3* embryos normalized to *gapdh*.

(F) Western blot detecting total Stat3 in WT, MZ*stat3* and MZ*stat3* embryos overexpressing Flag-tagged Stat3 at 6 hpf (see also Figure S1). β-actin was used as a loading control.

(G) Growth curve of $stat3^{stl28}$ homozygous fish and siblings.

(H) Survival rate of $stat3^{stl27}$ homozygous animals and siblings.

(I) Transcript levels of *tnfα* and *il6* detected by qRT-PCR.

(J-L) Live images, Alizarin staining, and μCT imaging showing body curvatures of *stat3* mutant and siblings (anterior to the left, see also Figure 2.2B). Bone mineral density (K) and bone/tissue volume ratio (Bv/Tv, L) were quantified according to μCT analysis.

*$p<0.05$, ***$p<0.001$, ****$p<0.0001$, error bars = standard error of the mean (SEM).

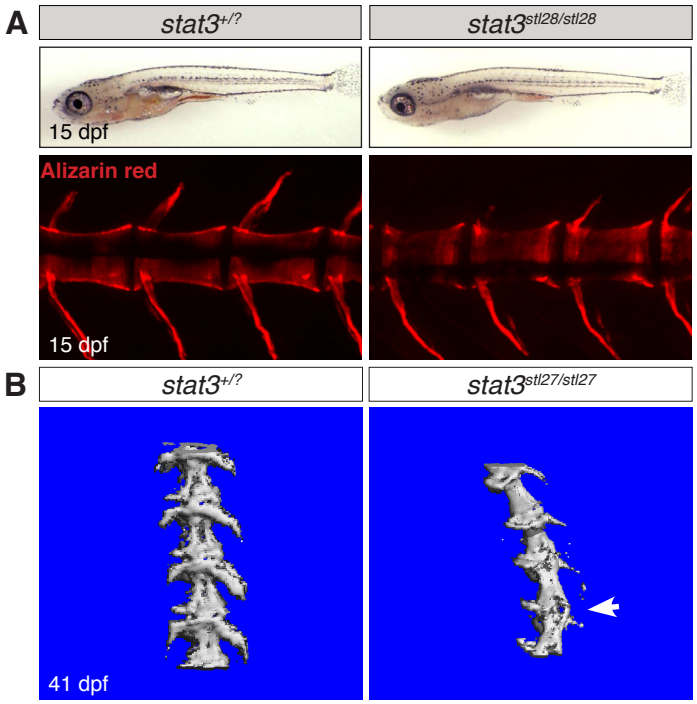

Figure 2.2 *stat3* deficient zebrafish do not exhibit structural defects in the vertebrae.

(A) Vertebral structure revealed by Alizarin red in live 15-dpf *stat3* mutant larvae and siblings (Lateral view, anterior to the left). Mutant larva did not show growth defect or scoliosis.

(B) Vertebral structure in 41 days old scoliotic *stat3* mutant juvenile and siblings (see also Figure 2.1J). White arrow, spinal curvature.

Interleukin (Il)-6 in *stat3*$^{stl27/stl27}$ larvae and juveniles (Figure 2.1I), temporally correlating with the manifestation of stunted growth and scoliotic phenotypes.

2.3.2 Maternal Zygotic *stat3* Gastrulae Exhibit Mild Extension Defect Independent of PCP Signaling

The lack of overt embryogenesis defects in *stat3* mutants generated by heterozygous parents was surprising given the previous morpholino results (Yamashita et al., 2002) and whole-mount *in situ* hybridization (WISH) studies that detected only zygotic expression of *stat3* in zebrafish embryos (Oates et al., 1999). However, using WISH and RT-PCR we found high levels of *stat3* maternal *stat3* transcripts (Figure 2.1C-D), *stat3* mRNA was expressed ubiquitously during blastula and gastrula stages and became enriched in the head and in neuromasts at 5 dpf (Figure 2.1C). To test whether maternal Stat3 function contributes to proper gastrulation movements, we generated maternal zygotic (MZ) *stat3*$^{stl27/stl27}$ mutants by germline transplantations (Ciruna et al., 2006). For simplicity, hereafter we use MZ*stat3*, Z*stat3*, and M*stat3* to refer to maternal zygotic (MZ*stat3*$^{stl27/stl27}$, from MZ*stat3* incrosses), zygotic (Z*stat3*$^{stl27/stl27}$, from heterozygous incrosses), and maternal (M*stat3*$^{stl27/+}$, from crosses of females harboring *stat3*$^{stl27/stl27}$ germline with *stat3*$^{stl27/+}$ or *stat3*$^{+/+}$ males) mutant, respectively, unless specified otherwise.

Unexpectedly, MZ*stat3* mutants progressed through embryogenesis and later manifested phenotypes described above for Z*stat3* mutants with no observable changes in the onset or severity. Using qRT-PCR and four different primer pairs spanning regions at, upstream of, or downstream of the *stat3*^{stl27} deletion in all three *stat3* transcript sequences annotated in the zv9 zebrafish genome assembly, we observed significant reduction of *stat3* transcripts in MZ*stat3* embryos (Figure 2.1C). In agreement, Western blotting with an antibody against the C-terminus

of zebrafish Stat3 (Experimental Procedures) failed to detect Stat3 protein in MZ*stat3* gastrulae (Figure 2.1F). Based on these results we conclude that *stl27* is a strong/null allele.

Previous studies proposed a requirement of *stat3* in Wnt/PCP signaling and mediolateral (ML) cell elongation essential for C&E (Miyagi et al., 2004). However, MZ*stat3* gastrulae did not exhibit severe C&E defects (Figure 2.3A) and showed normal AP body length by 30 hpf (Figure 2.3A-B). To detect any subtle morphogenetic defects, we visualized the nascent embryonic tissues that undergo dynamic C&E gastrulation movements using WISH (Jessen et al., 2002; Marlow et al., 1998). Whereas we failed to detect any defects in convergence of paraxial mesoderm revealed by the ML dimension of *paraxial protocadherin* (*papc*)-expression domain (Figure 2.3C-D), we noticed 13.2% and 14.2% reduction compared to WT in the AP extension of the notochord marked by expression of *no tail* (*ntl*) in M*stat3* and MZ*stat3* mutants, respectively (Figure 2.3E-F).

We next asked whether ML cell elongation, the hallmark of PCP signaling, was affected in *stat3*-deficient gastrulae. Our analyses of cell shape, or length-to-width ratio (LWR), and cell body orientation of the notochord cells revealed that the notochord cells in M*stat3* and MZ*stat3* gastrulae had a shorter long axis and a greater short axis, and consequently a reduced LWR (2.0±0.0) compared to WT cells with LWR of 2.5±0.0 (Figure 2.4A-F). However, in contrast to a typical PCP defect (Jessen et al., 2002), the mutant notochord cells aligned their long axes normally along the ML axis (Figure 2.4C). Moreover, we noted that M*stat3* and MZ*stat3* mutant cells were 11.6% and 17.3% larger compared to their WT counterparts, respectively (Figure 2.4G).

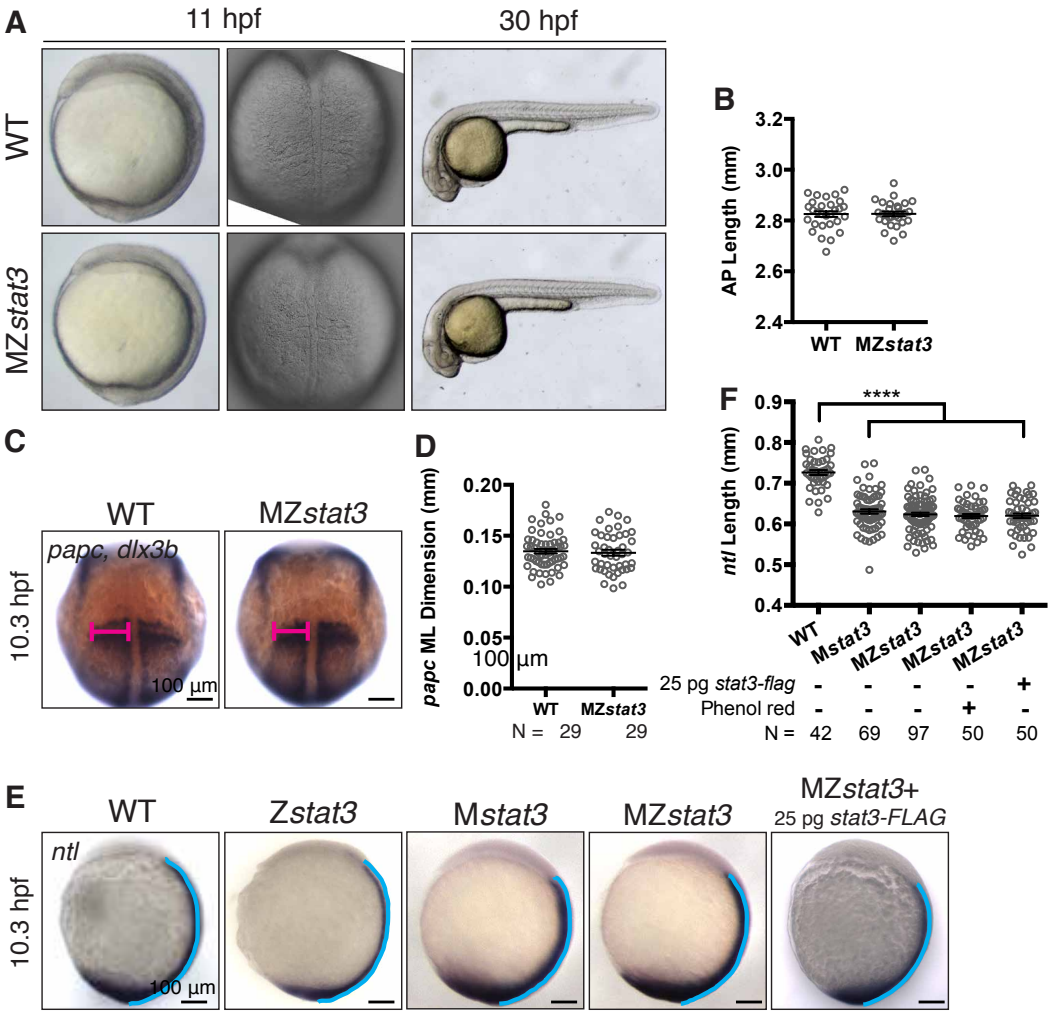

Figure 2.3 MZ*stat3* gastrulae exhibit mild extension defects in axial mesoderm.

(A and B) Live images of WT and MZ*stat3* embryos shown in lateral and dorsal view. AP axis extension in 30 hpf embryos was quantified in B.

(C) *papc* in presomitic mesoderm and *dlx3b* marking neuroectoderm boundary in 1-somite stage WT and MZ*stat3* embryos (dorsal view).

(D) Quantification of ML width of *papc* domain (pink in C).

(E) *ntl* in notochord and tail in 1-somite stage WT, Z*stat3,* M*stat3*, MZ*stat3*, and MZ*stat3* embryos overexpressing Stat3-Flag (lateral view). Phenol red was used as injection control.

(F) Quantification of notochord length (blue lines in E).

****p<0.0001, error bars = SEM.

These results argue against Stat3 being a key regulator of Wnt/PCP signaling during zebrafish gastrulation, but suggest a role of Stat3 in cell shape and size (see 2.4 Discussion).

To query further whether Stat3 plays any role in planar polarity or Wnt/PCP signaling in a sensitized background, we asked whether phenotypes of mutations disrupting Wnt/PCP components such as *trilobite(tri)/vangl2* (Jessen et al., 2002) or *silberblick(slb)/wnt11* (Heisenberg et al., 2000) could be exacerbated by simultaneous reduction of Stat3 function. A spectrum of eye separation phenotypes from partial to complete fusion of the eyes (Figure 2.4H), often associated with C&E defects, are commonly seen in both *tri* and *slb* embryos and are exacerbated in compound PCP mutants (Heisenberg and Nusslein-Volhard, 1997; Marlow et al., 1998). However, we found that Z*stat3;*Z*tri*^{vu67} and Z*stat3*;MZ*slb*^{tz216} compound mutants exhibited similar penetrance and expressivity of the eye separation defect compared to their single PCP mutant siblings (Figure 2.4H-J). Together, our data provide genetic evidence for an essential role of Stat3 in AP axis extension during zebrafish gastrulation. Moreover, Stat3 regulates cell size and shape during gastrulation without significantly affecting Wnt/PCP signaling.

2.3.3 Stat3 Promotes Cell Proliferation during Zebrafish Embryogenesis

In the above morphometric analyses, the enlarged cell size in MZ/M*stat3* mutant gastrulae stood out. Since Stat3 regulates cell proliferation in many biological contexts (Carpenter and Lo, 2014), we detected 31.2% and 33.7% reduction in mitosis in M*stat3* and MZ*stat3* mutants at 6 hpf compared to WT gastrulae, respectively, as revealed by phosphorylated Histone H3 (pH3, a mitotic marker) immunostaining (Figure 2.5A-B).

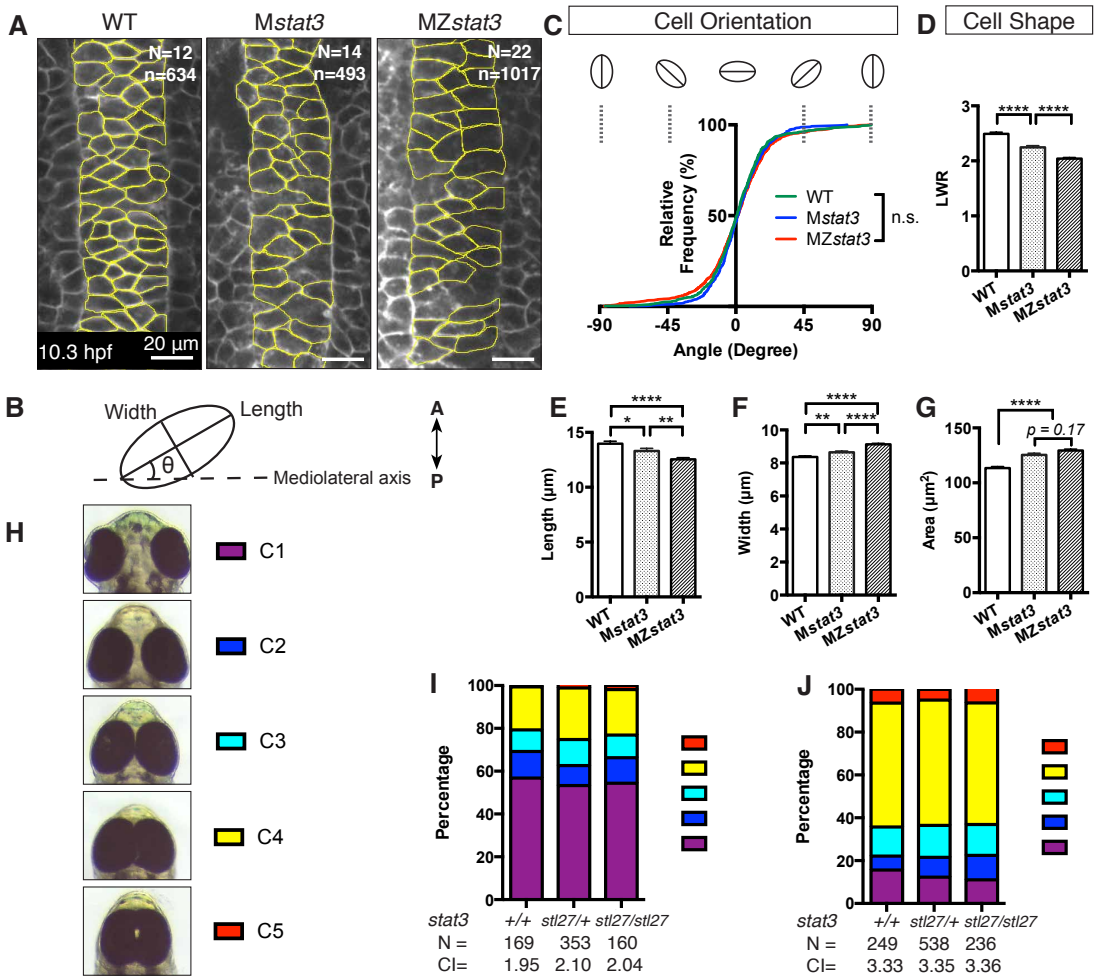

Figure 2.4 MZ*stat3* embryos show neither obvious cell polarity defects during C&E nor interaction with zebrafish PCP mutants.

(A-B) Dorsal view showing cells labeled with mGFP in WT, M*stat3*, and MZ*stat3* 1-somite stage embryos (anterior to the top). Cell shape and orientation of notochord cells were analyzed as illustrated in B.

(C) Cumulative distribution of notochord cell orientation in WT, M*stat3*, and MZ*stat3* embryos.

(D) Cell shape analysis represented by length-to-width ratio (LWR).

(E-G) Long axis (length, E), short axis (width, F) and average area (G) of in WT, M*stat3* and MZ*stat3* notochord cells.

(H) A spectrum of eye separation phenotypes with C1 representing WT eye spacing and C5 representing the most severe phenotype, cyclopia. Ventral view, anterior to the top.

(I) Eye phenotypes of Z*tri*, Z*tri*;Z*stat3*$^{stl27/+}$, and Z*tri*;Z*stat3* embryos at 3 dpf. CI, Cyclopia Index.

(J) Eye phenotypes of MZ*slb*, MZ*slb*;Z*stat3*$^{stl27/+}$, and MZ*slb*;Z*stat3* embryos at 3 dpf.

****$p<0.0001$, error bars = SEM.

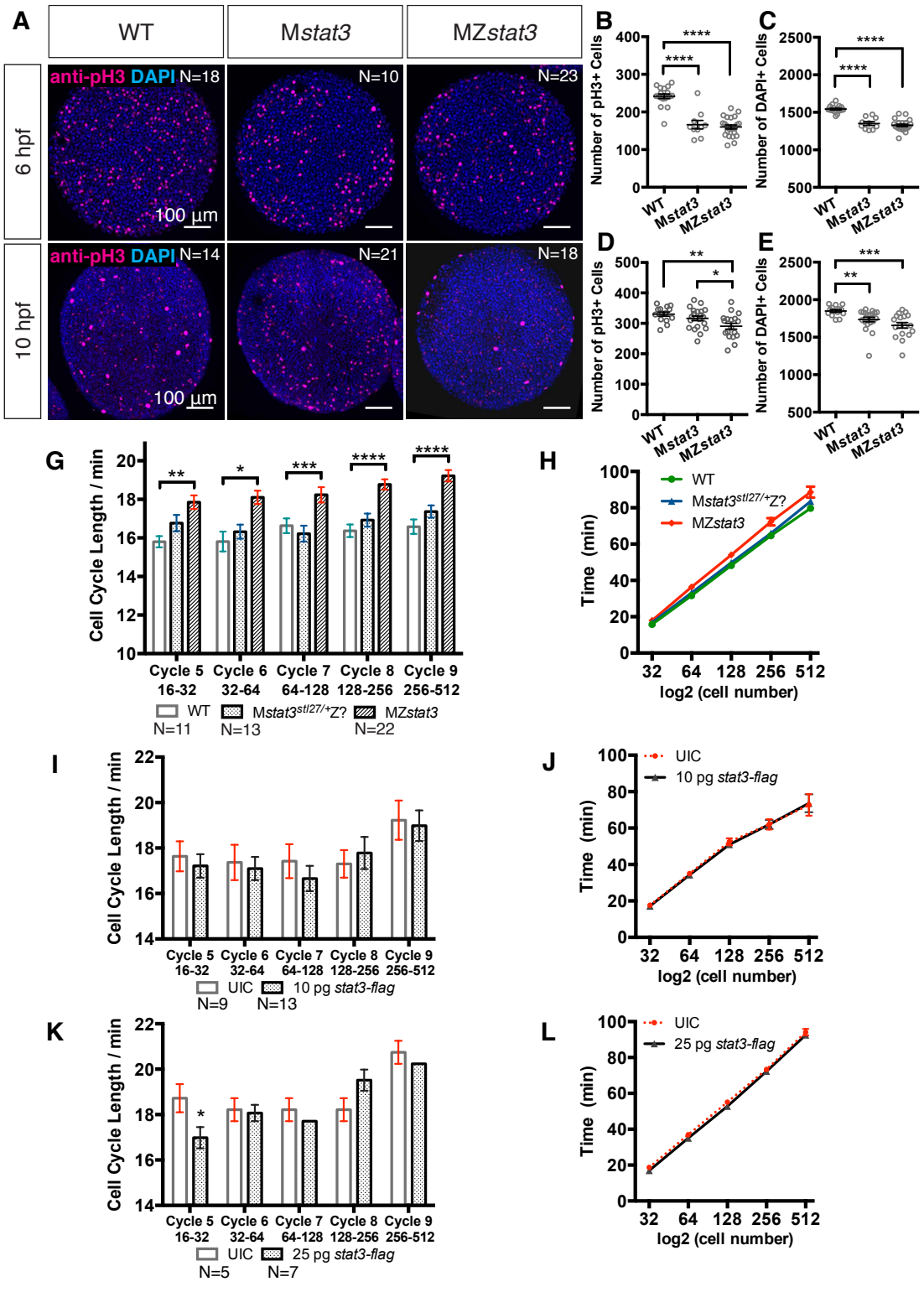

Figure 2.5 Stat3 promotes cell cycle progression during zebrafish embryogenesis.

(A-E) Cell proliferation (A) in WT, M*stat3*, MZ*stat3* embryos, and MZ*stat3* embryos overexpressing Stat3-FLAG at 6 hpf (animal view) and 10 hpf (dorsal view), with pH3 labeling proliferating cells (red, quantified in B and D) and DAPI labeling all nuclei (blue, quantified in C and E).

(G and H) Average length of each cell cycle (G) and timing of mitosis (H) from Cycle 5 to Cycle 9 in WT, maternal heterozygous, and MZ*stat3* embryos.

(I-L) Analyses of cell divisions from Cycle 5 to Cycle 9 in 10 pg (I and J) and 25 pg (K and L) *stat3-flag* injected MZ*stat3* embryos.

*p<0.05, **p<0.01, ***p<0.001, ****p<0.0001, error bars = SEM.

Total number of cells, as revealed by DAPI (+) nuclei, was also decreased by 12.5% and 14.1% in M*stat3* and MZ*stat3* mutants (Figure 2.5C), indicating comparable cell proliferation defects in these mutants at early gastrulation. By late gastrulation, however, M*stat3* gastrulae started to catch up and exhibited similar level of cell proliferation to that seen in WT (Figure 2.5D), whereas, their total cell number continued to be reduced (Figure 2.5E), suggesting a partial rescue of cell proliferation defect by zygotic Stat3 expression. However, both proliferation rate and total cell number in MZ*stat3* embryos remained low throughout gastrulation (Figure 2.5D-E). Together, these data indicate that Stat3 regulates cell proliferation during zebrafish embryogenesis. Moreover, one zygotic WT allele is not sufficient to compensate the cell number deficit caused by reduced cell proliferation in maternal *stat3* mutants, revealing a crucial role of maternal Stat3.

To investigate the maternal Stat3 function in cell proliferation, we analyzed the rapid cell divisions that depend exclusively on maternally deposited proteins and RNAs prior to MBT (Harvey et al., 2013) via *in vivo* confocal time-lapse imaging of embryos with Histone2B-RFP (H2B-RFP)-labeled nuclei (see also Experimental Procedures). Whereas WT embryos divided every 15.8 ~ 16.6 min from Cycle 5 (from 16 to 32 cells) to Cycle 9 (from 256 to 512 cells), pre-MBT cycles ranged from 17.6 min to 19.2 min in embryos lacking maternal *stat3* function (Figures 2.5G, 2.6), nearly 13% increase. Cumulatively, M*stat3* mutants took significantly longer to complete five pre-MBT cycles (Figure 2.5H). However, embryos from heterozygous females showed relatively normal pre-MBT cell divisions (Figure 2.5G-H).

We next asked whether Stat3 is required for post-MBT cell divisions. Our manual lineage tracing of individual blastomeres for the duration of five post-MBT divisions

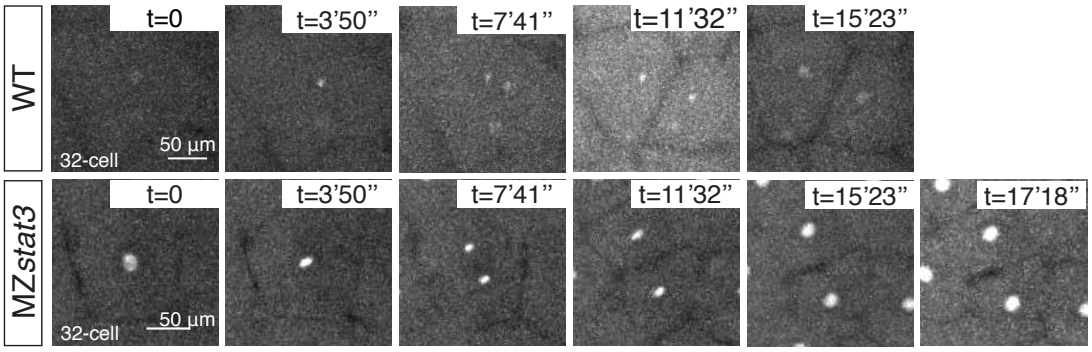

Figure 2.6 Pre-MBT cell divisions are lengthened in MZ*stat3* embryos compared to WT. Illustrated is a full pre-MBT cell cycle (Cycle 6, 32 cells to 64 cells) in WT and MZ*stat3* embryos from S phase to S phase.

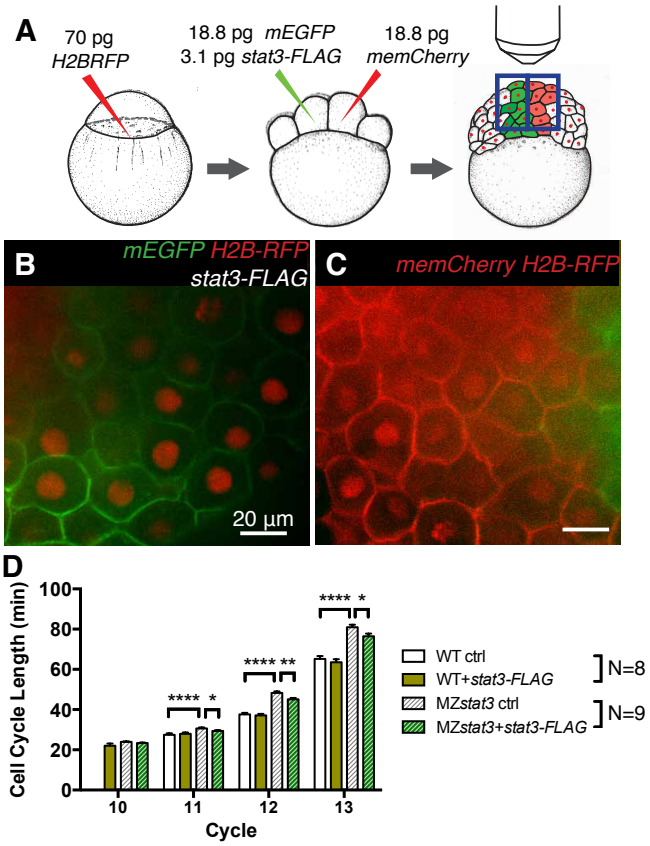

Figure 2.7 Stat3 promotes post-MBT cell divisions during zebrafish embryogenesis.

(A) Experimental design for post-MBT cell cycle analyses. Embryos labeled ubiquitously with H2B-RFP were mosaically labeled with *memCherry* or *mGFP* + *stat3-FLAG* mRNA at 8-cell stage for lineage tracing. Labeled clones (B and C) within the same embryo were monitored (See also Experimental Procedures).

(D) Analyses of cell cycle lengths for Cycle 10 - 13 in WT, WT overexpressing Stat3-FLAG, MZ*stat3*, and MZ*stat3* overexpressing Stat3-FLAG embryos.

*p<0.05, **p<0.01, ****p<0.0001, error bars = SEM.

(Figure 2.7A-C, see also Experimental Procedures) revealed that cell cycles gradually lengthened from MBT onward in both WT and MZ*stat3* embryos, consistent with previous observations (Dalle Nogare et al., 2009). Furthermore, cycles 10 through 13 were significantly longer in MZ*stat3* mutants than in WT (Figure 2.7D), demonstrating Stat3 was required for post-MBT cell cycle progression. Together, our results establish a key role of Stat3 in promoting cell proliferation throughout early embryogenesis.

2.3.4 *stat3* Deficiency Induces Apoptosis

Stat3 suppresses apoptosis in various biological contexts through transcriptional activation of anti-apoptotic genes (Carpenter and Lo, 2014). During zebrafish embryogenesis, apoptosis can be detected from early segmentation stages (Cole and Ross, 2001). Terminal deoxynucleotidyl transferase mediated dUTP Nick End Labeling (TUNEL) assay revealed a nearly 70% increase in the number of apoptotic cells in MZ*stat3* embryos compared to WT at both late gastrulation (Figure 2.8A-C) and early somitogenesis (Figure 2.8D-F). Using qRT-PCR, we further detected substantial downregulation of *birc5a*, the zebrafish homolog of known anti-apoptotic target of Stat3, *Survivin* (Delvaeye et al., 2009), in MZ*stat3* embryos (Figure 2.8G). Together, these data indicate that Stat3 suppresses apoptosis in zebrafish embryos likely through activating anti-apoptotic genes such as *birc5a/survivin*.

2.3.5 Reduced Cell Proliferation Impairs Axis Extension

AP tissue extension can be a result of ML cell intercalation that aligns cells one after another anteroposteriorly, simultaneously producing AP extension and ML convergence (Keller, 2002).

Confocal imaging at 3-somite stage revealed two rows of ML elongated axial mesodermal cells in the notochord in MZ*stat3* and WT embryos (Figure 2.9A-C),

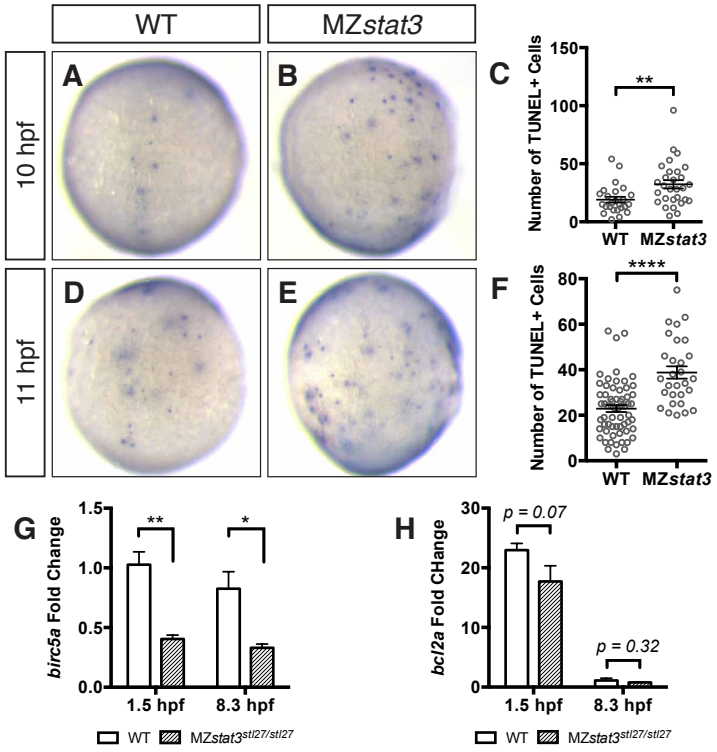

Figure 2.8 Stat3 suppresses apoptosis during zebrafish embryogenesis.

(A-E) Apoptosis in WT (A, D) and MZstat3 (B, E) embryos at 10 hpf (A, B) and 11 hpf (D, E) detected by TUNEL labeling (dorsal view, anterior to the top). Number of TUNEL-positive cells is quantified in C and F.

(G, H) *birc5a/survivin* (G) and *bcl2a* (H) expression levels in WT and MZstat3 embryos at 1.5 hpf and 8.3 hpf detected by qRT-PCR.

*p<0.05, **p<0.01, error bars = SEM.

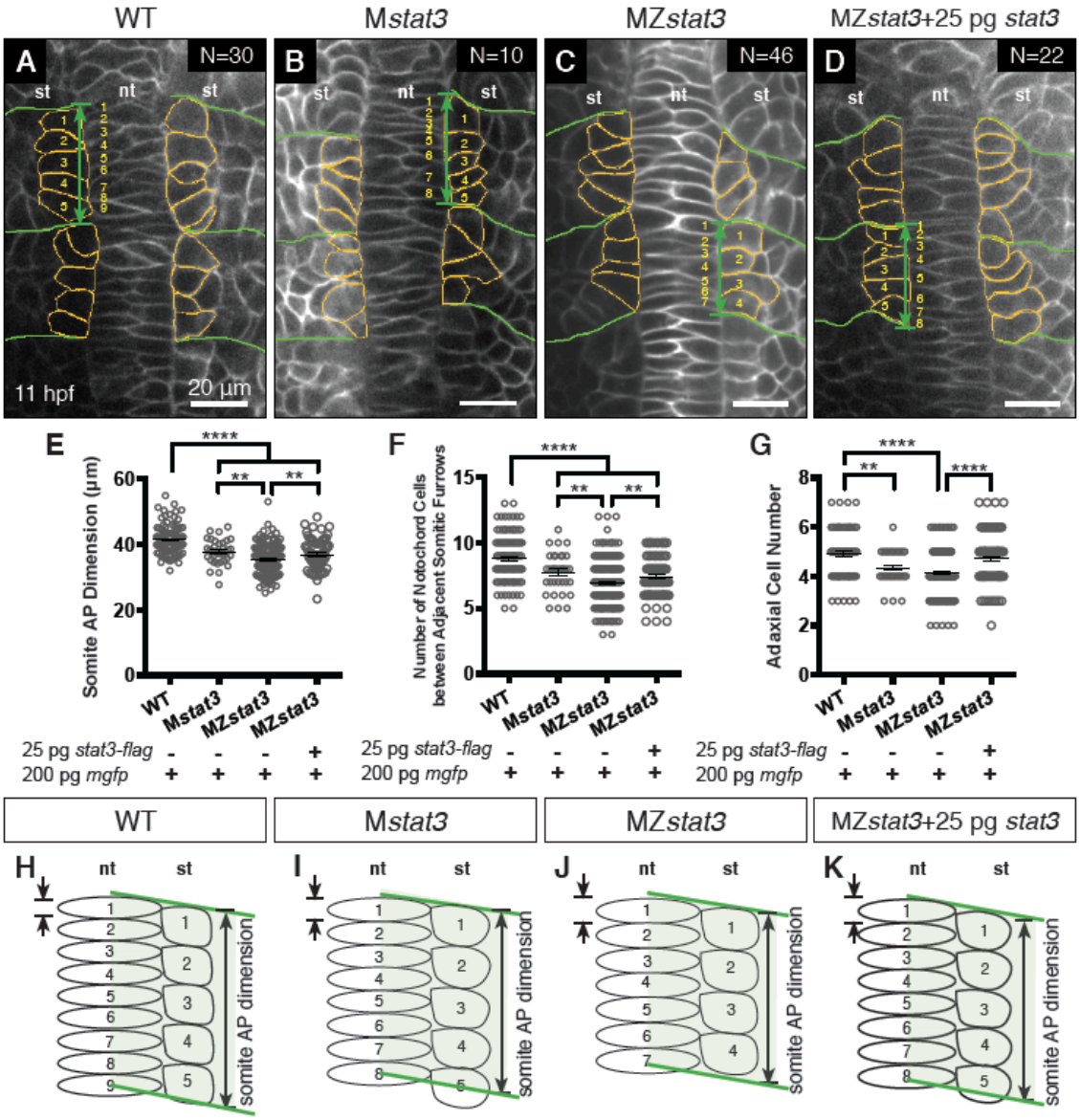

Figure 2.9 Cell number reduction correlates with axis extension defects in *stat3* mutant embryos.

(A-D) Dorsal view showing cells labeled with mGFP in WT (A), M*stat3* (B), MZ*stat3* (C) embryos, and MZ*stat3* embryos overexpressing Stat3-FLAG (D) at 11 hpf (anterior to the top). Somite boundaries are outlined in green. Adaxial cells are outlined in orange. Green arrows show AP dimension of each somite. Adaxial cells and notochord cells aligning along the AP axis are numbered in yellow.

(E-G) Quantification of the average somite AP dimension (E), number of notochord cells (F) and

number of adaxial cells (G) between adjacent somitic furrows.

(H-L) Illustration of AP extension of the notochord and presomitic mesoderm. st, somite; nt, notochord.

**p<0.01, ****p<0.0001, error bars = SEM.

arguing against defective ML intercalation. Rather, we reasoned that a shorter axis in MZ*stat3* gastrulae results from fewer cells aligning anteroposteriorly given the decreased cell number (Figure 2.5E). To test this, we analyzed the dimensions and numbers of cells in the notochord and adjacent first three somites in 3-somite stage embryos (see also Experimental Procedures). Within each somite, right adjacent to the notochord are the adaxial cells that will later give rise to slow muscles (Thisse et al., 1993). We found that somites were 8.9% and 14.7% shorter in AP dimension in M*stat3* and MZ*stat3* mutant embryos compared to WT, respectively (Figure 2.9E). In correlation with AP extension defect, somites exhibited 11.4% (M*stat3*) and 16.1% (MZ*stat3*) fewer adaxial cells compared to WT somites, which contained 4.9 ± 0.1 adaxial cells. Likewise, the adjacent notochord tissue contained 12.2% (M*stat3*) and 21.7% (MZ*stat3*) fewer cells than in WT embryos, in which the corresponding notochord fragment featured 8.8 ± 0.2 cells (Figure 2.9F-G). These results support the model whereby reduction of cell number in MZ*stat3* mutants contributes to morphogenetic defects in extension of axial and presomitic mesoderm (Figure 2.9H-J).

To further test this model, we asked whether chemical inhibition of cell proliferation in WT gastrulae could phenocopy MZ*stat3* axis extension defect. Blockage of mitosis in WT embryos with 150 μM aphidicolin and 20 mM hydroxyurea from early shield stage (5.7 hpf, Figure 2.10A-C) resulted in 22% reduction of total cells by late gastrulation (10 hpf, Figure 2.10E), similar to that in MZ*stat3* mutants. Moreover, compared to DMSO-treated controls, in drug-treated embryos *ntl*-expressing notochord was 10% shorter at 1-somite stage (Figure 2.10M-O). At 3-somite stage, somites were 20% shorter in AP dimension (Figure 2.10R), with 27.5% fewer adaxial cells, and the corresponding notochord fragment contained 34.3% fewer

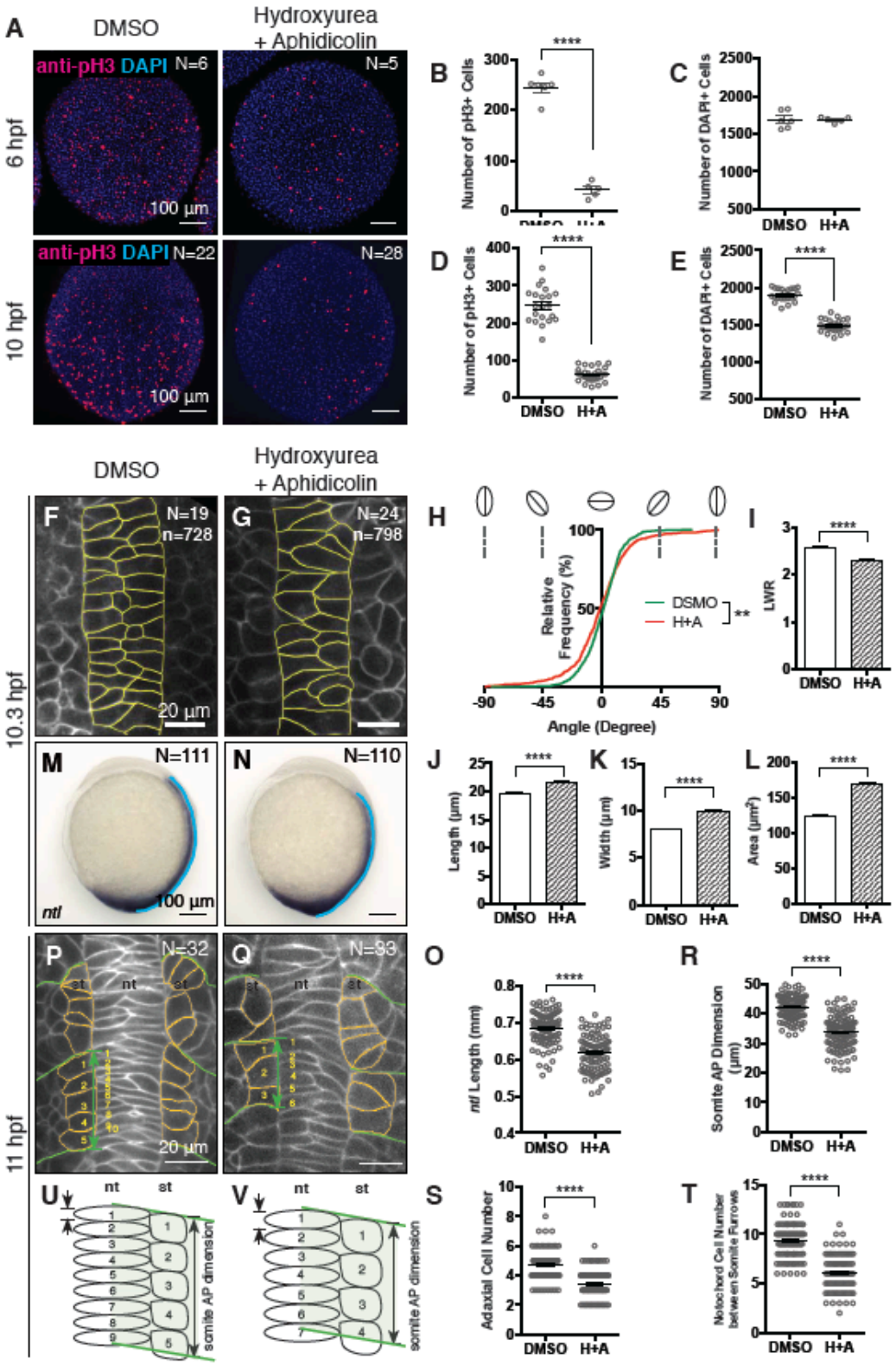

Figure 2.10 Inhibition of cell proliferation using hydroxyurea and aphidicolin leads to axis extension defects in zebrafish gastrulae.

(A) Proliferating cells and total nuclei are labeled with anti-pH3 staining (red) and DAPI labeling (blue) in DMSO-treated control embryos and hydroxyurea+aphidicolin (H+A)-treated embryos at 6 hpf (animal view) and 10 hpf (dorsal view, anterior to the top).

(B-E) Quantification of pH3+ cells (B and D) and DAPI+ cells (C and E) in A.

(F-L) Dorsal view showing cells labeled with mGFP in DMSO-treated (F) and drug-treated (G) embryos at 1-somite stage (anterior to the top). Notochord cells were analyzed for cell orientation (H), cell shape (I), cell size (J), long axis (length, K), and short axis (width, L).

(M and N) *ntl* in chordamesoderm at 1-somite stage (lateral view, anterior to the top).

(O) Quantification of notochord length (blue lines in M and N).

(P and Q) Dorsal view showing cells labeled with mGFP in 3-somite stage embryos with somite AP dimension illustrated with green arrow, somitic boundaries outlined in green, adaxial cells outlined in orange, adaxial cells and notochord cells between adjacent somitic boundaries numbered in yellow (dorsal view, anterior to the top).

(R-T) Quantification of somite AP dimension (R), numbers of adaxial cells (S) and notochord cells (T) in P and Q.

(U and V) Illustration of AP extension of the notochord and presomitic mesoderm. st, somite; nt, notochord.

****$p<0.0001$, error bars = SEM.

cells (Figure 2.10S-V). Together, these results indicate that drug inhibition of cell proliferation recapitulated both proliferation and morphogenetic phenotypes caused by loss of *stat3* function, supporting the model whereby reduced cell number in MZ*stat3* embryos due to proliferation defect could account for impaired extension. Hence, cell proliferation is required for axis extension during zebrafish gastrulation.

We next asked if the altered cell shape observed in MZ*stat3* gastrulae was due to increase cell size. Similarly to MZ*stat3* mutants, drug treatment increases cell size (Figure 2.10F, G, I) with only slight change in their ML alignment (Figure 2.10H). However, the enlarged cells in drug-treated embryos exhibited featured greater both long and short axes, and their cell elongation was only slightly reduced (LWR=2.3) compared to that of DMSO control cells (LWR=2.3 versus 2.6, Figure 2.10I). This contrasted the cell shape defect of MZ*stat3* mutants, where enlarged cells showed diminished long axis and strongly reduced LWR (2.0±0.0, Figure 2.4E-F). These results argue against the cell size increase alone causing the cell shape defect in MZ*stat3* gastrulae.

2.3.6 Stat3 Overexpression Partially Rescues Post-MBT Cell Proliferation Defect in MZ*stat3* mutants

We next asked whether restoring Stat3 expression could rescue proliferation and/or axis extension phenotypes in *stat3*-deficient embryos by injecting synthetic RNA encoding zebrafish Stat3 with FLAG tag at the C-terminus. However, injection of neither 10 pg nor 25 pg *stat3-FLAG* RNA altered the lengths of the pre-MBT cell cycles in MZ*stat3* mutants (Figure 2.5I-L). For post-MBT cell divisions, we mosaically overexpressed Stat3-FLAG in MZ*stat3* embryos labeled ubiquitously with H2B-RFP (Figure 2.7A; see also Experimental Procedures). Notably,

in MZ*stat3* cells overexpressing Stat3-Flag, Cycle 10~13 was shorter compared to uninjected mutant cells, but still longer than WT cycles (Figure 2.7D), indicating a partial rescue of post-MBT cell division defect. Interestingly, we did not observe significant changes of cell cycle length in WT cells overexpressing Stat3-Flag (Figure 2.7D). We also verified in WT and MZ*stat3* embryos that post-MBT cycle lengths were not altered in cells injected with RNA encoding fluorescent proteins (Figure 2.11).

Although we did not observe significant rescue of reduced axis extension via WISH in MZ*stat3* mutants upon injection at 1-cell stage of 25 pg *stat3-FLAG* RNA (Figure 2.3E-F), we did see partial rescue of the somite AP extension and notochord cell number phenotypes at 3-somite stage with the exception of adaxial cell number (Figure 2.9D-G, K). Hence, restoring Stat3 expression in MZ*stat3* could partially rescue phenotypes caused by defects in post-MBT processes such as post-MBT cell divisions; but failed to rescue the deficits caused by pre-MBT defects. These observations confirm the critical function of maternal Stat3, and imply that the role of Stat3 in cell proliferation during zebrafish embryogenesis is transcription-dependent.

2.3.7 Stat3 Regulates Cell Proliferation and Axis Extension by Promoting Cdc25a Expression

We next wished to define the molecular mechanism through which Stat3 regulates cell proliferation. Stat3 is known to regulate transcription of many cell cycle regulators (Carpenter and Lo, 2014). Accordingly, qRT-PCR revealed significant downregulation of *cdc25a* RNA in MZ*stat3* mutants during cleavage and gastrula stages (Figure 2.12A-B). In addition, expression of genes encoding Cyclins such as *ccna2, ccnb1, ccnb2*, etc. was

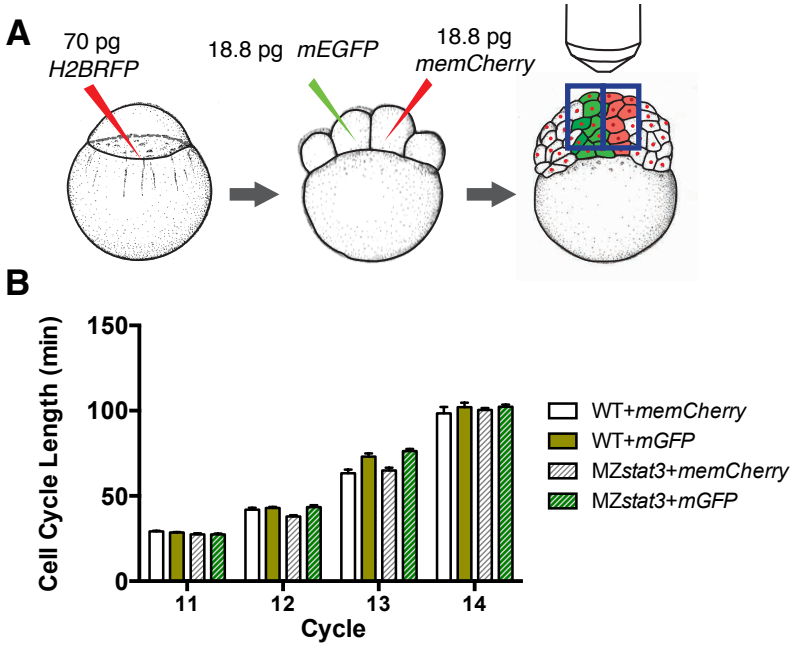

Figure 2.11 Control experiments for post-MBT cell cycle analyses.

(A) Experimental design for control post-MBT cell cycle analyses. Embroys labeled ubiquitously with H2B-RFP were mosaically labeled with *memCherry* or *mGFP* mRNA at 8-cell stage for lineage tracing (See also Figure 2.7 and Experimental Procedures).

(D) Analyses of cell cycle lengths for Cycle 10 - 13 in WT and MZ*stat3* embryos overexpressing mRNA or memCherry.

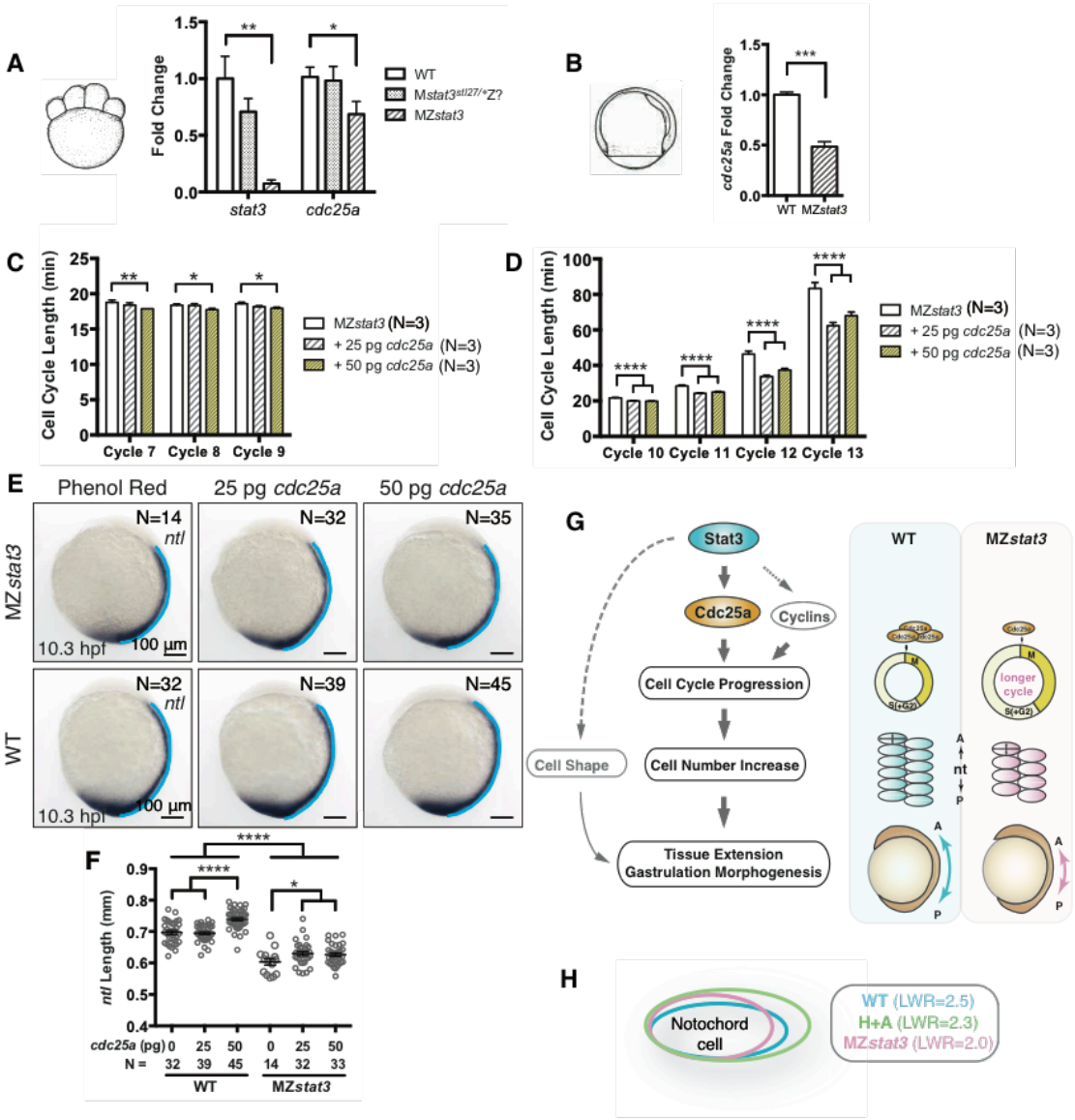

Figure 2.12 Stat3 promotes cell cycle progression during zebrafish embryogenesis via transcriptional activation of Cdc25a.

(A) qRT-PCT detecting *stat3* and *cdc25a* transcript levels at 1.5 hpf. All results shown were normalized to *gapdh*.

(B) qRT-PCR detecting *cdc25a* transcript levels at 8.3 hpf.

(C and D) Pre-MBT (C) and post-MBT (D) cell cycle length analyses in 1-somite stage MZ*stat3* embryos injected with 25 or 50 pg *cdc25a* RNA. Phenol Red was used as injection control.

(E and F) *ntl* in notochord in 1-somite stage MZ*stat3* and WT gastrulae with ectopic Cdc25a (lateral view, anterior to the top). Notochord length (blue) was quantified in F.

(G) Model of Stat3/Cdc25a regulating cell proliferation and morphogenesis during zebrafish embryogenesis. Normally Stat3, both maternal and zygotic, drives Cdc25a expression to promote mitotic entry throughout early development of zebrafish embryos. Loss of *stat3* leads to reduced Cdc25a level, longer cell cycle both pre- and post-MBT, and hence overall reduction of cell number. As a result, fewer cells accumulate in the axial and presomitic mesoderm along the AP axis, causing extension defects during gastrulation.

(H) Illustration of notochord cell shape in WT (blue), MZ*stat3* (pink) and drug-treated (green) 1-somite stage embryos.

*p<0.05, **p<0.01, ***p<0.001, ****p<0.0001, error bars = SEM.

slightly but not statistically significantly reduced (Figure 2.13A).

Cdc25a has a conserved role in promoting mitotic entry in early animal development (Dalle Nogare et al., 2009; Edgar and Datar, 1996; Kim et al., 1999). We asked if restoring *cdc25a* expression could suppress cell cycle and axis extension defects in MZ*stat3* mutants. We observed shortening of pre-MBT cycles (Cycle 7~9) in mutant embryos injected with 50 pg *cdc25a*, with cells dividing every 17.7~17.9 min compared to 18.4~18.8 min in control MZ*stat3* embryos (Figure 2.12C), but not to the WT values. Further, injection of either 25 pg or 50 pg *cdc25a* RNA fully suppressed post-MBT cell cycle phenotype (Figure 2.12D) partially suppressed notochord extension defect in MZ*stat3* gastrulae, and notably also resulted in excess notochord extension in WT gastrulae (Figure 2.12E-F). Based on these results we propose that Stat3 regulates cell proliferation in zebrafish embryogenesis in part by regulating c*dc25a* expression, and that Stat3/Cdc25a-dependent cell proliferation promotes axis extension during gastrulation.

2.4 Discussion

Previously Stat3 was reported to control convergence and extension movements during zebrafish gastrulation partly through promoting Wnt/PCP signaling (Miyagi et al., 2004; Yamashita et al., 2002). Our analyses of the newly generated zebrafish *stat3* null mutants do not support a requirement of Stat3 in convergence movements or in Wnt/PCP signaling. Instead, we propose an alternative model in which maternal and zygotic Stat3 function promotes axis extension by regulating Cdc25a-dependent cell proliferation (Figure 2.12G). Further, the scoliosis phenotype

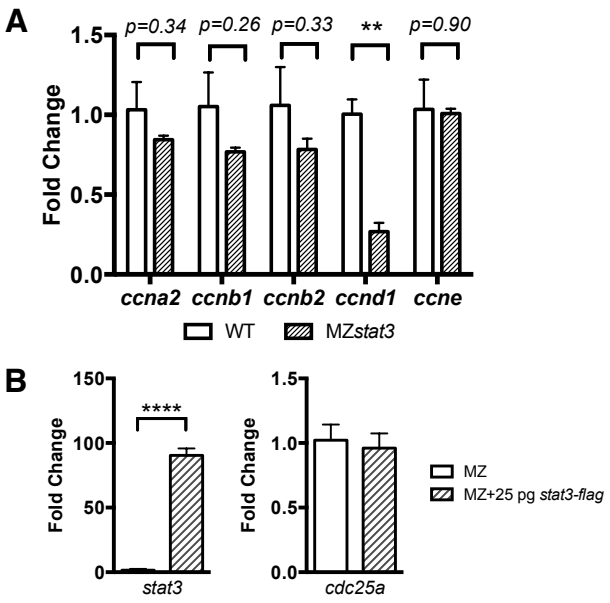

Figure 2.13 Stat3 may regulate cell proliferation via transcriptional activation of other cell cycle regulators.

(A) Maternal expression levels of cell cycle genes encoding zebrafish Cyclin a2, b1, b2, d1 and e in 16-cell stage WT and MZ*stat3* embryos detected by qRT-PCR.

(B) *cdc25a* transcript level in mid-gastrula stage (8.3 hpf) MZ*stat3* and MZ*stat3* embryos injected with 25 pg of *stat3-FLAG* RNA.

**p<0.01, ****p<0.0001, error bars = SEM.

of juvenile zebrafish *stat3* mutants affords a new model of STAT3-associated scoliosis in humans.

2.4.1 The Zebrafish *stat3* Mutant

We generated frame-shift mutations in the zebrafish *stat3* gene with the resulting alleles predicted to encode truncated proteins lacking all functional domains. Our *stat3*^{stl27} allele is likely a strong/null mutation as evidenced by significant reduction of *stat3* transcripts and undetectable level of Stat3 protein in the mutants (Figure 2.1E-F). In contrast to previous findings (Oates et al., 1999), we show that *stat3* is heavily expressed maternally, however, both zygotic and MZ *stat3* mutants complete embryogenesis (Figure 2.1C, G), indicating that *stat3* is not essential for embryonic development in zebrafish.

Contrasting the *stat3* morpholino studies (Yamashita et al., 2002), MZ*stat3* gastrulae exhibited normal convergence and only mild axis extension defects due to reduced cell proliferation. That both cell proliferation and axis extension defects could be partially rescued by Stat3 overexpression provides further support that the phenotypes caused by *stl27* and *stl28* alleles are specific to loss of *stat3* function (Figures 2.5, 2.7). This discrepancy between the *stat3* morphant and mutant phenotypes is consistent with the reports of poor correlation between morpholino-induced and mutant phenotypes in zebrafish and further questions the reliability of morpholinos as a loss-of-function tool (Kok et al., 2015). We consider our zebrafish *stat3* mutant a reliable tool to verify other functions of Stat3, such as in hair cell and retina regeneration (Nelson et al., 2012).

2.4.2 Stat3/Cdc25a Regulates Cell Proliferation in Development

We have established a requirement of Stat3, particularly maternal Stat3, in both pre- and post-MBT cell proliferation during zebrafish embryogenesis (Figures 2.5, 2.7). Moreover, *stat3*

mutants exhibited severe growth defects from late larval stage (Figure 2.1), suggesting a continuous requirement of Stat3 for cell proliferation throughout zebrafish development.

Cell cycle control is a conserved role of Stat3 in cancer and animal development (Carpenter and Lo, 2014). We propose that Stat3 promotes cell divisions during zebrafish embryogenesis mainly through transcriptional activation of Cdc25a, as in MZ*stat3* embryos *cdc25a* transcripts were significantly downregulated, and that ectopic *cdc25a* RNA suppressed both pre-MBT and post-MBT cell cycle phenotypes (Figure 2.12) while Stat3 overexpression from 1-cell stage could rescue only post-MBT but not pre-MBT cell cycle progression defect in MZ*stat3* embryos (Figures 2.5, 2.7). A key regulator of G1-S and G2-M transitions, Cdc25a is overexpressed in human cancers driving abnormal cell proliferation downstream of multiple signaling pathways including Stat3 (Boutros et al., 2007). In HepG2 carcinoma cells, for example, Stat3 binds directly to *CDC25a* promoter and activates its expression (Barre et al., 2005). Cdc25a is also a conserved regulator of cell divisions during embryogenesis from Drosophila to *Xenopus*, where pre-MBT mitotic entry is propelled by Cdc25a synthesized from maternal RNAs through activation of Cyclin B/Cdk1 complexes (Bouldin and Kimelman, 2014; Edgar and Datar, 1996; Kim et al., 1999; Tsai et al., 2014). Cdc25a activity is continuously required after MBT, as cells are arrested in G2 in the Drosophila *cdc25*/*string* mutant (Edgar and O'Farrell, 1990) and zebrafish *cdc25a*/*standstill* mutant (Verduzco et al., 2012). Whereas it was unclear how Cdc25a is activated in these early embryos, our studies point to Stat3 as a regulator of Cdc25a during zebrafish development, paralleling this role in cancer (Barre et al., 2005). Furthermore, Stat3/Cdc25a pathway may be conserved in mammalian embryogenesis. First, *Stat3* and *Cdc25a* knockout mouse embryos both die by early gastrulation; when cultured, both *Stat3-/-* and *Cdc25a-/-* mouse blastocysts showed growth defects (Lee et al., 2009; Takeda et al.,

1997). Second, *STAT3* mutant homozygotes have never been reported in human, while spontaneous dominant-negative *STAT3* mutations were linked to autosomal dominant HIES (Holland et al., 2007), a strong indication that *STAT3* inactivation may cause embryonic lethality. Hence, the Stat3/Cdc25a pathway may serve as a universal mechanism regulating cell proliferation during animal development.

However, our observations imply other players downstream of Stat3 are involved. First, we detected slight although not statistically significant downregulation of other cell cycle-regulating genes in MZ*stat3* embryos, including *ccnd1* encoding Cyclin D1 and *cdc25d* encoding a Cdc25 homolog (Figure 2.13A). Second, Stat3 overexpression failed to rescue *cdc25a* transcript level in whole MZ*stat3* gastrulae (Figure 2.13B). Given the tissue-specific requirement of Stat3 we observed (Figure 2.9), Stat3-dependent *cdc25a* activation may only occur within certain tissues. Besides, different Stat3 overexpression levels result in opposite effects on cell proliferation depending on the balance between positive and negative downstream regulators (Nichane et al., 2010). It is possible that the dose we used in our study (25 pg *stat3* RNA) induced positive and/or negative feedback loops in various tissues.

2.4.3 Cell Proliferation Promotes Axis Extension

Cell proliferation has been generally considered dispensable or even prohibitive for gastrulation movements and morphogenesis. For example, cell shape changes and ventral furrow formation in *Drosophila* require the inhibition of ventral cell proliferation through String/Cdc25 inhibitors Tribbles and Fruhstart (Grosshans and Wieschaus, 2000). In *Xenopus*, increased cell proliferation induced by inhibition of *wee2*, a Cdk inhibitor, impaired C&E in the paraxial mesoderm (Leise and Mueller, 2004). Conversely, zebrafish gastrulae still achieved relatively normal AP axis

extension when mitosis was chemically inhibited (Quesada-Hernandez et al., 2010). Indeed, a mathematical modeling of zebrafish gastrulation indicated that directed cell migration and polarized cell intercalation, the motile cell behaviors mediated by Wnt/PCP pathway, are sufficient to account for the morphogenesis of paraxial mesoderm, although a minor role of cell proliferation could not be excluded (Yin et al., 2008).

We present evidence in support of a small but significant contribution of cell proliferation to zebrafish gastrulation by showing that cell proliferation promotes AP extension of both the axial and paraxial mesoderm. The most compelling evidence comes from our pharmacological experiments where we inhibited mitosis in WT zebrafish embryos during gastrulation with hydroxyurea and aphidicolin (Quesada-Hernandez et al., 2010). Drug treatment during gastrulation recapitulated both proliferation and morphogenetic defects seen in MZ*stat3* gastrulae, as manifested by a shorter AP axis, as well as reduced AP dimensions of both axial and paraxial mesoderm cells, albeit larger in size, along the AP axis in these tissues (Figure 2.10). Moreover, cell intercalation seemed normal in MZ*stat3* embryos as evidenced by normal convergence (Figures 2, 2.4A, 2.9C). Therefore, we conclude that Stat3-mediated cell proliferation promotes extension morphogenesis during zebrafish gastrulation, most likely by providing sufficient building blocks necessary for intercalation-based extension.

Consistent with this model, loss of *cdc25a* function in the zebrafish *standstill* mutant led to bent and shorter body at 1 dpf (Verduzco et al., 2012); Ectopic *cdc25a* expression partially suppressed the extension phenotype in MZ*stat3* mutants (Figure 2.12). We also noticed while overexpression of Stat3 in MZ*stat3* could only rescue somite AP dimension and notochord cell number defects to M*stat3* level, reduction in adaxial cell number was fully rescued to WT level (Figure 2.9), suggesting a tissue-specific requirement of Stat3-dependent cell proliferation.

2.4.4 Stat3 Is Not Required for Planar Cell Polarity during Gastrulation

We gathered several lines of evidence arguing against Stat3 regulating C&E by promoting Wnt/PCP signaling and ML cell elongation (Miyagi et al., 2004). First, MZ*stat3* notochord cells, although rounder, exhibited normal ML orientation (Figure 2.4C). Second, MZ*stat3* mutants exhibit normal convergence of several tissues (Figure 2.3). Third, we failed to detect any genetic interactions between zygotic *stat3* inactivation with mutations disrupting Wnt/PCP pathway components (Figure 2.4H-J) with a caveat that maternal *stat3* function was not removed in these experiments.

However, our morphometric analyses implicate Stat3 in regulation of cell shape as MZ*stat3* axial mesodermal cells are rounder compared to WT with a bigger AP and a shorter ML dimension (Figure 2.4E-F, Figure 2.12H). One possibility is that the slightly reduced LWR is due to increased cell size. However, our observations support an alternative model where Stat3 plays a more direct role in cell shape regulation, as the enlarged cells resulting from the chemical inhibition of cell division increased in both dimensions compared to WT cells (Figure 2.10J-K). Indeed, in mouse keratinocytes and fibroblasts cytoplasmic Stat3 regulates microtubule and actin cytoskeleton through its interaction with Stathmin, a microtubule-destabilizing protein, and small Rho-GTPases, respectively (Ng et al., 2006; Teng et al., 2009). It will be interesting to investigate whether Stat3 utilizes similar mechanisms to shape gastrulating zebrafish cells.

2.4.5 Stat3 Loss-of-Function as a Model of Adolescent Idiopathic Scoliosis

We describe the first vertebrate *stat3* mutant that could survive beyond embryonic stages, opening new avenues for functional studies of Stat3 in later developmental processes and disease. Before they die as juveniles, *stat3* mutant fish exhibited late-onset idiopathic scoliosis

and excessive inflammation (Figure 2.1I-J). As a key regulator of immune responses, abnormal Stat3 activity has been associated with immunodeficiency such as HIES in human (Holland et al., 2007) and Crohn's disease-like conditions in mouse *Stat3* CKO (Welte et al., 2003). With a global disruption of Stat3, our *stat3* mutant zebrafish provides a new tool for studies of idiopathic scoliosis, HIES, and Crohn's disease.

In summary, we generated and characterized a valuable vertebrate *stat3* genetic model for further studies of development and disease. Our work provides direct evidence that cell proliferation promotes zebrafish axis extension, and clarifies the role of Stat3 in zebrafish gastrulation as proliferation regulator through Cdc25a activation. Further studies will verify whether cell cycle regulation function of Stat3 is conserved in larval and juvenile stages, and address the mechanisms underlying idiopathic scoliosis and other phenotypes associated with *stat3* zebrafish mutant.

2.5 Experimental Procedures

Zebrafish Stains and Staging

AB* or AB*/Tubingen WT, tri^{vu67} and slb^{tz216} mutant zebrafish (*Danio rerio*) lines were used. Embryos were collected from natural matings, maintained in 28.5°C, and staged according to Kimmel et al. (Kimmel et al., 1995).

Generation of *stat3* Mutant Line

A TALEN pair was designed to target the boundary of Intron 4 and Exon 5 of the zebrafish *stat3* gene. The targeting sequences for the TALEN arms are 5'- TAACCTCTTACTCATCCTCCA -3' and 5'-AAGAGGTTGTAGAAGTAGA-3', respectively. An NlaIII restriction site within the

15-base pair long spacer between the two TALEN arms was used for identifying disruption of this sequence in genomic DNA (Figure 1A). TALEN constructs were assembled using the Golden Gate method (Cermak et al., 2011) and used to generate indels in *stat3* target sequences as described (Shin et al., 2014). Two alleles, *stl27* and *stl28*, containing a 7-base pair and a 2-base pair deletion in Exon 5, respectively, were confirmed by sequencing and identified using PCR-based genotyping (forward primer 5'-AGCTATTGCTTGGGTATAACCTCTTACTC-3', reverse primer 5'-GCAGTCATACCTCCAGCACTC-3', followed by NlaIII digestion). *Stl27* allele can also be genotyped using allele-specific PCR amplification (common forward primer 5'-CCACCTGTGACCATATGACTGAA-3', WT allele primer 5'-CTCCAACATCTTCATCTTCTGCTCCA-3', *stl27* allele primer 5'-CTCCAACATCTTCATCTTCTGTCCTG-3'). *stl27* and *stl28* alleles are predicted to encode truncated proteins of 158 and 168 amino acids, respectively.

Plasmid Construction, RNA Synthesis and Injection

Full-length coding sequence of zebrafish *stat3* was subcloned from the previously published *stat3* construct (Oates et al., 1999) and FLAG-tagged at the C-terminus (Forward primer (CACC-*stat3*) 5'-CACCATGGCCCAGTGGAATCAGTTGCAG-3', reverse primer (*stat3*FLAGXho)5'-ctcgagTCActtatcgtcgtcatccttgtaatcAGCATTTCGGCAGGTGTCCATATCC-3'). Full length coding sequence of zebrafish *cdc25a* was subcloned from *cdc25* Tol2 construct (Bouldin et al., 2014) into pCS2 plasmid. Capped RNAs were synthesized using mMessage mMachine kit (Ambion), and injected at 1- or 8-cell stage with doses specified in Results.

Whole-Mount *in situ* Hybridization and Immunostaining

Embryos were fixed in 4% paraformaldehyde (PFA). *In situ* hybridization was carried out as described (Thisse and Thisse, 2008). Morphometric measurements were carried manually with Fiji software.

Immunostaining was carried out using a standard protocol. Antibodies used are: anti-phospho-Histone H3 antibody (1:3,000, rabbit, Upstate, 06-570), and Alexa Fluor 488 or 568 goat anti-rabbit (1:500, Invitrogen). Embryos were counterstained with DAPI (0.1 μg/mL, Invitrogen), mounted in 0.75% low melting temperature (LMT) agarose (Lonza), and imaged with the Quorum spinning disk confocal microscope (SDCM) using a 10x objective lens (10x). A z-stack of over 200 μm was acquired at a step size of 3 μm and projected in Fiji. The number of nuclei was quantified using Analyze Particles plugin in Fiji.

Western Blotting

Five to six embryos (6 hpf) were deyolked and homogenized in a modified RIPA buffer (Fang et al., 2013). Proteins were resolved in 4-12% NuPage Bis-Tris gels (Invitrogen) and transferred to PVDF membrane blocked with 10% milk in PBST. Primary antibodies used were: anti-Stat3 (1:250, AnaSpec, 55861), anti-FLAG (1:1,000, Sigma-Aldrich, F1804), and anti-β-actin (1:1,000, Sigma-Aldrich, A5441). Secondary antibodies used were: donkey anti-mouse HRP (1:5,000, Fisher Scientific, SA1100) and goat anti-rabbit HRP (1:5,000, Fisher Scientific, PR-W4011). Signals were detected with an ECL kit (Perkin Elmer) and imaged using film.

Quantitative Real-Time (qRT) PCR

Total RNA was isolated from 30-50 embryos with Trizol (Ambion) and treated with DNase (Zymo Research). For larvae and juveniles, whole animals were subjected to snap freezing in liquid nitrogen and homogenized using a mortar and pestle. cDNA was synthesized using iScript

kit (Bio-Rad). qRT-PCR was performed using CFX Connect Real-Time system and SYBR green (Bio-Rad), with at least three independent biological samples for each experiment. Primers are listed in the Table 2.1.

Pharmacological Treatment

WT embryos were dechorionated in 0.3x Danieau solution and incubated with 20 mM hydroxyurea (Sigma-Aldrich) and 150 μM aphidicolin (Sigma-Aldrich) in 4% dimethyl sulfoxide (DMSO, Sigma-Aldrich) from 5.7 hpf until desired stages (Zhang et al., 2008). Incubation in 4% DMSO was used as control.

Morphometric Analyses of Live Embryos

Embryos were injected with 200 pg *membraneEGFP* (*mEGFP*) RNA at 1-cell stage, mounted in 0.5% LMT agarose at desired stages and imaged on Quorum SDCM (40x). For cell body alignment and shape, image stacks were acquired and the top layer of the notochord cells were analyzed in Fiji (Jessen et al., 2002). To measure the AP dimension of the somite, five lines were drawn randomly in Fiji between two adjacent somitic furrows parallel to the notochord.

Cell Cycle Imaging and Analyses

For pre-MBT cell divisions, zygotes were injected within 20 minutes post-fertilization (mpf) with 70 pg *H2B-RFP* RNA and mounted in 0.3% LMT agarose at 4-8 cell stage. Time-lapse movies were taken at 28.5°C with Quorum SDCM using a 10x objective lens. A z stack covering 200 μm at a 3-4 μm step distance was acquired every 1-2 min for at least 4 hours. Cell divisions were manually tracked in Fiji by quantifying the length from telophase to telophase. As H2B-RFP signal became clearly visible from 8-16 cell stage, Cycles 5 (16 cells to 32 cells) to 9 (256 cells to 512 cells).

Post-MBT cell division experimental design was adapted with modifications from Dalle Nogare et al. (Dalle Nogare et al., 2009). Embryos were ubiquitously labeled with H2B-RFP. To minimize inter-individual and experimental variability, we performed mosaic labeling, which allowed us to compare experiment and control lineages within the same embryo. At 8-cell stage, one blastomere was injected with 18.8 pg (a dose equivalent to 150 pg at 1-cell stage) *membraneCherry* (*mCherry*) as control. An adjacent blastomere was injected with 18.8 pg *mEGFP* with or without 3.1 pg (a dose equivalent to 25 pg at 1-cell stage) *stat3-FLAG* or *cdc25a* RNA. Time-lapse movies were recorded separately for mEGFP- (Figure 2.7B) or mCherry- (Figure 2.7C) clones of each embryo with Quorum SDCM and a 40x objective at 2-minute interval for the duration of 5-6 post-MBT cycles. At each time point, a z stack spanning 100 μm was acquired at a step size of 4 μm. Movies were converted to hyperstacks in Fiji. Cell divisions were manually tracked using MtrackJ plugin in Fiji.

Bone Analyses

Juvenile fish were fixed in 4% PFA, bleached in 3% hydrogen peroxide/1% KOH, and stained with 1 mg/mL Alizarin Red in 1% KOH overnight for whole-mount bone staining. Soft tissues were cleared with 1% trypsin in 2% borax for up to a week. Larval vertebrae were stained with Alizarin Red (1 mg/mL) for 2 hours before imaging live on Quorum SDCM. Microcomputed tomography (Scanco uCT40) was used for 3D reconstruction and analyses of bone parameters (threshold set as ~150) of the juvenile vertebrae.

Statistical Analyses

WISH and immunostaining quantification, and morphometric analysis were performed blindly. Data were collected in Excel (Microsoft), analyzed and graphed with GraphPad Prism

(GraphPad Software). Student's *t* test was applied to determine statistical significance ($p<0.05$) between two datasets. Kolmogorov-Smirnov test was used to compare angle distributions. All results are shown as Mean±SEM.

Acknowledgements

We thank David Kimelman for *cdc25* Tol2 plasmid; Drs. John Rawls, Margot Williams, Ryan Gray for comments on the manuscript; and the LSK lab for advice. This project was supported by NIH grant RO1 GM55101.

Table 2.1 Nucleotide sequences of RT primers

Primer	Forward Sequence (5'-3')	Reverse Sequence (5'-3')
stat3_RT[1]	ACAGCAGGATGGCCAGGTTGC	TCTGTCTGGTGGCTGCTGCCT
stat3_RT1[1]	CCCATGGAGCTCCGACAGTT	ACGATGCGGGCAATCTCCAT
stat3_RT2[1]	TTTGGCAAATACTGCCGCCC	ATGAGAGAGTCGAGCGTGCG
sta3_RT3[1]	CTGTGTCACCCCGTGTCCTT	GCCTCAGCAGCTTCGTTGTG
il6	ACGCGAATCTACAGCGTCCT	CACCTGCAGCTGGCTGTTTA
tnfα	ACCAGGCCTTTTCTTCAGGT	GCATGGCTCATAAGCACTTGTT
bcl2a	GAACTGGGGGCGGATCATTG	CCACGAAGGCATCCCAACC
birc5a	TGCACTCCAGAAAACATGGCT	ATCACAGCTGGGAGAATGCG
cdc25a (pair1)[2]	TCGCTCTCCTGCCTTCAAGA	GACAGCGAATGACAGGCGAA
cdc25a (pair2)[2]	TCCCTCCCGTTATGGAGTGT	GGGTGGTGGGGAGAGCATTA
cdc25d	AGCGAGCCATTAAGCGACTG	CATTGGATCCACCGCCTCTG
ccna2	GAGGCGCTAAACAGGGGTCT	AGGTGCTTTCTTGGAGCACG
ccnb1	GCAGCGAGAATCAGAACGCT	GGTGCAACCTTCACCTCCTTC
ccnb2	CATGGAAATGCACGCTCTGC	ACAACCTTCTTTGTCTGAACTGGT
ccnd1	TGGGATCTGGCCTCAGTGAC	TGAAGTTGACGTCTGTCGCAC
ccne	TCAGGGCTGAAGTGGTGTGA	GGAGTGAACCTTTCCCAGCC

[1] Four pairs of primers were used to detect *stat3* transcript. *Stat3_RT* span the deletion site in both *stl27* and *stl28* alleles; *stat3-RT1* amplifies a coding region upstream of deletion site in all three splicing variants; *stat3_RT3* only amplifies a coding region downstream of deletion site in the full length splicing variant; and *stat3-RT2* spans an alternative splicing site downstream of deletion site, and detects two longer splicing variants.

[2] Two pairs of primers were used to detect *cdc25a* transcript in zebrafish embryos.

Chapter 3

Fam132a/C1qdc2 Inhibits Cell Contact and Tissue Cohesion Underlying the Collective Mesoderm Migration during Gastrulation

3.1 Summary

Vertebrate gastrulation is a fundamental morphogenetic process during which germ layers are formed, patterned and shaped into a body plan with organ rudiments. Gastrulation is driven by a set of conserved cellular behaviors including individual and collective cell migration and cell intercalation. The Wnt/Planar Cell Polarity (Wnt/PCP) pathway mediates planar cell polarity that underlies several polarized gastrulation cell behaviors. *stat3*–deficient zebrafish mutants complete gastrulation or embryogenesis despite mild proliferation and axis extension defects. However, *stat3* morpholino induced severe defects in both convergence and extension (C&E) gastrulation movements, likely due to downregulation of genes essential for this process.

Therefore in this study we used *stat3* morpholino as a tool to uncover novel regulators of C&E by gene expression profiling. We identified six candidate genes downregulated in *stat3* zebrafish morphant gastrulae, including *fam132a*, which encodes a conserved secreted peptide. Ectopic Fam132a independently led to dorsoventral patterning defect and severe C&E defects in the axial mesoderm. In particular, Fam132a overexpression impaired mediolateral planar intercalation of the notochord progenitor cells and collective anterior migration of the prechordal plate progenitor (PPP) cells likely independent of Wnt/PCP signaling. Moreover, excess Fam132a disrupted cell contact maintenance and tissue cohesiveness, impairing persistence and coherence of PPP collective cell migration. Whereas genetic disruption of the *fam132a* gene did not impair gastrulation of wild-type embryos, it partially suppressed defects in cell contact, tissue cohesion and coherent migration of PPP cells in *silberblick* (*slb*)/*wnt11* mutant gastrulae, suggesting that Fam132a regulates collective migration during gastrulation by suppressing cell contact and tissue cohesion. We further demonstrate that the requirement for Fam132a varies in different tissues. Together, our studies identified Fam132a as a secreted regulator of C&E movements, which modulates collective migration and morphogenesis via cell contact inhibition.

3.2 Introduction

Gastrulation is a fundamental process during early metazoan development, during which an orchestrated sequence of inductive and morphogenetic processes establish a nascent body plan (Solnica-Krezel and Sepich, 2012; Tam and Loebel, 2007). Convergence and extension (C&E) are evolutionarily conserved gastrulation movements that narrow the embryonic tissues along the mediolateral (ML) axis and elongate it along the anteroposterior (AP) axis (Keller, 2002). At the onset of zebrafish gastrulation, the embryonic shield, the equivalent of the amphibian Spemann-

Mangold gastrula organizer, forms on the dorsal side (refs). Specified at the high and medium levels of the Nodal morphogen gradient, respectively, the anterior and posterior regions of the shield give rise to prechordal plate (anterior axial mesoderm) and chordamesoderm (posterior axial mesoderm that will differentiate into notochord) (Schier, 2001; Ulrich et al., 2003). C&E of the zebrafish axial mesoderm are achieved by two cellular behaviors: cell intercalation and cell migration (Tada and Heisenberg, 2012). ML planar intercalation is employed largely by the chordamesodermal cells, which adopt an elongated shape and align their long axis mediolaterally. Prechordal plate precursors, on the other hand, undergo collective migration anteriorly, thus contributing to anteroposterior (AP) extension of the entire axial mesoderm (Gray et al., 2011; Tada and Heisenberg, 2012). Conserved from *Drosophila* to vertebrates, Wnt/Planar Cell Polarity (Wnt/PCP) signaling is a key regulator of cell polarity within the plane of tissue (Axelrod and McNeill, 2002; Gray et al., 2011; Strutt and Strutt, 2009). During vertebrate gastrulation, Wnt/PCP is essential for C&E, with mutations in its component genes resulting in AP shorter and ML wider embryonic tissues and more posteriorly-positioned prechordal plate (Gray et al., 2011). Similar severe morphogenetic phenotypes were also reported for antisense morpholino-mediated loss of *stat3* function in zebrafish (Yamashita et al., 2002). However, my studies of *stat3* null mutants described in Chapter 2 of this thesis provided evidence arguing against such severe C&E defects being Stat3-dependent, raising a question of what genes are actually responsible for *stat3* morpholino-induced C&E phenotypes. In this chapter I describe my experiments addressing this question.

Collective cell migration of a cohesive cell group is widely adopted during development as an efficient way to achieve tissue morphogenesis. During gastrulation, collective migration involves either actin-driven epithelial sheet migration characterized by stable cell contacts, such

as *Drosophila* dorsal closure (Kiehart et al., 2000), or migration of mesenchymal-like cell groups that make dynamic cell contacts, such as prechordal plate migration and dorsal convergence of the lateral mesoderm in zebrafish (Montero et al., 2005; Sepich et al., 2000; Warga and Kimmel, 1990; Weijer, 2009). In addition to gastrulation, cells also migrate in groups during various development processes including migration of *Drosophila* border cells, lateral line primordia in zebrafish, neural crest migration in vertebrates, tracheal branching in *Drosophila*, and wound healing (Friedl and Gilmour, 2009; Weijer, 2009). This mode of cell migration is also prevalent during metastasis of many invasive tumors such as squamous carcinoma and breast cancer (Friedl and Gilmour, 2009). In this study we use zebrafish prechordal plate progenitor (PPP) migration as a model to further explore the mechanisms underlying collective migration. During gastrulation, these mesodermal cells migrate as a cohesive group with highly aligned trajectories and similar movement behaviors, and rarely exchange neighbors regardless of their positions in the group (Dumortier et al., 2012). During *Xenopus* gastrulation, PPP cells migrate anteriorly across the blastocoel roof (BCR) in response to an endogenous Platelet-derived growth factor (PDGF) gradient formed by the overlying ectoderm with extensive protrusive activity at their leading edges (Weijer, 2009). In fish, although PPP cells are able to respond *in vitro* to a PDGF source in a phosphoinositide 3-kinase (PI3K)-dependent manner to extend cell protrusions and gain motility (Montero et al., 2003), directional cues are proposed to be generated from within the cohesive group and transmitted through cell-cell contacts, as single cells migrated in random directions (Dumortier et al., 2012). Indeed, recent evidence suggests that tissue cohesion, mainly achieved through cell-cell adhesion, provides the foundation for directionality in collective migration in part through enabling mechanosensitive polarization. In *Xenopus* PPP cells, cadherin adhesion-generated tension is sensed and transduced through a ϒ catenin/plakoglobin-

keratin intermediate filament network. Attachment of PPP cells at the rear to the chordamesoderm tissue is proposed to provide the unidirectional asymmetry of intercellular tension, and as a result all cellular protrusions are polarized toward anterior (Behrndt and Heisenberg, 2012; Weber et al., 2012)

Cell-cell adhesion is a major contributor to tissue integrity and its dynamic regulation underlies different modes of cell movements, including directed cell migration, radial and planar intercalations and collective migration. Cell adhesion within the zebrafish presumptive prechordal plate domain is mainly mediated by E-cadherin/Cadherin 1 (Chd1) (Montero et al., 2005). *chd1*-deficient PPP cells, when transplanted to a wild-type (WT) gastrula, lagged behind WT PPP cells during their anterior migration, indicating a requirement of E-cadherin-mediated cell-cell adhesion in collective migration (Montero et al., 2005; Shimizu et al., 2005b). On one hand, different adhesion levels are required for tissue separation, known as the "Differential Adhesion Theory" (Steinberg, 2007), as ectopic E-cadherin induced by reduced expression of zebrafish *snail1b,* encoding a transcriptional repressor of the *cdh1* gene, led to mixing of prechordal and chordamesoderm cells (Blanco et al., 2007). On the other hand, cell-cell adhesion needs to be tightly controlled as too much or too little adhesion both interfere with cell migration (Blaser et al., 2005; Speirs et al., 2010). Multiple mechanisms, both transcriptional and post-transcriptional, have been implicated in regulation of E-cadherin expression, membrane localization and adhesive activity. In zebrafish, for example, interference with expression or stability of Snail1a and Snail1b (Batlle et al., 2000), altered levels of E-cadherin/Cdh1 transcript and protein and led to defective anterior migration of PPP cells (Blanco et al., 2007; Speirs et al., 2010; Yamashita et al., 2004). Similar mechanism was also proposed for impaired migration of PPP cells in *stat3* morphants (i.e. *stat3* morpholino-injected embryos). Liv1/Slc39a6, a zinc

transporter, was proposed to regulate nuclear translocation of Snail downstream of Stat3, as downregulation of Liv1 expression in *stat3* morphants led to more packed PPP cells and their defective anterior migration, phenocopying defects observed in *snail1a* morphants (Yamashita et al., 2004). In addition, emerging evidence suggests that besides its expression level, dynamic E-cadherin membrane localization is essential during collective migration to allow rapid assembly and disassembly of cell junctions (Hammerschmidt and Wedlich, 2008). Wnt11 was reported to regulate E-cadherin endocytosis via Rab5c in zebrafish PPP cells; in both *silberblick* (*slb*)/*wnt11* mutant and *rab5c* morphant gastrulae PPP cells appeared less cohesive and failed to migrate anteriorly despite increased E-cadherin accumulation on their membranes (Ulrich et al., 2005). Similarly, normal epiboly movements in zebrafish require Pou5f1-dependent Epidermal growth factor (EGF) expression, which in turn regulates E-cadherin endocytosis and cell adhesion (Song et al., 2013). Via a yet different mechanism, Gα12/13 heterotrimeric G proteins were also shown to inhibit E-cadherin activity during epiboly without affecting its expression level or intracellular distribution (Lin et al., 2009). However, many more cell cohesion mechanisms underlying collective migration of the zebrafish prechordal plate are likely yet to be uncovered, given the variety of cell adhesion molecules identified in other developmental and pathological processes (Hammerschmidt and Wedlich, 2008).

Other than cell-cell adhesion, cell adhesion to extracellular matrix (ECM) also affects tissue cohesion and migration, and plays important roles during morphogenesis. ECM is a collection of a variety of extracellular molecules including glycosaminoglycans, proteoglycans, collagens and non-collagenous glycoproteins that are synthesized and secreted by surrounding cells (Rozario and DeSimone, 2010). ECM plays critical roles in morphogenesis by providing structural support, serving as a repository for growth factors, and by generating forces and

mechanical signals through cell-matrix interaction (Rozario and DeSimone, 2010). Cells need intermediate concentration of ECM to allow dynamic formation and disassembly of the cell-matrix contacts (Rozario and DeSimone, 2010). In *Xenopus*, the assembly of fibronectin (FN) matrix on the surface of BCR depends on cell adhesion-generated tissue tension of the BCR as well as Wnt/PCP signaling, and is essential for anterior migration of PPP cells and ML intercalation of chordamesoderm (Davidson et al., 2006; Dzamba et al., 2009). Similarly in zebrafish, FN and laminin (LM)-containing ECM is assembled during gastrulation at ectoderm-mesoderm and mesoderm-endoderm interfaces under the regulation of Wnt/PCP signaling, and disruption of the FN network resulted in C&E phenotypes (Dohn et al., 2013; Latimer and Jessen, 2010). Recent work further indicates that formation of FN and LM-containing ECM beneath the migrating PPP cell layer depends on Efemp2, an ECM protein, and is crucial for the collective migration of PPP cells (Zhang et al., 2014). Cell-ECM interaction is mainly mediated by integrins, a superfamily of transmembrane cell surface receptors that bind to ECM components. *Xenopus* gastrulating cells rely on integrin $\alpha_5\beta_1$ for growth and orientation of cellular processes (Davidson et al., 2006). However, how cells interact with ECM in zebrafish gastrulae is still poorly understood.

Cell-cell and cell-matrix adhesions constantly regulate each other. *Xenopus* FN matrix assembly depends on Cadherin-mediated cell-cell adhesion between BCR cells (Dzamba et al., 2009). In turn, FN-integrin signaling affects ML intercalation by modulating Cadherin-dependent adhesion between chordamesodermal cells (Marsden and DeSimone, 2003). The two competing adhesions are simultaneously required for cell migration and need to be coordinated to achieve effective migration. Indeed, manipulation of cell-cell and cell-matrix interactions *in vitro* could both affect tissue cohesion and invasion pattern of migrating cells (Hegedus et al., 2006).

Stat3 was previously shown to regulate C&E gastrulation movements of zebrafish PPP cells, chordamesoderm and lateral mesoderm in part by regulating polarized cell behaviors via Wnt/PCP pathway (Miyagi et al., 2004; Yamashita et al., 2002). Later studies identified Liv1 and Efemp2 as downstream targets of Stat3 that mediate PPP cell migration by regulating E-cadherin-dependent cohesion and ECM assembly, respectively (Yamashita et al., 2004; Zhang et al., 2014). However, my recent studies described in Chapter 2 demonstrated that zebrafish embryos lacking both maternal and zygotic *stat3* expression complete gastrulation with only mild axis extension defects and normal prechordal plate morphogenesis (Liu and Solnica-Krezel, 2015), indicating that the *stat3* morpholino-induced C&E phenotypes are largely *stat3*-independent. Therefore, in this study we sought for factors downregulated in *stat3* morphants during zebrafish gastrulation. We report identification of several genes downregulated in *stat3* morphants and functional characterization of one such secreted molecule, Fam132a, in the collective migration of PPP cells.

Fam132a/C1q-domain containing 2 (C1qdc2) belongs to the C1q/TNF superfamily, members of which all contain the globular C1q (gC1q) domain. C1q and other members of the family have diverse functions in many physiological and pathological processes including inflammation, adaptive immunity, as well as cell adhesion and chemotaxis (Nayak et al., 2010). C1q and its canonical receptor gC1qr, for example, can both interact with multiple ECM components and regulate cell adhesion and spreading (Nayak et al., 2010). Human FAM132a, also designated as CTRP12 or Adipolin, was recently identified as a member of the emerging adipokine family, members of which all contain C1q domain and are secreted (or predicted to be secreted) to plasma in mammals (Enomoto et al., 2011). Secreted by adipocytes, FAM132a is an

endocrine factor improving insulin sensitivity (Wei et al., 2012b). However, its function during development has not been investigated.

We identified Fam132a among several genes downregulated in *stat3* morphants using microarray and qRT-PCR experiments. Our functional studies of Fam132a indicate that it is a secreted molecule, which negatively regulates tissue cohesiveness and integrity underlying the collective migration of PPP cells. Overexpression of Fam132a caused dispersion and frequent neighbor exchange between PPP cells and loss of coherence in their anterior migration toward the animal pole. By contrast, loss of *fam132a* function partially suppressed defects in tissue cohesiveness and migration coherence of PPP cells in *slb*/*wnt11* mutant. Excess Fam132a also impaired ML intercalation of the chordamesoderm cells without significantly affecting their ML cell elongation, suggesting a Wnt/PCP-independent activity. Together, our study identified a novel developmental role for this secreted molecule in modulating morphogenesis and collective cell migration during zebrafish gastrulation.

3.3 Results

3.3.1 Identification of Non-specific Target Genes of *stat3* Morpholino in Zebrafish C&E movements

The discrepancy between *stat3* morpholino-induced and mutant C&E phenotypes in *stat3* gene (Chapter 2) (Liu and Solnica-Krezel, 2015; Yamashita et al., 2002) lead us to conclude that the morpholino-induced C&E phenotypes are largely *stat3*-independent. Accordingly, cell proliferation and chordamesoderm morphogenesis defects of MZ*stat3* mutants but not the strong C&E defects of *stat3* morphants could be rescued by expression of Stat3-Flag fusion protein (Chapter 2 and data not shown). To search for the genes misregulated in *stat3* morphants that

could underlie the C&E movement defects, we compared gene expression profiles of uninjected WT control and *stat3* morphant gastrulae in a microarray experiment. Injection of 10 ng of MO1-*stat3* induced dose-dependent C&E defects confirmed by morphology and whole-mount *in situ* hybridization (WISH) analyses at early segmentation of expression of several cell type specific genes, including (*no tail* (*ntl*) marking chordamesoderm, *myoD* marking paraxial mesoderm, data not shown) as previously described (Yamashita et al., 2002). Microarray analyses of RNA isolated from *stat3*-MO-injected and control embryos at late gastrula stage (9 hours post fertilization (hpf)) followed by bioinformatic analysis identified numerous candidate genes misregulated in *stat3* morphant gastrulae (Figure 3.1A). According to Yamashita et al, *stat3* deficiency caused severe C&E gastrulation defects via both cell-autonomous and non cell-autonomous mechanisms, implying that transcriptional activity of Stat3 promotes expression of a secreted factor(s) guiding dorsal cell convergence (Yamashita et al., 2002). Therefore, we prioritized this candidate list by focusing on genes previously implicated in cell movement and on predicted to encode secreted proteins, and identified 19 candidate genes (Table 3.1). Next, we validated their expression level in *stat3* morphants at late gastrula stage using RT- and qRT-PCR (Table 3.1), which further narrowed the list to six candidate genes including *cart prepropeptide* (*cartpt*), *hatching enzyme 1a* (*he1a*), *family with sequence similarity 132a* (*fam132a*), *sulfatase modifying factor 2* (*sumf2*), *arrestin domain containing 3 like* (*arrdc3l*), and *thymosin β* (*tmsb*). We also determined their expression during zebrafish embryogenesis by RT- and qRT-PCR, what revealed that they are all expressed during gastrulation (Figure 3.1B). Genes

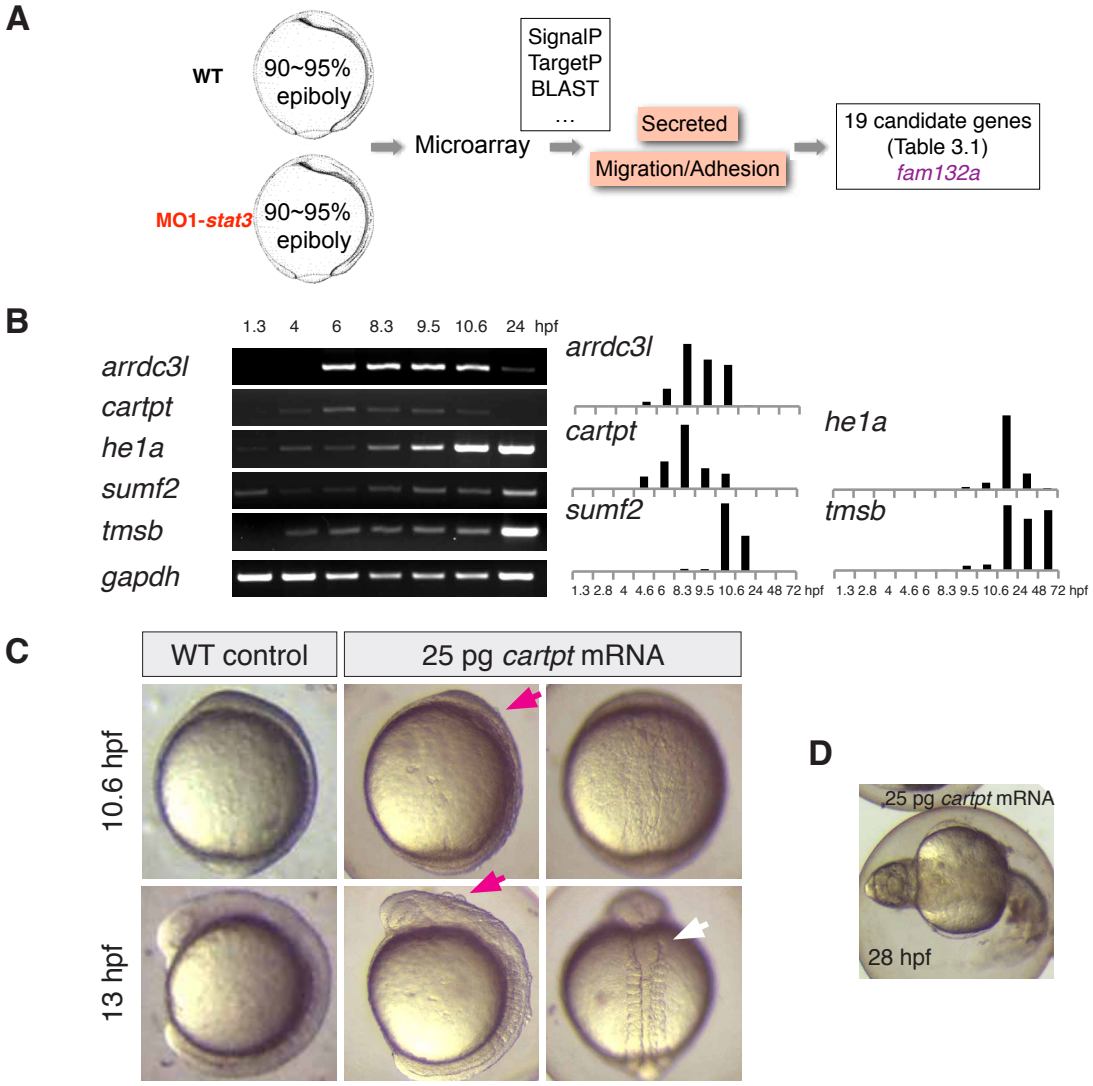

Figure 3.1 Identification of the novel C&E regulators. (A) Overview of microarray and bioinformatics analyses used to identify novel zebrafish C&E regulators that are downregulated by *stat3* morpholino (see also Table 3.1 for a full list of 19 candidate genes). (B) Temporal expression patterns of 5 validated candidate genes (labeled red in Table 3.1) during early zebrafish development detected by RT- and qRT-PCR. *gapdh* was used as an internal control. (C) Live images of zebrafish embryos overexpressing Cartpt at early somite stages. Loose cells

(red arrow) and split notochord (white arrow) were often observed. (D) Cartpt-overexpressing embryos exhibited eye spacing defects.

Table 3.1 19 Candidate genes selected from microarray analysis

Gene Symbol	Description	Predicted localication	MO/WT in Micro-arrays	RT-PCR		qRT-PCR	
				WT	10ng MO1-*stat3*	10ng MO1-*stat3*	WT
papl	*iron/zinc purple acid phostatase-like*	Secreted	-9.42				
ntn1b	*netrin 1b*	Secreted	-7.98				
cpa2	*carboxypeptide A2*	Secreted	-7.68				
cartpt[1]	*CART prepropeptide*	Maybe secreted	-7.50				
fetub	*fetuin B*	Maybe secreted	-5.93	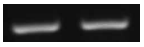			
he1a	*hatching enzyme 1a*	Secreted	-5.45				
fam132a	*family with sequence similarity 132*	Secreted	-4.77				
p4ha2	*prolyl 4-hydroxylase, α polypeptide II*	Secreted	-4.53				
sumf2	*sulfatase modifying factor 2*	Secreted	-4.28				
col7a1	*homolog to human Collagen trpe VII, α1*	Secreted	-7.41				
arrdc3l	*arrestin domain containing 3 like*	Cytoplasm	-71.94				
inosb	*inducible nitric oxide synthase 2*	Cytoplasm	-15.35				
tmsb	*thymosin β*	Cytoplasm	-8.46				
gpm6aa	*glycoprotein M6A a*	Membrane	-7.00				
ccdc88a	*coiled-coil doamin containing 88Ab*	Cytoplasm/Nucleus	-6.47				
osbpl3a	*oxysterol binding protein-like 3a*	Membrane/Nucleus	-5.66				
dpysl5a	*dihydropyrimidinase-like 5a*	Cytoplasm	-5.45	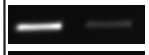			
dsg4	*homolog to human Desmoglein 4*	Cytoplasm	-5.38	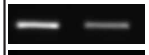			
stx2	*syntaxin 2*	Cytoplasm/Nucleus	-4.30				

[1]Red, candidate genes chosen for gain-of-function screen

that were not significantly downregulated (explain how this was determined) in *stat3* morphant gastrulae were not analyzed further.

Given previous observations that both loss-of-function (LOF) and gain-of-function (GOF) of many cell migration and cell polarity regulators impair C&E movements (Jessen et al., 2002), we undertook an overexpression approach as the first step of functional analyses of the candidate genes. We injected synthetic RNAs encoding these candidate genes into zebrafish embryos at one-cell stage and assessed their morphology at early segmentation (1-5 somites stages). These experiments identified two genes that upon overexpression generated gastrulation defects: *cartpt* and *fam132a*. *cartpt* encodes a hypothetical protein, which shares sequence similarity with human Cocain- and Amphetamine- Regulated Transcript Prepropeptide (CARTPT). CARTPT is normally cleaved to generate several active CART peptides, which are widely distributed in the central nervous system (CNS) and characterized as neurotransmitters and hormones involved in body weight, addiction, neuroregeneration, and cell migration (Luo et al., 2013; Rogge et al., 2008). *cartpt* appears to be only zygotically expressed during the course of gastrulation (Figure 3.1B). The predicted protein encoded by this gene contains a signal peptide (SP) at the N-terminus and a CART domain at the C-terminus. Injection of synthetic RNA of *cartpt* into one-cell stage zebrafish embryos resulted in shorter and wider body axes at early segmentation stages (Figure 3.1C), suggesting severe C&E defects. Penetrance of this phenotype increased in dose-dependent manner (data not shown). At 1 day post fertilization (dpf), *cartpt*-overexpressing embryos remained shorter compared to uninjected WT controls, and a subset exhibited cyclopia (Figure 3.1D), an eye field-fusion phenotype commonly associated with C&E defects (Marlow et al., 1998). These preliminary results suggest that *cartpt* may

regulate C&E movements and it will be worthwhile to continue characterizing the functions of this gene during zebrafish embryogenesis in the future.

3.3.2 Fam132a is a Conserved Secreted Molecule

The second candidate gene that emerged from our microarray screen is *fam132a*, or C1qdc2, is conserved among vertebrates (Figure 3.2A). Zebrafish *fam132a* encodes a 318-amino acid protein predicted to contain a leading SP at its N-terminus, a C-terminal C1q domain, and a stalk in between with unknown functions. RT-PCR detected high level of maternal *fam132a* transcripts, which decrease shortly after mid-blastrula transition (MBT) and zygotic transcripts start to accumulate during gastrulation (Figure 3.2B). qRT-PCR experiments showed that *fam132a* expression was significantly downregulated in *stat3* morphants at late gastrula stage (Figure 3.2C, Table 3.1), but was not significantly affected in MZ*stat3*$^{stl27/stl27}$ mutant embryos at several stages of development (Figure 3.2D). WISH experiments revealed that *fam132a* transcripts concentrate in the anterior and posterior region of the forming dorsal midline during gastrulation and later become enriched in the developing eyes, ears, heart, and other tissues to be identified (Figure 3.2E).

To obtain an insight into the subcellular localization of Fam132a we injected synthetic RNA coding Fam132a with GFP or Myc fused at its C- terminus. Live imaging revealed that Fam132a-GFP protein was found as stable or dynamic puncta at cell contacts and extracellular space in zebrafish blastulae (Figure 3.2F). Whole mount immunostaining experiments using anti-Myc antibodies also detected Fam132a-Myc in extracellular space (Figure 3.2G). When mosaically expressed, Fam132a puncta could be observed several cell diameters away in all

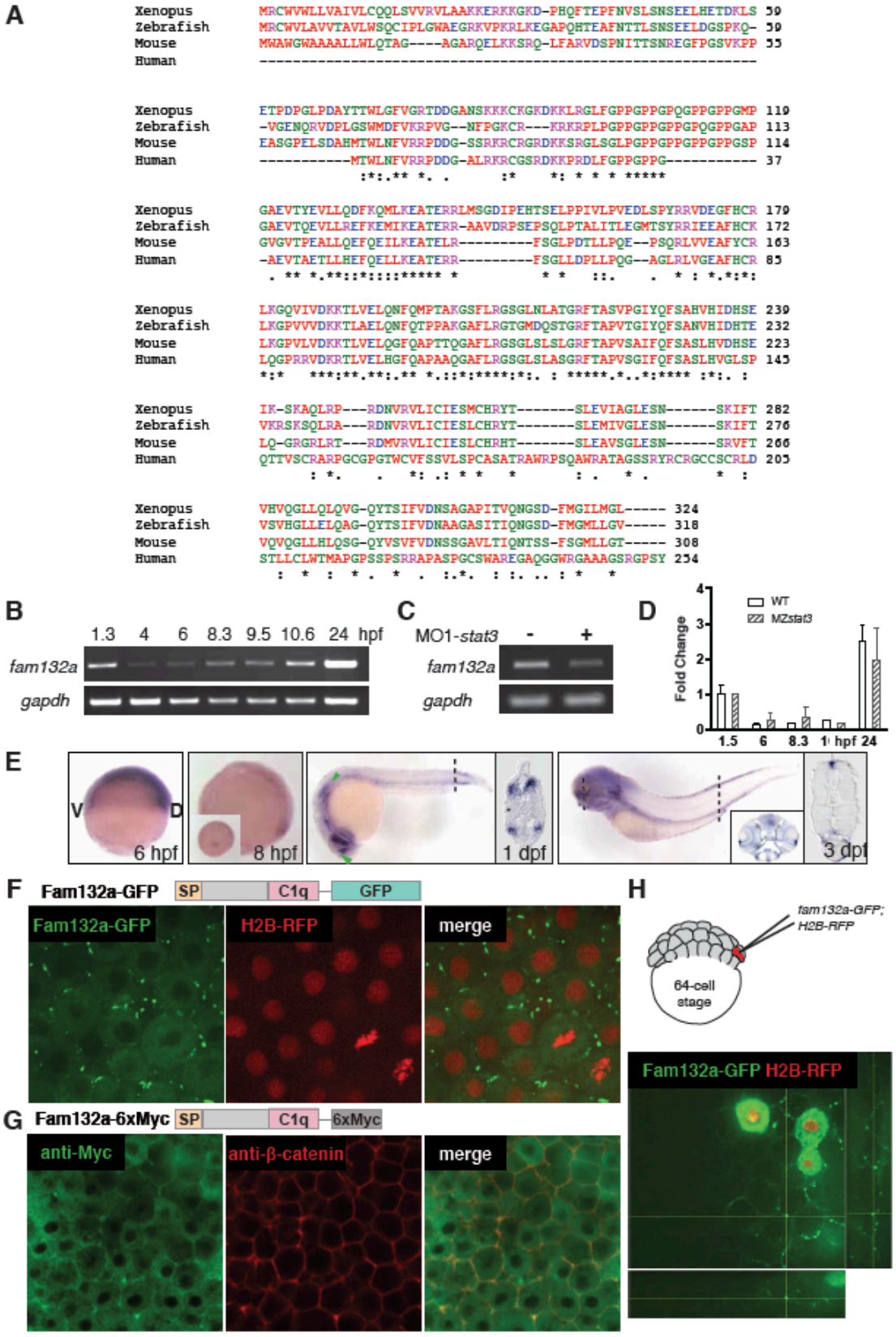

Figure 3.2 Fam132a is a conserved and secreted molecule expressed during zebrafish

embryogenesis. (A) ClustalW2 multiple protein sequence alignment of Fam132a amino acid sequences from four vertebrates. Asterisk, colon and period indicate fully conserved, strongly similar and weakly similar residues, respectively. (B-D) Temporal expression pattern of *fam132a* during early zebrafish development defected by RT- and qRT-PCR. *fam132a* expression was downregulated in *stat3* morphant at late gastrula stage (C), and seemed unaffected in MZ*stat3* mutant embryos throughout early embryogenesis (D). (E) Spatial expression pattern of *fam132a* transcripts detected by WISH (lateral view). Insets, transverse section. (F-G) Subcellular localization of Fam132a-GFP (F) and Fam132a-Myc (G) fusion proteins in zebrafish blastulae detected with live imaging and whole-mount immunostaining, respectively. Fusion proteins were expressed ubiquitously by injecting synthetic RNA into 1-cell stage embryos. (H) Subcellular localization of Fam132a-GFP in live embryos that were mosaically co-labeled with Fam132a-GFP and H2B-RFP. Error bars = SEM.

directions from the expressing cells co-labeled with Histone2B-RFP (Figure 3.2H, Materials and Methods), indicating that zebrafish Fam132a is indeed a secreted molecule.

3.3.3 Fam132a Regulates Cell Fates and C&E Movements Independent of PCP

fam132a stood out in our GOF screen as overexpression of the gene in zebrafish embryos resulted in oval yolk shape during early somitogenesis and dorsalized phenotype at 1 dpf in (Figure 3.3A-B). Marker analyses using WISH and qRT-PCR further detected that at early gastrula stage (6 hpf), while expression of genes downstream of the dorsal β-catenin signaling such as *bozozok* (*boz*)/*dharma* and *goosecoid* (*gsc*) remained unchanged, transcripts levels of genes encoding Bmp signaling components such as *bmp2b*, *bmp4*, *eve1* and *sizzled* (*szl*) were decreased to various degrees (Figure 3.2B and D). These results suggest that Fam132a may interact with Bmp signaling to regulate dorsoventral patterning during zebrafish embryogenesis.

In contrast to a simply dorsalized phenotype resulting from inhibition of Bmp signaling (Mullins et al., 1996), *fam132a*-overexpressing embryos also displayed C&E movement defects. At early somite stage (10.3 hpf), the anterior presumptive prechordal plate marked by *hgg1* that normally resides anteriorly to the *dlx3b*-expressing neuroectoderm boundary was located more posteriorly due to *fam132a* overexpression (Figure 3.3E). Later during somitogenesis, Fam132a-overexpressing embryos exhibited anteroposteriorly shorter and mediolaterally wider embryonic tissues compared to uninjected WT controls, as revealed by WISH using *hgg1*, *myoD* marking the paraxial mesoderm, and *pax2a* in the mid-hindbrain boundary, otic placode and the developing pronephros (Figure 3.3F). At the end of embryogenesis (30 hpf), I observed partial or complete fusion of the eye field in *fam132a*-overexpressing embryos (Figure 3.3A), a phenotype

typically associated with C&E movement defects as seen in Wnt/PCP signaling component mutants (Marlow et al., 1998), but not reported for even severely dorsalized mutants such as *snailhouse* (*snh*) (Mullins et al., 1996). Together, these results suggest that Fam132a regulates C&E movements independent of dorsoventral patterning.

Excess Fam132a affected C&E of multiple tissues during zebrafish gastrulation (Figure 3.3). We next focused on the morphogenesis of the axial mesoderm. Detailed analysis of axial mesoderm markers *flh* and *hgg1* marking the presumptive notochord and hatching gland, respectively, at different time points during gastrulation revealed that gain of Fam132a function resulted in a much shorter and wider forming notochord compared to WT gastrulae, and largely reduced anterior migration of prechordal plate progenitor (PPP) cells (Figure 3.4A). Strikingly, instead of intact domains as observed in WT gastrulae, both the forming notochord and the future prechordal plate in *fam132a*-overexpressing embryos lost tissue integrity, showing irregular shape and loose organization with cells scattered around. In some cases the notochord appeared as two separate structures (Figure 3.4A).

To further determine how Fam132a affects C&E movements in the axial mesoderm, we performed confocal time-lapse imaging using *Tg[lhx1a:EGFP]* line with notochord and intermediate mesodermal cells labeled in green (Swanhart et al., 2010). Mediolateral (ML) cell intercalation is known to be the main cell behavior driving C&E of the axial mesoderm (Gray et al., 2011; Keller et al., 2000). Cell tracing analysis also confirmed that during gastrulation, chordamesodermal cells emerging from the margin actively rearranged and intercalated between one another in WT embryos to form an anteroposteriorly elongated dorsal axis (Figure 3.4B-C). However, such ML intercalation was strongly reduced and chordamesoderm was much shorter in the AP dimension and mediolaterally wider in Fam132a-overexpressing gastrulae (Figure 3.4B-

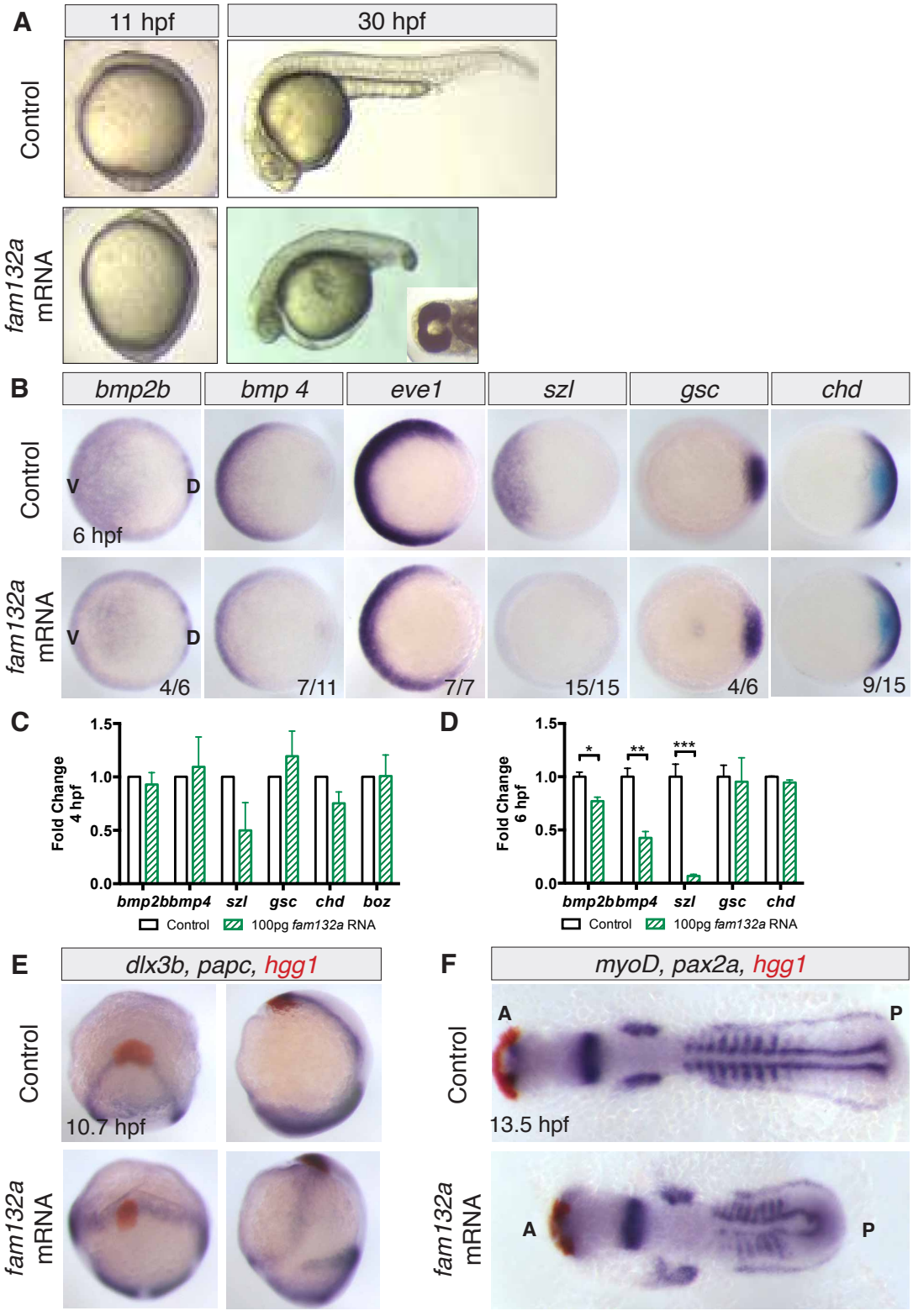

Figure 3.3 *fam132a* GOF causes mild dorsalization and C&E defects in zebrafish embryos. (A)

Lateral view showing WT control and Fam132a-overexpressing live embryos, a subset of which exhibited cyclopia and synophthalmia eye-spacing phenotypes (inset). (B) Marker gene analysis of DV patterning in early gastrula stage (6 hpf) WT control and embryos injected with 100 pg *fam132a* RNA detected by WISH. Animal view, dorsal to the right. Marker gene expression was affected in all Fam132a-overexpressing embryos to various extends. Images and numbers shown reflect the most prevalent expression pattern. (C-D) qRT-PCR showing DV patterning marker gene transcript levels in blastrula (4 hpf, C) and early gastrula (6 hpf, D) stage control and Fam132a-overexpressing embryos detected normalized to *gapdh*. (E) Animal and lateral views showing *hgg1* in prechordal plate mesoderm, *papc* in presomitic mesoderm and *dlx3b* marking neuroectoderm boundary in 2-somite embryos. (F) *myoD* marking somites, *pax2a* in eye, mindbrain-hindbrain boundary, otic placode and pronephric mesoderm, and *hgg1* in flat-mounted embryos. (*$p<0.05$, **$p<0.01$, ***<0.001, error bars = SEM.)

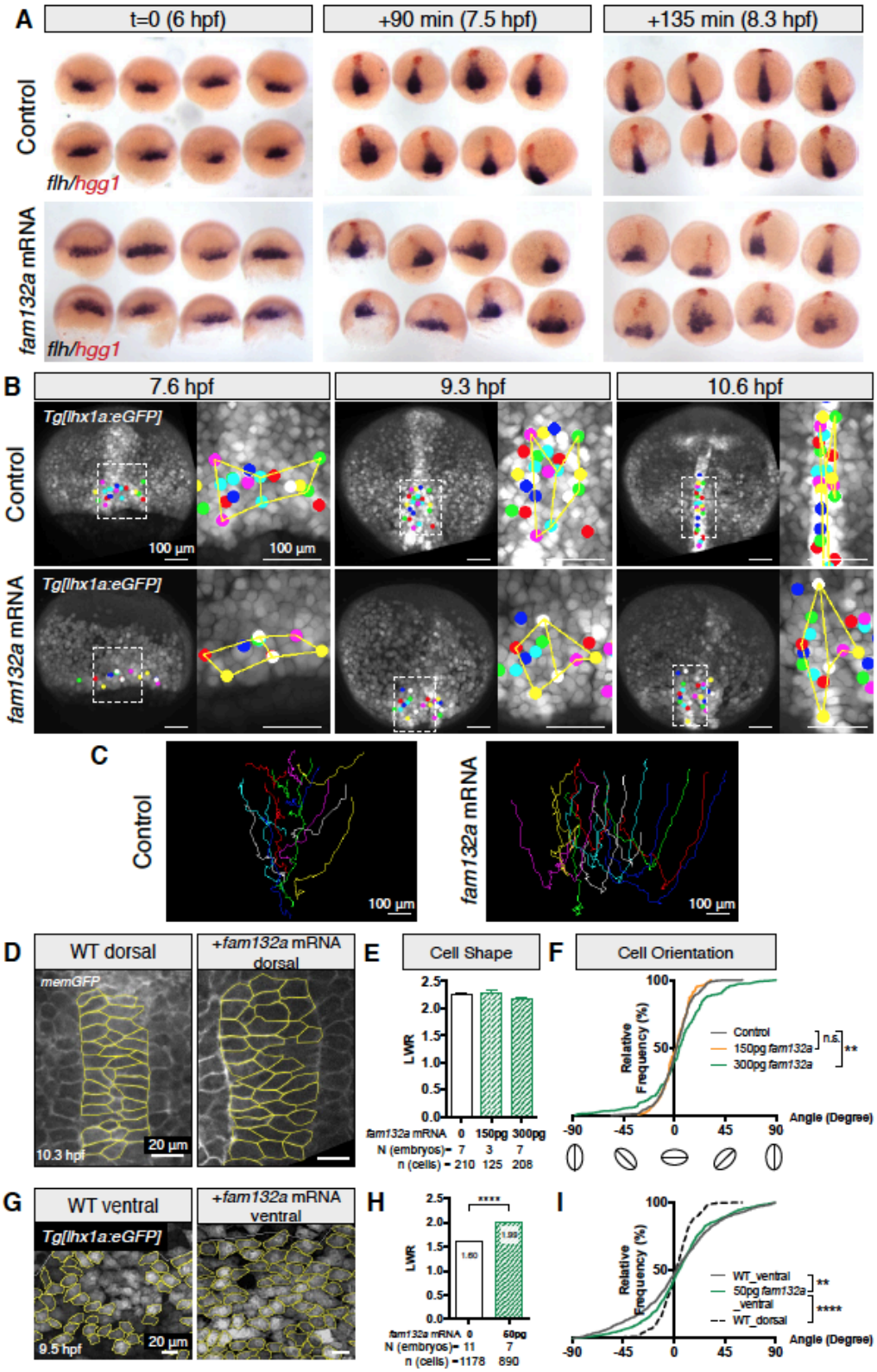

Figure 3.4 *fam132a* GOF leads to C&E defects in the axial mesodermal cells without affecting planar cell polarity. (A) Dorsal view (animal to the top) showing *hgg1* marking PPP domain and

flh marking the forming notochord in control embryos and embryos injected with 100 pg *fam132a* RNA during gastrulation. (B) Still images of confocal time-lapse movies recording C&E movements of chordamesoderm in control and Fam132a-overexpressing (300 pg RNA) *Tg[lhx1a:eGFP]* gastrulae with dots overlaying individual cells tracked. Lines connecting six cells in order represent the change of the relative position of cells over time. Insets show enlarged views of boxed region. Trajectories of chordamesodermal cells are shown in C. (D-F) Dorsal view showing notochord cells labeled with mGFP in WT and Fam132a-overexpressing (150 and 300 pg RNA) embryos at 1-somite stage (D). Cell shape (length-to-width ratio) and orientation (cumulative distribution) are quantified in E and F, respectively. (G-I) Cell shape and orientation analyses of ventral cells in control and Fam132a-overexpressing (50 pg RNA) *Tg[lhx1a:eGFP]* embryos. (n.s. not significant, **p<0.01, ****p<0.0001, error bars = SEM.)

C), suggesting that Fam132a regulates ML intercalation of the axial mesoderm during C&E.

Looking for the cellular mechanisms by which Fam132a regulates ML intercalation, we wished to examine whether it affects planar cell polarity where cells are elongated mediolaterally across the tissue. Planar polarity has been shown to be a prerequisite for ML intercalation during gastrulation, and its disruption, for example by manipulating Wnt/PCP signaling, impairs ML cell intercalation (Gray et al., 2011). We performed morphometric analyses of GFP-labeled notochord cells in 1-somite stage (10.3 hpf) embryos (Figure 3.4D), and found that elongation of notochord cells appeared normal in *fam132a*-RNA-injected embryos compared to WT (Figure 3.4E). Fam132a-overexpressing notochord cells were also able to align their long axis mediolaterally, except for a slight misorientation of cells in embryos injected with the highest doses of *fam132a* RNA (Figure 3.4F). In addition, even cells on the ventral side of the *fam132a*-overexpressing gastrulae were ML elongated as opposed to a rounder shape and more randomized orientation normally seen in WT (Figure 3.4G-I), similar to previous observations in dorsalized embryos such as *somitabun (sbn)/smad5* (Myers et al., 2002). Together, these results indicate that Fam132a regulates cell intercalation in a PCP-independent fashion.

3.3.4 *fam132a* GOF Results in Reduced Cell Contact Persistence and Less Coherent Migration of the Prechordal Plate Progenitor (PPP) Cells

To closely examine the anterior migration of PPP cells, we performed live cell imaging recording PPP cell migration for a total of 20 minutes at different gastrula stages in both WT and *fam132a*-overexpressing gastrulae using *Tg[gsc:GFP-CAAX]* transgenic line (From Dr. M. Tada, UCL, UK) that labels PPP cells with membrane GFP (Figure 3.5A-D). During zebrafish gastrulation, PPP cells migrate anteriorly as a cohesive cluster with cells staying in contact and

keeping their relative positions in a coherent manner with all cells within the tissue migrating with a similar speed in a uniform direction (Dumortier et al., 2012; Tada and Heisenberg, 2012). Live imaging revealed that GOF cells appeared to be highly protrusive and polarized as control cells, however the orientation of cellular processes were randomized compared to anteriorly biased cytoplasmic extensions in WT (Figure 3.5C-D). This observation was confirmed by co-labeling with Lifeact-mCherry fusion protein that marks the actin-rich protrusions (Figure 3.5L). In addition, we performed cell tracing and cell trajectories revealed that whereas WT PPP cells at all stages examined migrated only toward anterior, *fam132a* GOF PPP cells migrated in random directions (Figure 3.5E-F). To further characterize how Fam132a affects the migration behaviors of PPP cells, we quantified the net migration speed, persistence (or the ability of cells maintaining their migration directions), and coherence which indicates cells within a cohesive group follow highly aligned tracks in the same direction (see also Materials and Methods). The effect of Fam132a on net speed appeared to be random (Figure 3.5I). However, *fam132a* GOF led to less persistent migration and significantly reduced coherence (Figure 3.5J-K), suggesting that those PPP cells migrated more individually rather than collectively.

Consistent with tissue integrity defects in the *fam132a*-overexpressing prechordal plate described earlier (Figure 3.4A), those PPP cells failed to maintain stable contact and dynamically changed neighbors. By tracking neighboring cells during the 20 minute duration of the time-lapse movies, we observed that in WT embryos, only about a third of neighbor cell pairs separated from each other at 65%-epiboly stage (7.3 hpf). As development progressed, nearly no separation events took place, and neighbor cells maintained in contact during almost the entire movies (Figure 3.5G-H). Strikingly, although PPP cells progressively improved in contact

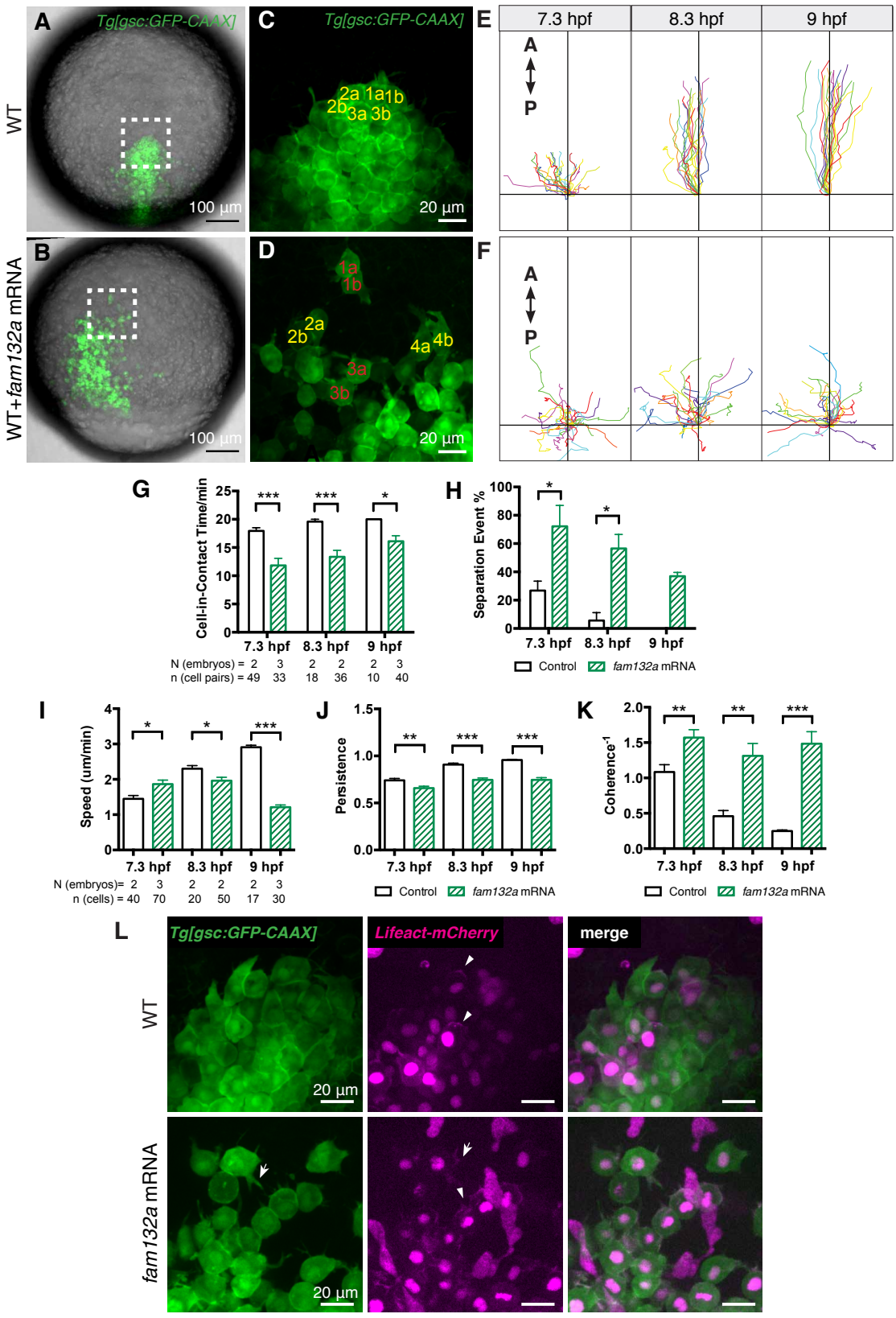

Figure 3.5 *fam132a* GOF leads to reduced cell contact persistence and less coherent anterior

migration of zebrafish PPP cells. (A-B) Confocal images of *Tg[gsc:CAAX-GFP]* embryos with axial mesodermal cell labeled with membrane GFP. Boxed areas were chosen for time-lapse movies. (C-K) Still images from time-lapse movies recording anterior migration of PPP cells in control (C) and Fam132a-overexpressing (D) embryos (anterior to the top). Trajectories are shown in E and F. Migration net speed, persistence and coherence are quantified in I-K (see also Materials and Methods). Neighbor cells were chosen and tracked for analysis of their ability of maintaining cell-cell contact, as exemplified by numbers labeled. Some pairs were able to maintain contact throughout the movie (yellow), while others separated (red). Frequency of separation events and average cell-contact time are quantified in G and H. (L) Mosaic labeling of Lifeact-mCherry (co-labeled with H2B-RFP) showing actin-rich cytoplasmic extensions in PPP cells (anterior to the top). White arrowheads and arrows show extensions oriented toward and away from anterior, respectively. (*$p<0.05$, **$p<0.01$, ***$p<0.001$, ****$p<0.0001$, error bars = SEM.)

maintenance over time, separation events significantly increased in *fam132* GOF prechordal plate, and the average time for neighbor cells to stay in contact was reduced (Figure 3.5G-H). Tissue cohesion and cell contact maintenance have been shown to be crucial for the directed migration of PPP cells (Montero et al., 2005; Ulrich et al., 2005), and were recently proposed to provide intrinsic directionality (Dumortier et al., 2012). Together, our results suggest that Fam132a regulates the coherent migration of PPP cells through negative regulation of tissue cohesiveness and integrity.

3.3.5 Fam132a LOF Suppresses Tissue Cohesiveness and Directional Migration Defects of MZ*slb/wnt11* PPP Cells

Similar defects in tissue cohesiveness, cell migration coherence, and prechordal plate morphogenesis seen in *fam132a* GOF were reported before in *slb*/*wnt11* mutant embryos (Montero et al., 2005; Ulrich et al., 2005), suggesting potential interactions between *fam132a* and *wnt11*. To address this, we generated *fam132a* zebrafish mutants using transcription activator-like effector nuclease (TALEN) method. Mutations in Exon 1 in the *stl8* and *stl9* alleles lead to frameshift and pre-mature stop codons, and the resulting protein is 73 and 57 amino acids in length, respectively (Figure 3.6A-B). Zygotic *fam132a* homozygous (Z*fam132a*) mutants did not show obvious developmental defects and could grow into viable and fertile adults (data not shown). Given the abundant maternal *fam132a* RNA (Figure 3.2B), we generated maternal zygotic *fam132a* homozygous (MZ*fam132a*) mutant embryos by incrossing Z*fam132a* parents. However, MZ*fam132a* embryos also developed relatively normally throughout development (Figure 3.6C), indicating that *fam132a* is not essential for zebrafish embryogenesis (see 3.4 Discussion).

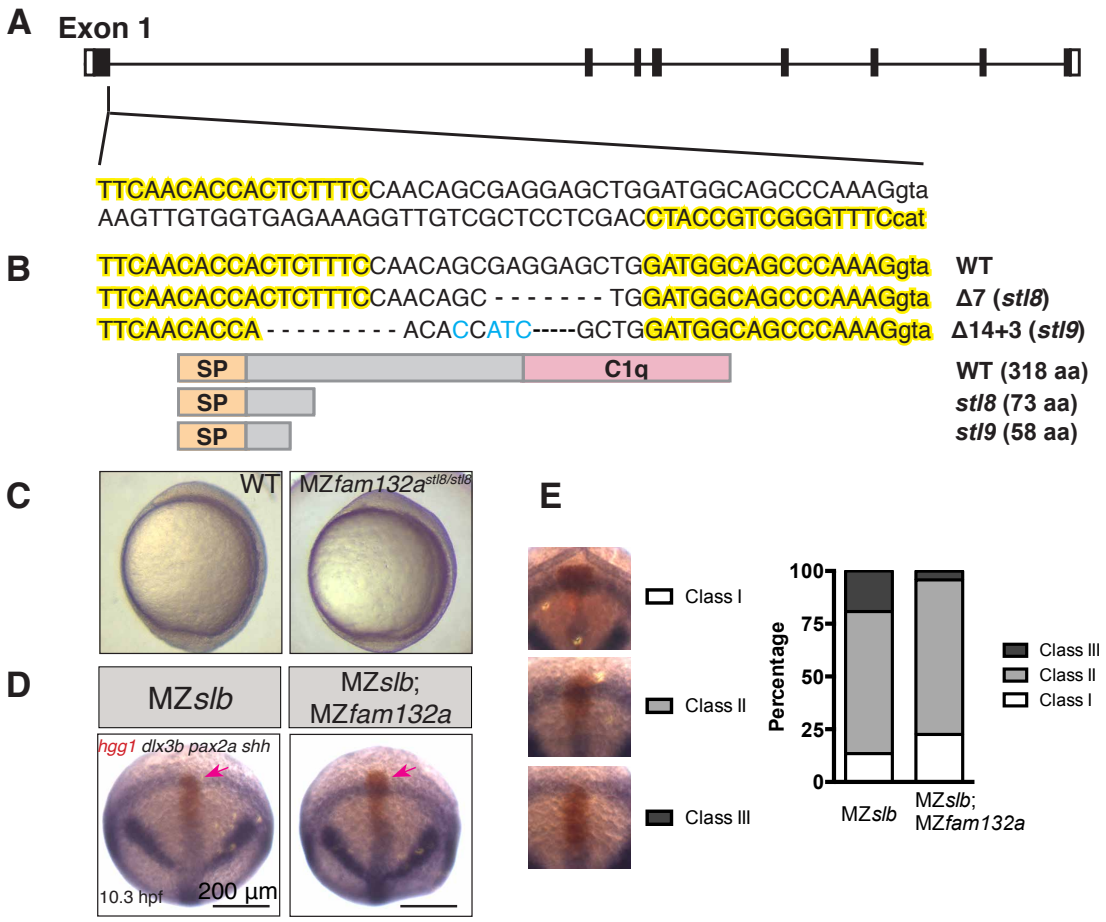

Figure 3.6 Loss of *fam132a* function partially suppresses extension defects of the MZ*slb* prechordal mesoderm. (A) Design of TALEN pair targeting zebrafish *stat3* gene. (B) Sequence alignments and diagrams of encoded proteins of *stl8* and *stl9* alleles. (C) Live images of WT and MZ*fam132a* embryos at early somite stage (lateral view, animal to the top). (D) Position of *hgg1*-expressing PPP domain with respect to neuroectoderm boundary labeled by *dlx3b* in MZ*slb* and MZ*slb*; MZ*fam132a* embryos (animal view). Relative position of the two domains are classified into three groups and quantified in E.

Using both *fam132a* alleles, we generated *slb*; *fam132a* compound mutants and analyzed anterior migration of PPP cells in MZ*slb*; MZ*fam132a* mutant gastrulae. Due to variability in severity of gastrulation phenotypes seen among different *slb* clutches, we performed our analyses in MZ*slb*; M*fam132a*$^{+/-}$ (MZ*slb* for short) and MZ*slb*; MZ*fam132a* embryos obtained from the same clutch of eggs (see 3.5 Materials and Methods), which also allowed us to examine exclusively the zygotic Fam132a function. *hgg1*-expressing prechordal plate domain usually displays a spectrum of morphogenetic phenotypes (Heisenberg and Nusslein-Volhard, 1997). We categorized these various phenotypes based on severity, with Class I representing the least severe situation where majority of the *slb* PPP cells migrate anteriorly passing the *dlx3b*-expressing neuroectoderm boundary, Class III being the most severe where almost the entire *hgg1* domain is located posterior to the neuroectoderm, and Class II being the intermediate phenotype where prechordal plate partially migrates over the neuroectoderm boundary (Figure 3.6E). Loss of *fam132a* function, however, partially suppressed this morphogenetic phenotype by shifting the phenotypic spectrum towards the less severe phenotype (Figure 3.6E). Together, these results indicate that despite being dispensable in WT, disruption of Fam132a function promotes the directed migration of the anterior axial mesoderm in a sensitized background such as *slb* mutant.

To explore the cellular mechanisms underlying the partial suppression of PPP cell migration phenotype in the double mutants, we performed DIC time-lapse imaging recording PPP cell migration for the duration of 30 minutes at the onset of gastrulation (Figure 3.7A). Neighbor MZ*slb* PPP cells separated from each other during the course of movies much more frequently and maintained in contact for a shorter period of time on average compared to their WT counterparts (Figure 3.7B) (Witzel et al., 2006), both of which were partially suppressed in MZ*slb*; MZ*fam132a* double mutant gastrulae (Figure 3.7B), suggesting a partial suppression of

cohesion defect. By analyzing migration parameters, we observed significantly reduced net speed, persistence and coherence in the anterior migration of MZ*slb* PPP cells compare to WT, similar to previous studies (Figure 3.7C) (Kai et al., 2008). Without affecting migration speed, loss of Fam132a function significantly increased persistence and coherence of MZ*slb* PPP cell migration (Figure 3.7C). Our results suggest that compromised Fam132a function could suppress tissue cohesion defect in *slb* mutant prechordal plate precursors, which may account for the partial rescue of the less coherent migration phenotype. We also overexpressed a very low dose of Fam132a (5 pg RNA) in MZ*slb* embryos. Although we did not observe significant changes in neighbor separation and contact time (Figure 3.7D), excess Fam132a reduced persistence and coherence in MZ*slb* PPP cell migration (Figure 3.7E). Together, our results support a model where Fam132a negatively regulates cell contact maintenance and tissue cohesiveness underlying the coherent anterior migration of PPP cells during zebrafish gastrulation. We also demonstrated that Fam132a exerts its function in complete absence of Wnt11, suggesting a Wnt11-independent role of Fam132a.

3.3.6 Fam132a Function Is Tissue-Specific

Partial (synophthalmia) or complete (cyclopia) eye fusion phenotype was observed in both *fam132a* GOF as shown earlier and *slb* mutant embryos (Heisenberg and Nusslein-Volhard, 1997). Given a partial rescue of cell behaviors and PPP cell migration defects in double mutants, we next asked whether *slb* eye phenotype could also be suppressed by loss of *fam132a* function. We classified MZ*slb* and MZ*slb*; MZ*fam132a* embryos according to their eye phenotype severity as described previously, with C1 representing WT eye spacing and C5 representing the most severe phenotype, cyclopia (Marlow et al., 1998). Surprisingly, loss of Fam132a function

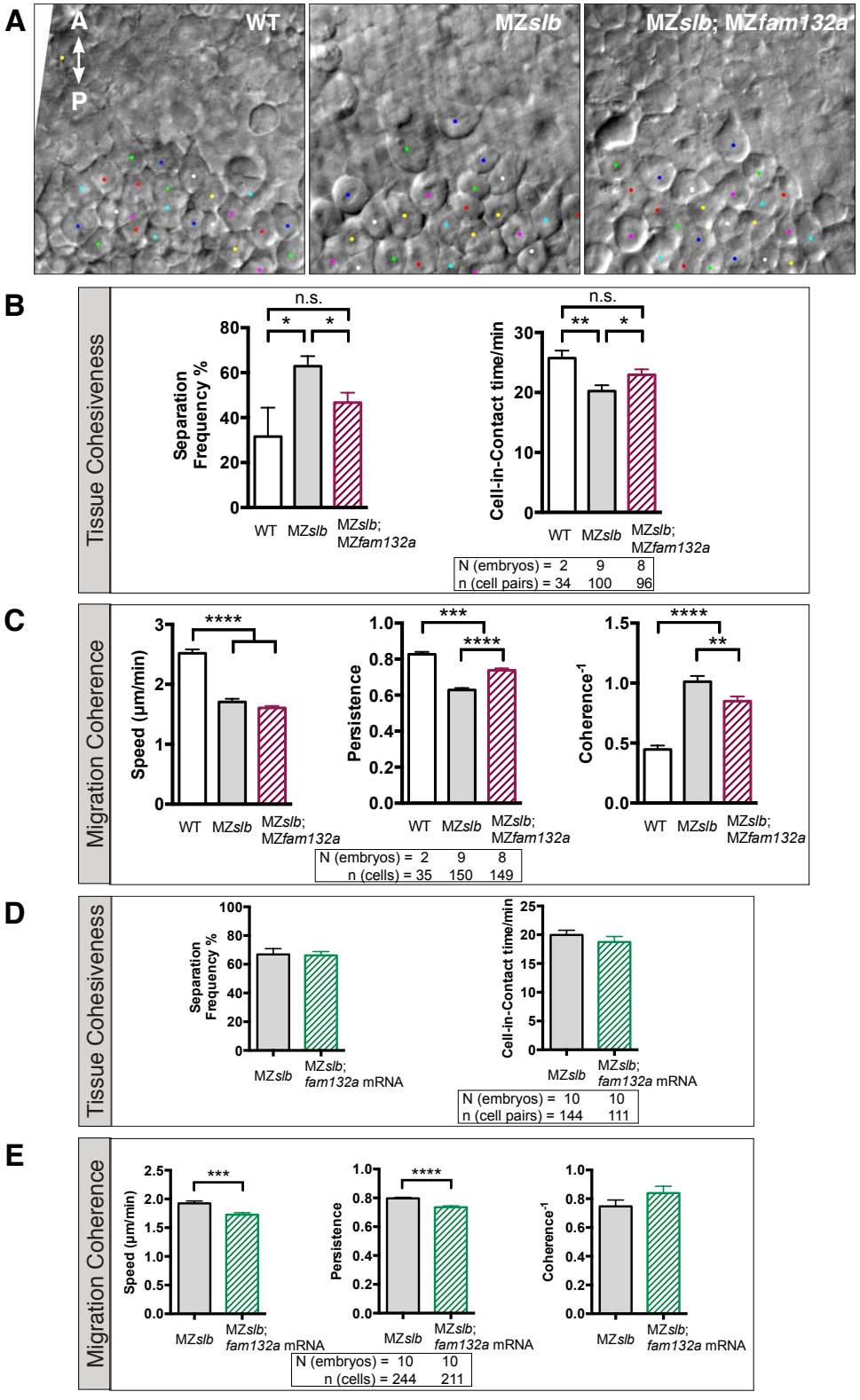

Figure 3.7 Loss of *fam132a* function partially suppresses defects in tissue cohesiveness and migration coherence of the MZ*slb* PPP cells. (A) DIC time-lapse analysis of migration PPP cells

in WT, MZ*slb* and MZ*slb*; MZ*fam132a* embryos at early gastrula stage. Dots represent cells that are tracked. (B) Frequency of neighbor cell separation and average time of cell-contact maintenance in WT, MZ*slb* and MZ*slb*; MZ*fam132a* PPP domain. (C) Migration speed, persistence and coherence of WT, MZ*slb* and MZ*slb*; MZ*fam132a* PPP cells. (D, E) Cell-contact maintenance (D) and migration parameter analyses (E) in MZ*slb* and MZ*slb* embryos expressing low dose of ectopic Fam132a (5 pg RNA) at the same stage. (n.s. not significant, *$p<0.05$, **$p<0.01$, ***$p<0.001$, ****$p<0.0001$, error bars = SEM.)

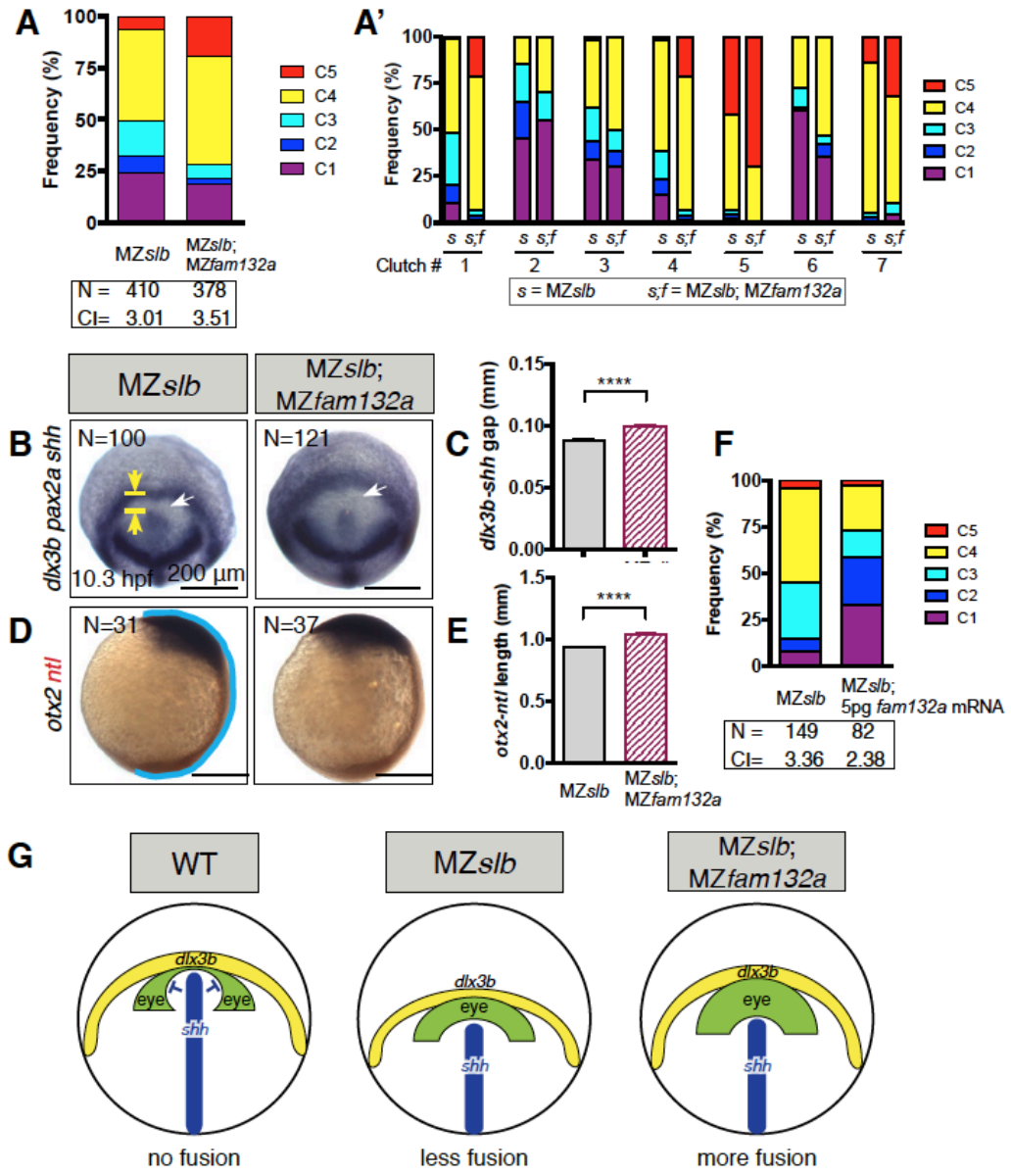

Figure 3.8 Tissue-specific requirement of *fam132a* for zebrafish C&E movements. (A, A') Eye spacing phenotypes in MZ*slb* and MZ*slb*; MZ*fam132a* embryos at 3 dpf quantified in each individual experiment (A') or with all experiments combined (A). CI, cyclopia index, was calculated as previously described (Marlow et al., 1998). (B) *shh* in floor plate and notochord, and *dlx3b* in neuroectoderm boundary in single and *slb*, *fam132a* compound mutant embryos (animal view). Distance between the anterior edge of *shh* domain and posterior edge of *dlx3b* domain is quantified in C. (D) Lateral view showing extension of neuroectoderm labeled by *otx2*

and chordamesoderm labeled by *ntl*. Embryonic extension is quantified in E. (F) Eye spacing phenotypes in MZ*slb* control and Fam132a-overexpressing (low dose, 5 pg RNA) embryos at 3 dpf. (G) Model of eye spacing phenotypes in correlation with tissue morphogenesis. Eye field separation is a result of coordinated morphogenetic movements of neuroectoderm and mesoderm tissues. Normally the extension of axial mesoderm and neuroectoderm results in a relatively narrow gap between *shh* and *dlx3b* which allows Hh signaling to suppress Pax6 expression and eye specification in the midline. In *slb* embryos, extension of both axial mesoderm and neuroectoderm was impaired, leaving a wider *shh-dlx3b* gap. Without Hh signaling eyes are excessively specified even in the midline region, leading to partial or complete fusion of the eye fields. The bigger the gap is, the more severe eye spacing phenotype would be. Loss of *fam132a* function partially suppressed extension defects in these tissues to different extends. Neuroectoderm was able to extend anteriorly to a greater degree than axial mesoderm. As a result, an even wider gap between *shh* and *dlx3b* was created, hence the more severe eye spacing phenotype in the double mutant embryos compared to *slb* embryos.

exacerbated the *slb* eye spacing phenotype with the phenotype spectrum shifting toward C4 and C5 (Figure 3.8A and A'). Eye field separation in zebrafish embryos depends on the suppression of *pax6* expression and eye structure specification by Hedgehog (Hh) expressed by the axial mesodermal cells. In many Wnt/PCP mutants, C&E defects create abnormal distance between *hh*-expressing axial mesoderm and *dlx3b*-expressing anterior neural plate, resulting in eye fusion phenotypes (Marlow et al., 1998). Therefore, we analyzed the *shh-dlx3b* gap in these mutants, and found that compared to MZ*slb,* MZ*slb*; MZ*fam132a* double mutant gastrulae indeed contained a larger gap (Figure 3.8B, C and G), possibly due to a more anterior position of the *otx2*-expressing neuroectoderm with respect to *shh*-expressing dorsal midline (Figure 3.8D, E and G). Surprisingly, low dose Fam132a overexpression also partially suppressed the eye spacing phenotype in MZ*slb* embryos (Figure 3.8F), possibly due to less extension of neuroectoderm and consequently a narrower *dlx3b-shh* gap. These results indicate that Fam132a function is required differently among tissues. Loss of Fam132a function leads to uncoordinated morphogenetic movements of neuroectoderm and axial mesoderm, hence the exacerbation of eye fusion phenotypes in *slb* mutants.

3.4 Discussion

Previous antisense morpholino-mediated knockdown of Stat3 expression in zebrafish dramatically impaired C&E gastrulation movements, positing that Stat3 transcription factor regulates C&E in both cell-autonomous and non-cell autonomous manner (Yamashita et al., 2002). Against this notion, my recent analyses of null *stat3* mutants indicated the morpholino-induced phenotypes are largely Stat3-independent (Liu and Solnica-Krezel, 2015). Nevertheless, we reasoned that exploration of the genes misregulated in *stat3* morphants with severe C&E

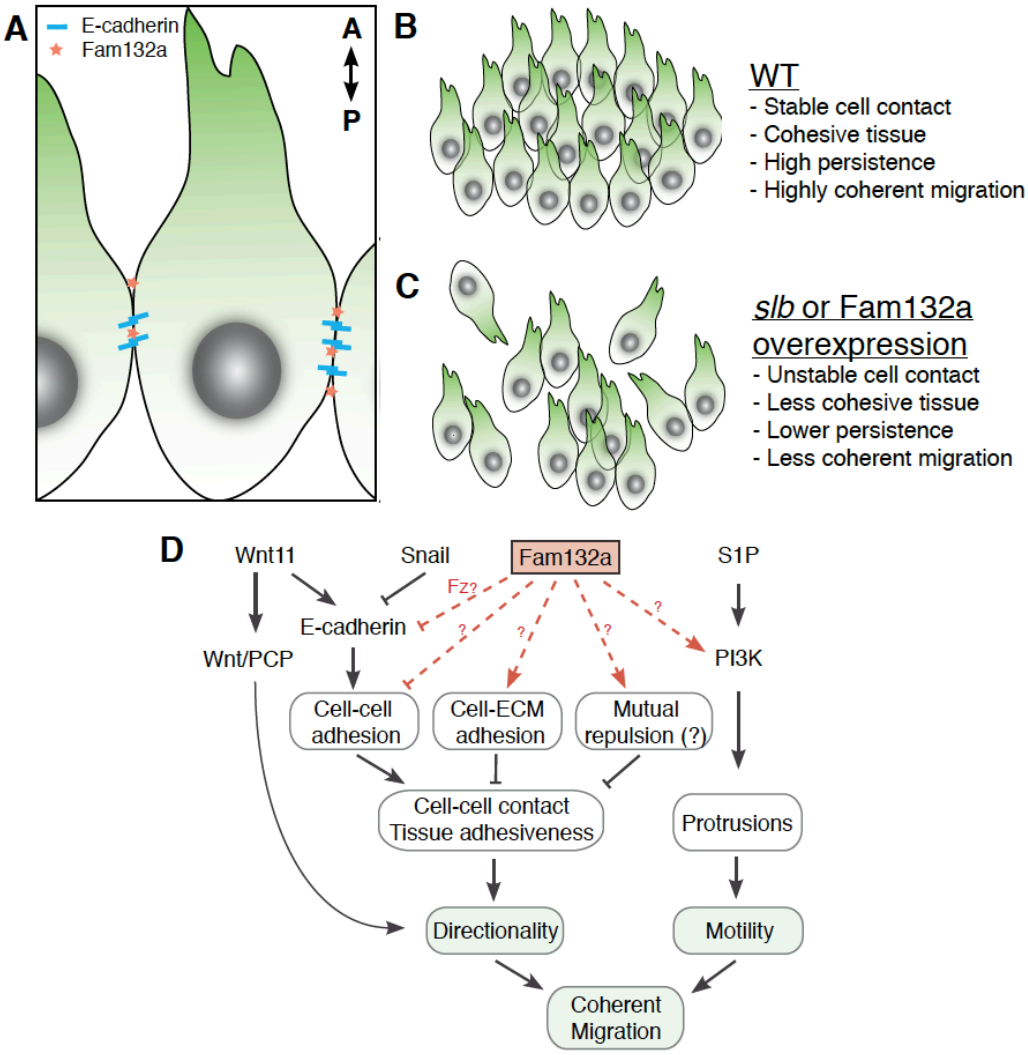

Figure 3.9 Model of Fam132a regulating collective prechordal plate migration. (A) E-cadherin contributes to cell adhesion among zebrafish PPP cells. Fam132a is likely to localize extracellularly. (B) PPP cells normally move coherently toward anterior as a cohesive group. In both *slb* and Fam132a-overexpressing embryos cells lose their ability to maintain contact, and their migration is less persistent and coherent. Loss of *fam132a* function could partially suppress cohesion and migration defects of PPP cells in *slb* embryos. (D) Potential mechanisms by which Fam132a regulates tissue cohesiveness and coherent migration (black arrows, known components/pathways in PPP cell migration; red arrows, potential functions of Fam132a). See Discussion for details.

defects will help identify existing and/or novel genes and processes underlying C&E gastrulation movements. In this study, using microarray gene expression profiling of control WT and *stat3* morphant gastrulae, we identified six candidate C&E regulators, and report functional analyses of Fam132a. We demonstrate that this conserved secreted C1q domain-containing molecule mediates the collective anterior migration of the zebrafish prechordal plate precursors by negatively regulating the cohesiveness and integrity of tissue (Figure 3.9).

3.4.1 *fam132a* Nonsense Mutations Are Non-Phenotypic during Zebrafish Embryogenesis

By comparing gene expression profiles in WT control and *stat3* morphant gastrulae, we identified Fam132a as a downstream effector of the *stat3* morpholino during zebrafish gastrulation. We validated using RT- and qRT-PCR that *fam132a* was downregulated in *stat3* morphants (Figure 3.2C, Table 3.1), but its expression is not affected in MZ*stat3* embryos throughout early development (Figure 3.2D). qRT-PCR revealed that *fam132a* is both maternally and zygotically expressed throughout embryogenesis. WISH further showed that *fam132a* transcripts reside in the dorsal side of the gastrulae, in particular in the anteriormost and posteriormost of the extending axial mesoderm (Figure 3.2), indicating its potential roles in gastrulation. Given that excess and reduction of function of many gastrulation regulators interfere with gastrulation movements (Yin et al., 2009), we carried both gain- and loss-of-function studies of Fam132a. We observed severe patterning and morphogenetic defects upon overexpression of Fam132a in the zebrafish gastrulae. However, both Z*fam132a* and MZ*fam132a* single mutant embryos are viable with no overt developmental defects (data not shown) and can grow to fertile adults, indicating *fam132a* is not essential for gastrulation or

embryogenesis. In a sensitized background such as *slb* mutant embryos harboring a mutation in the zebrafish *wnt11* gene, however, we did observe morphogenetic and cell behavioral phenotypes associated with *fam132a* (Figures 3.6-3.8), indicating a facilitating role of endogenous Fam132a during zebrafish gastrulation.

Although careful morphometric analyses remain to further test if *fam132a* plays any role in gastrulation movements, we explored the possibilities of mild-to-no phenotypes seen in *fam132a* loss of function and found redundancy as the most likely reason. Fam132a belongs to a large C1q family conserved in invertebrate and vertebrate genomes. 32 C1q containing open reading frames (ORFs) have been identified in human, and 52 found in zebrafish (Carland and Gerwick, 2010). The globular C1q domain shared by all family members is also found to share structural similarity with the multifunctional tumor necrosis factor (TNF), hence the C1q-TNF superfamily (Ghai et al., 2007). Besides structural and functional similarities to various extends among all family members, there are also a few closely related members including *fam132b*.

The murine Fam132b, or Ctrp15, is a myonectin mediating a cross-talk between skeletal muscle and other tissues to enhance lipid uptake in adipose tissue and liver (Seldin et al., 2012). Whereas the zebrafish *fam132b* homolog has not yet been characterized, it is predicted to encode a secreted protein of 294 amino acids, with 31% amino acids identical to Fam132a in protein sequence (Figure 3.10A). Similar to Fam132a, it is also comprised of a signal peptide at the N-terminus, a C1q domain at the C-terminus and a stalk in between (Figure 3.11B). Maternal *fam132b* mRNA seems to be quickly degraded around MBT and replaced by zygotic transcripts (Figure 3.10B). While we have not determined the spatial expression pattern of *fam132a* in WT zebrafish blastulae and gastrulae, we did observe its transcripts in the otic vesicle from 1 dpf (Figure 3.10C). We cloned *fam132b* from zebrafish cDNA library synthesized using total RNA

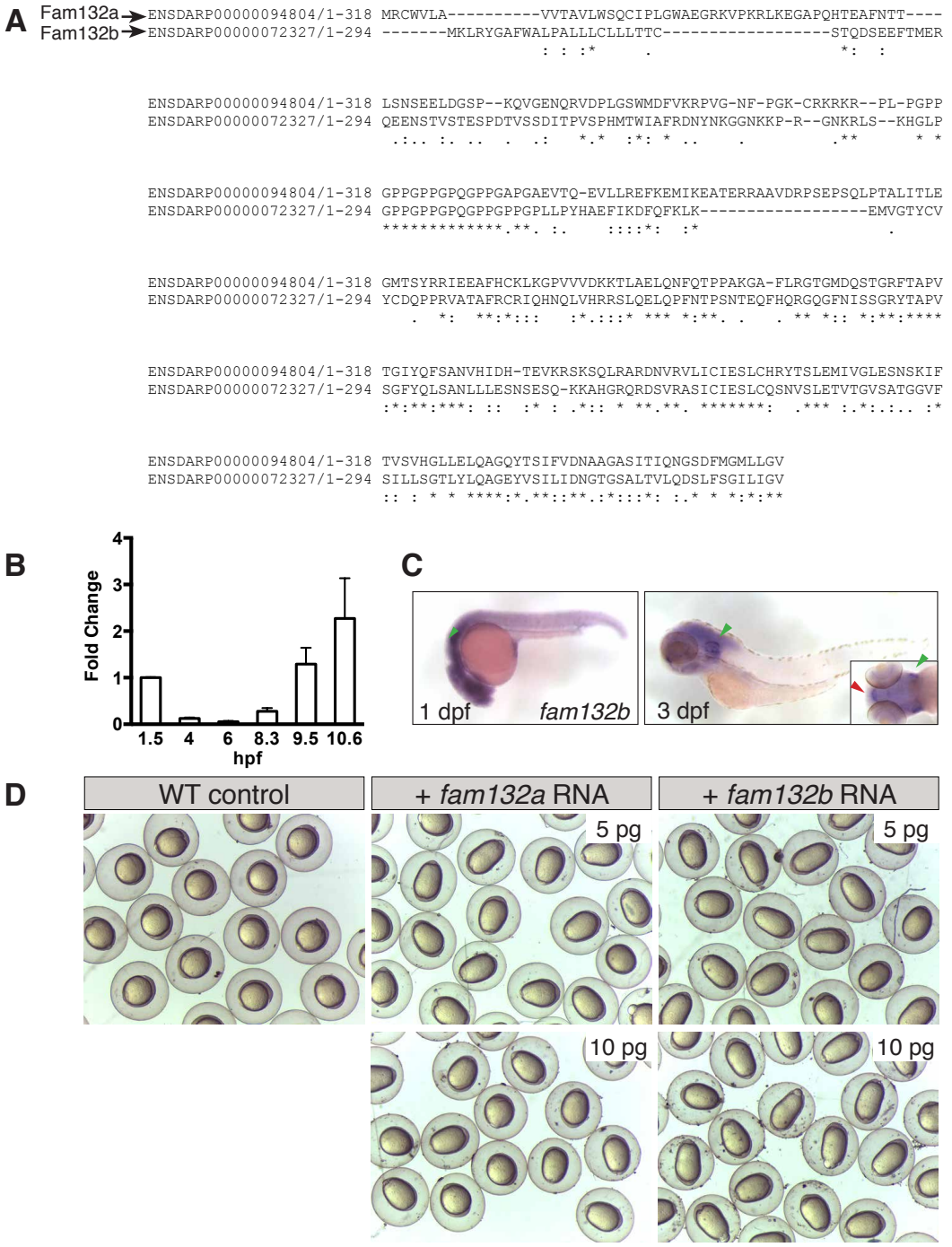

Figure 3.10 Fam132b is a homolog of Fam132a. (A) ClusterW2 alignment of amino acid sequences of zebrafish Fam132a and Fam132b. Asterisk, colon and period indicate fully conserved, strongly similar and weakly similar residues, respectively. (B, C) Expression patterns

of *fam132a* during zebrafish embryogenesis. (D) Live images of WT control embryos and embryos injected with low doses of *fam132a*, or *fam132b*, or both at early somite stage. (error bars = SEM.)

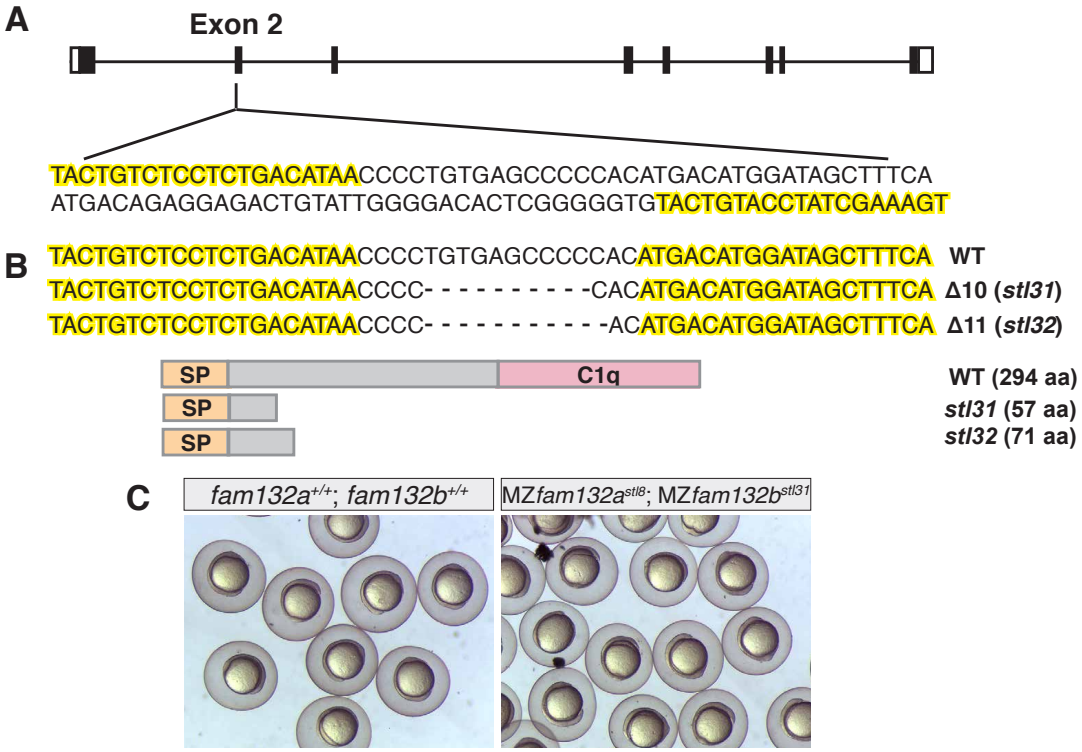

Figure 3.11 Generation of zebrafish *fam132a*; *fam132b* compound mutations. (A) Design of TALEN pair targeting zebrafish *fam132b* gene. (B) Sequence alignments and domain diagrams of encoded proteins of *stl31* and *stl32* alleles. (C) Live images showing control and MZ*fam132a*; MZ*fam132b* compound mutant embryo at early somite stage.

extracted from 1-somite stage WT embryos. Injection of *fam132b* synthetic RNA into 1-cell stage embryos led to a much more severe dorsalization phenotype compared to *fam132a* overexpression (Figure 3.10D, Figure 3.3). We generated TALEN-based zebrafish *fam132b* mutants, *stl31* and *stl32*, containing 10- and 11-base pair deletion in *fam132b* coding region, and are predicted to encode truncated protein of 57 and 71 amino acids long, respectively (Figure 3.11A-B). Our initial results showed that single mutants Z*fam132b* and MZ*fam132b* undergo normal gastrulation and embryogenesis. We also observed that MZ*fam132a*; MZ*fam132b* compound mutants developed to adulthood (data not shown), suggesting that other genes may compensate for the functions of these secreted peptides in zebrafish development (Figure 3.11C). Indeed, it was reported that in a large-scale phenotypic analysis of more than 1,000 zebrafish protein-coding genes, only less than 10% nonsense and critical splice site mutations showed embryonic phenotypes, and paralog redundancy due to teleost-specific genome duplication is considered one of the most significant contributors (Kettleborough et al., 2013). However, any mild and/or transient gastrulation defects in either single or compound *fam132a* and *fam132b* mutants cannot currently be excluded and further morphometric and patterning analyses are warranted.

3.4.2 Fam132a in Adhesion and Migration

We propose in this study that Fam132a regulates the collective migration of the zebrafish PPP cells during gastrulation by destabilizing cell-cell contacts. During zebrafish gastrulation, PPP cells migrate coherently as a cohesive group with cells maintaining contacts with neighbors (Tada and Heisenberg, 2012). Overexpression of Fam132a led to dispersion of PPP cells, loss of cell contact maintenance, loss of integrity of the tissue, decreased coherence in their anterior migration with reduced directionality persistence, and hence morphogenetic defects in the

prechordal plate (Figures 3.4-3.5). Whereas loss of *fam132a* function did not affect PPP cell migration or gastrulation in general, it partially suppressed the cell contact persistence defect reported in the MZ*slb/wnt11* mutant PPP cells (Witzel et al., 2006), as migration of PPP cells in MZ*slb/wnt11*; MZ*fam132a* double mutant gastrulae was more persistent and coherent (Figure 3.7). Adhesion and cell migration are conserved roles of C1q and its members. As early as over two decades ago, people discovered C1q as a mediator of cell-ECM adhesion for human fibroblasts partially through its binding to the fibroblast C1q receptor (Bordin et al., 1990). Such C1q-mediated cell-matrix adhesion and spreading was later reported critical for human endothelial cells (Feng et al., 2002) and trophoblast invasion (Agostinis et al., 2010).

To better understand the mechanisms by which Fam132a regulates zebrafish PPP cell adhesion and collective migration, it will be important to identify its receptor(s) expressed on the surface of PPP cells. So far no receptors have been reported for Fam132a. However, some clues are provided by previous studies on C1q. Several cell surface receptors have been implicated in C1q or C1q domain containing molecule-mediated adhesion, including C1q receptor (gC1qR) (Feng et al., 2002), adhesion G-Protein Coupled Receptor (aGPCR) Bai3 (Bolliger et al., 2011), adiponectin receptors, $\alpha_2\beta_1$ integrin (Zutter and Edelson, 2007), and $\alpha_4\beta_1$ integrin (Agostinis et al., 2010). Firstly, the functions of zebrafish gCq1R/C1q binding protein (C1qbp) have not characterized. However, its transcripts are observed exclusively in presomitic mesoderm and neural plate (Thisse et al., 2001, ZFIN direct data submission, unpublished), making it a less likely candidate for a Fam132a receptor in zebrafish PPP cell migration during gastrulation. Secondly, *bai3* belongs to Group VII of the aGPCR family along with *bai1a, bai1b*, and *bai2*. Only *bai2* is expressed during early embryogenesis (Harty et al., 2015), with its spatial expression pattern and developmental functions yet to be characterized. Thirdly, due to

similarities between murine Fam132a and Adiponectin, both of which are members of the adipokine family (Wei et al., 2012b), adiponectin receptors might also be able to bind Fam132a. So far functions of adiponectin receptors during animal development have not been described. Three adiponectin receptors have been identified in zebrafish, including *adipor1a*, *adipor1b*, and *adipor2*. *adipor1b* is the only receptor gene expressed during gastrulation (Nishio et al., 2008), with its transcripts accumulating in the prechordal plate and later hatching gland (Thisse et al., 2004, ZFIN direct data submission) as well as other tissues (Nishio et al., 2008). The overlapping expression pattern of *adipor1b* and *fam132a* in the anterior axial mesoderm during gastrulation raises strong possibility that *adipor1b* could be a Fam132a receptor in regulating zebrafish PPP cell migration. Finally, zebrafish *itga2* gene encoding α_2 integrin subunit is maternally and zygotically expressed and has been implicated in angiogenesis in adults (San Antonio et al., 2009). However its spatial expression pattern during embryogenesis is unknown. Four integrin β_1 homologs have been described in zebrafish, including *itgb1a*, *itgb1b*, *itgb1b.1*, and *itgb1b.2* (Wang et al., 2014). Except *itgb1b.2*, all the other three genes are maternally expressed, and all four genes are expressed in the notochord. Despite various expression patterns in other tissues, *itgb1a*, *itgb1b* and *itgb1b.2* share common expression in the otic vesicle with *fam132a* and *fam132b*, suggesting that β_1 integrins are likely receptors for Fam132a in zebrafish. In accordance with this hypothesis, β_1 integrin is also shown to mediate cell-matrix interaction during *Xenopus* convergent extension movements (Davidson et al., 2006).

3.4.3 Potential Mechanisms Underlying Fam132's Role in Tissue Cohesiveness and Integrity

Zebrafish prechordal plate (PP) is a cohesive cell population. However in Fam132a overexpressing embryos, PP lost tissue integrity with cells dispersed around (Figures 3.4-3.5). Tissue integrity arises as a result of the competition among cell-cell adhesion, cell-matrix adhesion (Hegedus et al., 2006) and other processes. In an *in vitro* study, for example, people described the invasion patterns of brain tumor cell lines in 3D matrix by providing different collagen concentrations in the 3D gel and found that increasing collagen level was able to cause dispersion of cells during invasion (Hegedus et al., 2006), similar to inducing epithelial-to-mesenchymal transition (EMT). Epithelial cells form and maintain apicobasal polarity and stable cell-cell adhesion, and are generally less motile; while mesenchymal cells exhibit little cell-cell adhesion and more motile (Montell, 2008). EMT is prevalent in many developmental and pathological processes to promote migratory and invasive properties, and is considered to result from downregulation of cadherin-mediated cell-cell adhesion and upregulation of cell-matrix interaction (Montell, 2008). Zebrafish PPP cells have been suggested to undergo EMT triggered by Liv1-mediated nuclear translocation of Snail (Yamashita et al., 2004). Whether EMT takes place in zebrafish PPP cell migration is controversial, as these mesodermal cells show no clear apicobasal polarity and therefore are not epithelial cells at all times (Montero et al., 2005), arguing against the traditional concept of EMT. However, it is proposed recently that EMT may include a gradation of phenotypes between a typical epithelial status with high-level cell-cell adhesion and a typical mesenchymal status with no cell-cell junctions (Theveneau and Mayor, 2013). Indeed, even migrating PPP cells are not entirely typical mesenchymal cells, as E-cadherin is required to maintain a certain level of cell-cell adhesion between zebrafish PPP cells (Montero et al., 2005) which is necessary for the directionality and coherence of the collective migration of PPP cells (Dumortier et al., 2012; Witzel et al., 2006). It is therefore tempting to

consider that PPP cells normally undergo a switch from a "less mesenchymal" status to a "moderate mesenchymal" status during anterior migration, whereas Fam132a GOF PPP cells appear to be "super-mesenchymal cells" with very low cell-cell cohesion and/or upregulated cell-matrix interaction. Thus, we hypothesize that Fam132a negatively regulates cell-cell adhesion and/or promotes cell-matrix adhesion. In addition, the dispersion configuration of Fam132a GOF prechordal plate could also result from increased mutual repulsion among PPP cells. We will discuss each of these hypotheses and future directions.

a. Cell-Cell Adhesion

Cadherins and cadherin-dependent cell-cell adhesion are crucial for gastrulation from *Drosophila* to mouse (Hammerschmidt and Wedlich, 2008; Takeichi, 1988). Cell adhesion in the zebrafish gastrula including among the zebrafish PPP cells is mainly mediated by E-cadherin (Kane et al., 2005; Montero et al., 2005; Shimizu et al., 2005b), which is tightly regulated at both transcriptional level and post-transcriptional level. Alteration of its expression level (*e-cadherin*/*cdh1* morpholino (Montero et al., 2005), *snail* morpholino and mRNA (Blanco et al., 2007)) or dynamics in cellular distribution (*wnt11*/*slb* mutant (Ulrich et al., 2005)) could both impair anterior migration of PPP cells. To determine if manipulation of Fam132a affects cell-cell adhesion, future studies could focus on analyzing E-cadherin expression level and distribution in WT, Fam132a GOF, MZ*slb*, and MZ*slb*; MZ*fam132a* gastrulae. Cell-cell adhesion could also be assessed with functional assays. First, cell sorting experiment will help assess cadherin activity or adhesion levels between cell groups based on "Differential Adhesion Hypothesis", where cells with different adhesion types or levels when mixed together will sort out and aggregate separately (Steinberg, 2007). Therefore, WT and Fam132a-overexpressing cells could be dissociated and mixed together, and formation of separate aggregates could indicate different

adhesion levels between the two groups of cells; Second, cell-cell adhesion assay involves coating the FN and/or LM containing substrate with WT cells and quantifying the number of Fam132a-overexpressing cells adhering to the WT cell-coated substrate and vice versa, providing a more quantitative tool to assess adhesion differences (Carmona-Fontaine et al., 2011).

More recently, "Differential Adhesion Hypothesis" has been questioned for being insufficient to explain cell-sorting behaviors in the first functional assay described above. Instead, it is proposed that tissue cohesion is influenced by not only cell-cell adhesion but also cortical tension (Hammerschmidt and Wedlich, 2008). In fact, both *intro* and *in vivo* experiments showed that aggregate formation and cell sorting of zebrafish progenitors cells result from a combination of actomyosin-dependent cell-cortex tension under the regulation of Nodal/Transforming Growth Factor β (TGFβ) signaling and cadherin-dependent cell cohesion (Krieg et al., 2008). High cell-cell adhesion, high cell-matrix tension and low cell-cortical tension cause high tissue surface tension. Therefore to dissect contributions of adhesion and cortical tension in cell sorting experiment, besides using cells dissociated from WT control and *fam132a* mRNA-injected embryos, one could overexpress in the embryos dominant-negative (dn) Rho kinase 2 (Rok2), an upstream of actomyosin activity, to abolish potential effects of Fam132 on cortical tension without affecting adhesion (Krieg et al., 2008; Marlow et al., 2002). If control and Fam132a-overexpressing cells aggregate separately in cell sorting experiment independent of dnRok2, it strongly indicates that Fam132a regulates cell-cell adhesion rather than cortical tension. If expression of dnRok2 interferes with cell segregation, it suggests that Fam132a may regulate cortical tension.

b. Cell-Matrix Adhesion

Migrating cells on a substrate require dynamic interactions with the surrounding ECM for adhesion, spreading and deadhesion. C1q family and their receptors have been shown to promote cell-matrix adhesion (Nayak et al., 2010). C1q, a secreted molecule, was proposed to act like a matrix component and stimulate fibroblasts and endothelial cells to adhere to and spread along ECM through its receptor C1qR and β_1 integrin (Bordin et al., 1990; Feng et al., 2002). Similarly, by expressing Fam132a-GFP fusion protein in zebrafish blastulae, we demonstrated that endogenous Fam132a is likely to be secreted to extracellular space (Figure 3.2). To test whether functional Fam132a serves as a matrix protein and promote cell-matrix interactions, cell-substrate adhesion assay should be performed (Humphries, 2001) using WT zebrafish gastrula cells and FN and/or LM-coated substrate with or without Fam132a.

c. Fam132a as a Mutual Repellent

Other than cell-cell and cell-matrix adhesion, a different mechanism, named co-attraction, was recently proposed to regulate the cohesive arrangement of a group of migrating cells. Migrating *Xenopus* and zebrafish neural crest cells are predicted to disperse by nature due to contact inhibition of locomotion (CIL). It is proposed that mutual cell-cell attraction achieved by complement component C3 and its receptor C3R is the main mechanism through which neural crest cells maintain in contact (Carmona-Fontaine et al., 2011). Therefore, the cell dispersion phenotype in GOF embryos suggests that Fam132a is likely to induce mutual repulsion between the migrating zebrafish PPP cells. To further test this hypothesis, groups of PPP cells with or without ectopic Fam132a could be plated in juxtaposition on a FN and/or LM-coated substrate. If WT cells migrate away from the Fam132a-overexpressing PPP cell group, it will be a strong indication that Fam132a is a repellent mediating mutual repulsion within the zebrafish prechordal plate domain during its anterior migration.

d. Fam132a-Frizzeled Interaction

Frizzeled (Fz) is the common receptor of Wnt ligands mediating both canonical and noncanonical Wnt signaling (Angers and Moon, 2009). Activated by Wnt11 ligand, Fz7 together with atypical cadherin Flamingo regulate cell contact persistence in the zebrafish PPP cells (Witzel et al., 2006). Recent evidence also indicates that C1q activates canonical Wnt signaling in mammals via binding to Fz receptors and inducing subsequent cleavage of Wnt coreceptor low-density lipoprotein receptor-related protein 6 (LRP6) (Naito et al., 2012). It is therefore likely that Fam132a competes with Wnt11 in zebrafish PPP cells by binding to Fz receptor, and in turn affects cell contact maintenance and tissue cohesiveness and integrity. This could be further addressed using *in vitro* pull-down experiment determining binding of Fam132a and Fz7, and *in vivo* co-localization experiments detecting protein co-localization of Fam132a-GFP and Fz7-CFP.

e. Fam132a-PI3K pathway

It was recently reported that Fam132a/Ctrp12 activates PI3K-Akt pathway to promote glucose uptake in the murine adipocytes (Wei et al., 2012b). PI3K is a key regulator of outgrowth and polarity of cellular processes during zebrafish PPP cell migration. Elevated PI3K activity led to more numerous and polarized protrusions, and increased cell motility; while inhibiting PI3K activity reduced the number and randomized the orientation of protrusions, decreased cell motility, and hence impaired anterior migration of PPP cells (Montero et al., 2003). Against the notion that Fam132a regulates PI3K activity in PPP cells, manipulation of Fam132a level did not seem to have a significant effect on PPP cell motility (Figures 3.5 and 3.7). Although the prechordal plate domain lost cohesiveness and cells scattered around in Fam132a GOF embryos, cells were still elaborated protrusions (Figure 3.5L). These observations differ from the dramatic

effects of PI3K on protrusion outgrowth and cell motility reported previously (Montero et al., 2003), making PI3K an unlikely underlying mechanism for Fam132a. However, further quantification of protrusion types, lengths, number and orientation will provide insight into whether Fam132a interacts in any way with PI3K in regulating PPP migration.

3.4.4 Fam132a and Planar Cell Polarity

Wnt/PCP signaling is a conserved regulator of ML cell polarization underlying C&E movements during zebrafish gastrulation. Abnormal activity of this pathway impairs C&E movements, including defects in ML cell intercalation defects in the chordamesoderm, and anterior migration of PPP cells (Gray et al., 2011). Our observations showed that excess Fam132a during gastrulation impaired both cellular behaviors, ML intercalation and anterior migration, and hence morphogenetic defects in notochord and prechordal plate (Figures 3.3-3.5). One possibility is that Fam132a regulates PCP during zebrafish gastrulation. However, our morphometric analyses of the notochord cells at the end of gastrulation showed that cell elongation (assayed by LWR), was not affected by Fam132a overexpression. Low to medium doses of ectopic Fam132a also did not interfere with the ML orientation of those notochord cells, although cells were slightly misoriented in embryos injected with the highest dose of *fam132a* mRNA (Figure 3.4). These observations contrast the typically severe cell elongation and orientation defects seen in zebrafish PCP mutants (Jessen et al., 2002), arguing against an involvement of Fam132a in planar cell polarity.

3.4.5 Fam132a in DV Patterning

One intriguing consequence of Fam132a overexpression in zebrafish embryos was dorsalization manifested by elongated embryo shape at early segmentation stages and tail truncations at the

end of embryogenesis (Figure 3.3). Further, we observed significant downregulation of ventrally expressed *bmp2*, *bmp4* as well as *eve1* and *szl* genes that are critical in specification of ventral cell fates (Figure 3.3) (Schier and Talbot, 2005). Strikingly, at early gastrula stage expression of genes downstream of the dorsal β-catenin signaling such as *gsc* and *chordin* remained unaffected in these dorsalized embryos, indicating the dorsalization effect of Fam132a is likely independent of β-catenin signaling (Figure 3.3). Fgf/Mapk signaling in zebrafish is known to regulate DV patterning by downregulating Bmp expression (Furthauer et al., 2004). On the other hand, it was shown that Fam132a/Ctrp12 activates mitogen-activated protein kinase (MAPK) in mouse hepotacytes and adipocytes (Wei et al., 2012a). Therefore, it is plausible that Fam132a acts through Fgf/Mapk signaling to mediate DV patterning.

3.4.6 Other Candidate Targets of *stat3* Morpholino

Fam132a is not the only non-specific target of *stat3* morpholino in controlling the anterior migration of the zebrafish prechordal plate progenitors. In fact, Liv1 (Yamashita et al., 2004) and recently Efemp2 (Zhang et al., 2014) were identified as downregulated in *stat3* morphants and proposed to act as downstream targets of Stat3 in the same process by regulating Snail activity and ECM assembly, respectively. Before further analyses are performed to determine if they are Stat3 targets by detecting their expression levels in the MZ*stat3* mutant embryos, there remains a possibility that they are unrelated to Stat3 signaling and are non-specific targets of *stat3* morpholino instead.

In addition, our microarray analyses identified other candidate targets of *stat3* morpholino (Table 3.1). *cartpt* the functions of which have never been characterized during development of all organisms, for example, led to interesting C&E defects and cyclopia

phenotype when overexpressed (Figure 3.1). Further studies of this gene and other candidate genes may lead to identification of novel signaling pathways underlying zebrafish C&E gastrulation movements.

3.5 Materials and Methods

Zebrafish Strains

Embryos were obtained by natural spawning of AB* or AB*/Tubingen WT, *slb*^{tz216} and *stat3*^{stl27} mutant, *Tg[lhx1a:EGFP]* and *Tg[gsc:GFP-CAAX]* transgenic zebrafish (*Danio rerio*). For strict internal control due to heterogeneity, *in vitro* fertilization was performed to generate MZ*slb*; MZ*fam132a* embryos and MZ*slb* control embryos using the same clutch of eggs collected from *slb*; *fam132a*$^{stl8 \text{ or } stl9}$ females. One half of the clutch was fertilized with sperm samples collected from *slb*; *fam132a* males (hence MZ*slb*; MZ*fam132a* embryos), and the other half with sperm from *slb*; *fam132a*$^{stl8/+ \text{ or } stl9/+}$ males (hence MZ*slb*; M*fam132a*, or MZ*slb* control embryos). Embryos were maintained in 28.5°C and staged according to Kimmel et al. (Kimmel et al., 1995).

Microarray Analysis

Total RNA used for microarray was extracted with Trizol (Invitrogen) method from 90~95% epiboly stage WT control embryos and embryos injected with 10 ng MO1-*stat3* (Yamashita et al., 2002), and treated with RNase (Qiagen). Agilent Zebrafish Gene Expression Array, which carries 34,788 targets representing 16,870 distinct genes based on Zv8 Zebrafish genome (Ensembl and UCSC genome browsers), was performed with two replicates and analyzed by the Vanderbilt Functional Genomics Shared Resource (FGSR) (Figure 1A). Genes that are statistically significantly downregulated by at least two-fold in *stat3* morphants compared to WT

control embryos were identified. About 90% of the genes were poorly characterized at the time of analysis based on Zv9. To identify genes encoding secreted molecules, SignalP, TargetP, and other bioinformatics tools were used to predict the subcellular localization of gene products (Emanuelsson et al., 2007). NCBI-BLAST was also performed to identify candidate genes of which the encoded products have been implicated in cell migration in other organisms (Altschul et al., 1990).

RT-PCR and qRT-PCR

Total RNA was isolated from 30-50 zebrafish embryos with Trizol (Ambion) at indicated stages. cDNA was synthesized with iScript kit (Bio-Rad). Gene-specific primers that amplify 130-240 base-pair fragments and preferentially span exon-exon junctions were designed and listed in Table 3.2. RT-PCR was performed with GoTaq Flexi DNA polymerase (Promega); qRT-PCR was performed using CFX Connect Real-Time system and SYBR green (Bio-Rad) with at least three independent biological samples for each experiment.

Cloning of Candidate Genes, RNA Synthesis and Injection

Full length sequences coding *arrdc3l* (zgc:110353), *he1a* (ZFIN:ZDB-GENE-021211-3), *cartpt* (ZFIN:ZDB-GENE-060503-15), *tmsb* (ZFIN:ZDB-GENE-050307-5) and *fam132b* (ENSDARG00000055498.5) were amplified from cDNA synthesized as described above using primers listed in Table 3.3 and high fidelity PfuUltra II Fusion HS DNA polymerase (Agilent Technologies), and cloned into pENTR and subsequently pCSDest2 vector with Gateway LR clonase II (Invitrogen). Full length sequences coding *sumpf2* (ZFIN:ZDB-GENE-041010-55) and *fam132a* (ZFIN:ZDB-GENE-061215-120) were amplified and subcloned from *Sumf2*-

pExpress1 and *fam132a*-pCMVSPORT6.1 cDNA plasmids (OpenBiosystems) into pCS2 vector using primers listed in Table 3.3.

Constructs encoding Fam132a-GFP or Fam132a-6xMyc fusion proteins were synthesized with multi-way Gateway cloning method and Gateway LR clonase II Plus enzyme (Invitrogen). Reverse primer that excludes the endogenous stop codon (ΔStop) in the *fam132a* sequence was used (Table 3.3).

Capped RNAs were synthesized from linearlized pCSDest or pCS2 constructs containing full-length cDNA sequence of genes of interest using SP6 mMessage mMachines kit (Ambion), and injected into zebrafish embryos at 1-cell stage. For gain-of-function (GOF) screening, a dose ranging from 50 pg to 300 pg of RNA was injected. 100 to 300 pg of *fam132a*, *fam132a-GFP*, and *fam132a-6xMyc* synthetic RNA was injected for overexpression experiments.

Generation of *fam132a* and *fam132a* Mutant Lines

Joung Lab REAL Assembly (Sander et al., 2011)- and Golden Gate (Cermak et al., 2011)-based Transcription activator-like effector nuclease (TALEN) method was used to generate mutations in *fam132a* and *fam132b* target sequences, respectively. For *fam132a,* a TALEN pair was designed to target Exon 1 (TALEN arm sequences: 5'-TTCAACACCACTCTTT-3' and 5'-TACCTTTGGGCTGCCATC-3') and span a BseRI restriction site. One-cell stage F0 embryos were injected with 35-105 pg of each synthetic TALEN RNA, and at 24 hpf analyzed for lesions in the target *fam132a* sequence using BseRI digestion. A subset of F0 embryos was raised to adulthood and outcrossed to WT to generate F1 fish. From those F1, two alleles, *stl8* and *stl9*, were identified and confirmed by sequencing as containing a 7-base pair deletion and 14-base pair deletion in combination with addition of 3 base pairs in Exon 1, respectively, which caused

frameshift and premature stop codons in the *fam132a* gene. They are predicted to encode proteins that are 73 and 58 amino acids long, respectively. Both alleles can be identified using PCR-based genotyping (forward primer 5'- AAGGTGCCTAAGAGGCTGAAG-3', reverse primer 5'-CGAGCTGCTGTATAGCCCTAA-3') followed by BseRI digestion. Alternatively, *stl8* can be identified via PCR using allele-specific primers that span the deletion site (common forward primer 5'-GAGCCAGTGCATCCCTCTAGGGTG-3', WT allele reverse primer 5'-TGGGGCTGCCATCCAGCTCCTC-3' (annealing temperature = 65°C), *stl8* allele primer 5'-CTTTGGGCTGCCATCCAGCTGTT-3' (annealing temperature = 67°C)). WT allele specific primers are not able to amplify *stl8* allele under certain condition (for example, 65°C as annealing temperature) and vice versa. By directly dissolving PCR products on an agarose gel, *stl8* heterozygous and homozygous animals can be identified. *stl9* can be genotyped using the same method (common forward primer: same as *stl8*, WT allele reverse primer 5'-CAGCTCCTCGCTGTTGGAAAGAGTGGTG-3' (annealing temperature = 65°C), *stl9* allele reverse primer 5'-CTGCCATCCAGCAGTGGTGTTGGTG-3' (annealing temperature = 66°C)).

Fam132b TALEN pair was designed to target Exon 2. The targeting sequences for the TALEN arms are 5'-TACTGTCTCCTCTGACATAA-3' and 5'-TGAAAGCTATCCATGTCAT-3', between which a BanII restriction site was used for genotyping (Figure 9E). 18-56 pg of each synthetic TALEN RNA was injected into F0 embryos. F1 progenies were raised and screened for mutations in *fam132b* gene as described above. *stl31* and *stl32* alleles contain a 10-base pair and a 11-base pair deletion in Exon 2, and are predicted to encode truncated proteins of 57 and 71 amino acids long, respectively. Both alleles can be genotyped using PCR amplification (forward primer 5'-AAGGTGCCTAAGAGGCTGAAG-3', reverse primer 5'-CGAGCTGCTGTATAGCCCTAA-3') followed by BanII digestion.

Probe Synthesis and Whole-Mount *in situ* Hybridization

Digoxigenin (DIG)- or Fluorescein-labeled antisense probes were synthesized using RNA labeling kits (Roche). pCSDest2 and pCS2 constructs containing genes cloned as described above were used as templates, and T7 polymerase was used for probe synthesis. Embryos were fixed in 4% paraformaldehyde (PFA). Whole-mount *in situ* hybridization was carried out as described (Thisse and Thisse, 2008)

Whole-Mount Immunostaining

Embryos were fixed in 4% PFA. Immunostaining was carried out using a standard protocol. Primary antibodies used were: anti-Myc-tag (9B11) antibody (1:500, mouse, Cell Signaling, #2276), anti-β-catenin (H-102) antibody (1:1,000, rabbit, Santa Cruz, sc-7199). Secondary antibodies used were Alexa Fluor 488 goat anti-mouse (1:500, Invitrogen) and 568 goat anti-rabbit (1:500, Invitrogen). Embryos were mounted in 0.75% low melting temperature (LMT) agarose (Lonza) and imaged with the Quorum spinning disk confocal microscope (SDCM, Olympus).

Morphometric Analyses

WT embryos injected with 200 pg *membraneEGFP* (*mEGFP*) RNA at 1-cell stage, or *Tg[lhx1a:eGFP]* transgenic embryos, were injected with 150 to 300 pg of *fam132a* RNA for overexpression experiments. Embryos were mounted in 0.5% LMT agarose and imaged on Quorum SDCM at 1-somite stage (10.3 hours postfertilization (hpf)) using 40x and 20x objectives, respectively. A z-stack was acquired at a step size of 0.5 μm and the top layer of the notochord cells were analyzed for cell shape and orientation in Fiji (Jessen et al., 2002).

Time-Lapse Imaging

For subcellular localization of Fam132a-GFP fusion protein, embryos were injected with *fam132a-GFP* synthetic RNA at one-cell stage and mounted in 2% methylcellulose. Time-lapse movies were taken using Quorum SDCM and a 60x objective lens every 15 seconds for 5 minutes. For mosaic expression of Fam132a-GFP protein, one blastomere in 64-cell stage embryos was coinjected with RNA encoding Fam132a-GFP and H2B-RFP. H2B-RFP-positive clones were mounted and imaged similarly.

To monitor C&E of the axial mesoderm, control and *fam132a* RNA injected *Tg[lhx1a:eGFP]* embryos were mounted at shield stage (6 hpf) in 0.5% LMT agarose, and imaged with a 10x objective every 3 minutes for about 6 hours at 28.5°C maintained by a stage heater. At each time point, a z-stack covering 200 μm at a 3 μm step distance was acquired. Z projection was obtained for each time point on MetaMorph, and image segmentation including "Gaussian Blur", "Minimum" and "Unsharpen mask" was performed in Fiji to detect individual cells, as cell bodies and edges were not sharp enough for subsequent analysis due to relatively weak and uneven cytoplasmic labeling of GFP. Cells that ended up in the notochord at the end of the movies were tracked backwards to mid-gastrula stage, and trajectories were generated in Fiji.

For analysis of PPP cell migration in Fam132a GOF experiments, *Tg[gsc:GFP-CAAX]* embryos with GFP specifically labeling the membranes of PPP cells were used. Control and Fam132a-overexpressing embryos were mounted in 2% methylcellulose and imaged on Quorum SDCM (40x objective). Time-lapse movies were captured at a single z plane every 15 seconds for 20 minutes at different stages during gastrulation. PPP cells were manually tracked in Fiji

using “Manual Tracking” plugin. Coordinates of each cell at each time point were collected and subsequently analyzed in Matlab.

PPP cell migration was also monitored with DIC time-lapse movies. WT, MZ*slb*, MZ*slb*; MZ*fam132a*, and MZ*slb* embryos injected with low dose (5 pg) of *fam132a* were mounted at shield stage (6 hpf) in 0.5% LMT agarose. Movies were taken from 60% epiboly stage (about 6.5 hpf) for 30 minutes with a 40x DIC objective at one-minute interval. At each time point a z-stack covering 30 μm at a step size of 1.5 μm was acquired. The first two to three rows of PPP cells were manually tracked in Fiji and late analyzed in Matlab for multiple migration parameters.

PPP Cell Migration Analyses

Coordinates of tracked cells at different time points were collected and analyzed for speed, persistence and coherence as previously described (Kai et al., 2008). Net speed (μm/min) was measured as the total distance a cell traveled during the course of the movie (i.e. 20 minutes for overexpression/*Tg[gsc:GFPCAAX]* fluorescent time-lapse movies, and 30 minutes for *slb* and *fam132a* mutant DIC time-lapse movies) divided by total time; Persistence was calculated as the ratio of net distance over gross distance a cell traveled every 10 minutes; Coherence^{-1} was a parameter measuring the change of relative positions within each cell pair every 10 minutes by taking both speed and direction into account. If n cells were tracked in a movie, and coherence^{-1} was calculated for each cell within a random cell pair, considering there were n(n-1)/2 cell pairs, n(n-1) different foherence^{-1} values would be generated. Median was used to represent the total coherence^{-1} for every 10 minutes analyzed. Speed, persistence, coherence and trajectory were written in scripts and analyzed using Matlab.

Statistical Analyses

Data were collected in Excel (Microsoft) and Matlab (Mathworks), analyzed and graphed in GraphPad Prism (GraphPad Software) and Matlab. Student's *t* test was used to determine statistical significance ($p<0.05$) between two datasets. Kolmogorov-Smirnov test was applied to compare distributions of two cell orientation/angle datasets. All results are shown as Mean±SEM.

Acknowledgement

We thank Dr. Masa Tada for the *Tg[gsc:GFPCAAX]* transgenic line, Dr. Isabella Roszko for comments on the manuscript, Dr. Yuecheng Shen for Matlab help, and the LSK lab for advice. This project was supported by NIH grant RO1 GM55101.

Table 3.2 Nucleotide sequences of RT- and qRT-PCR primers

Primer	Forward Sequence (5'-3')	Reverse Sequence (5'-3')
arrdc3l	TAACATCGCTTACGGTGCAG	AGATGGCAGACTTTGGTTGG
nos2b	CAGGAGGATCACAGACAGCA	GTCAGGAGAGGAGCTGATGG
papl	TCAGTCCATCGCTGCTTATG	CCAGGCCGTATTCCAGATAA
tmsb	CGACAAACCCAACATGACTG	ACGGTGTGGACTCTCCTTGT
ntn1b	GGGACCAGAGTGTGACAGGT	TTCAGGCAGACTCCTCCACT
cpa2	GAACCGTCCCATGTATGTCC	GGTGGGAGAAGACGTATCCA
cartpt	ACGGAAGCGACAAGAGATGT	AGGGTGAGGTCACAATGTCC
col7a	CAGCTGGAGATTCTGCTTCC	TATCGGCTTCCCATCTTGTC
gpm6aa	CATTTGCCAAAACACCACTG	GGCAGACAGAACCATCAGGT
ccdc88ab	CAGCAGGAGTCATCAGGACA	CCTTCAGCTTGGAGAAGTCG
fetub	GAATTTGCGCACAAAGGATT	GTTTTGGTGTGATCGTGTGC
osbpl3a	AGGCCGGACCAAAGATTACT	ATCCTTCCTGAGCTCCCAAT
he1a	GTGGTCTCCCTCAACAGGAA	GCCGTTTTTCCATAGTGCAT
dpysl5a	CCTGCATATGGGAGTGACCT	GCCACAGCACCAATATCCTT
dsg4	TGTTGCAGCATCCTTGAGTC	CTGGATGGTGCTAGTGCTGA
fam132a	TGTGGTCGTGGACAAAAAGA	GGACGTTGTCTCTGGCTCTC
p4ha2	ACTGTCAGGAGCTGGGCTAA	CATCCTCCTCATCTGGGAAA
stx2	GGCGAATTATCAGCCCACTA	TCATTGCCAAACAGCTCAAG
sumf2	GGACTGGAAGGCAGGTCATA	CTGAGCTCCAGGAAAACTGG
p2y	TCACCCTTCCGTTTCTCATC	TGGGTGTTCAACAAGGACAA
fam132b	CTATGGAGCGTCAGGAGGAG	GGAAGACCATGCTTGGAGAG
bmp2b	GGAGACACACACCGGAGCGAAC	ACAGTGCCTCGAAAGCCTCTTCG
bmp4	CCATCATGAAGAGCACCTGGAGGA	TCCCGTGGCGCCTTTAACACC
chd	GGGCTCGACAGGGGAAGTGC	TGACGCCATGGTCACACCAGC
szl	AACGACTTCGCGGTGAAGGTGA	CGATGGATCCACCAGCACGCA
gsc	TCGGTGAATGGAAGGATAGG	GCTGTAGCTCGGTTCTGGAC
gapdh	GATACACGGAGCACCAGGTT	GCCATCAGGTCACATACACG

Table 3.3 Nucleotide sequences of cloning primers

Primer	Forward Sequence (5'-3')	Reverse Sequence (5'-3')
arrdc3l	CACCATGACTATCCGGAACTTCGCC	TTAATTGGAAATCTTCATTTTTGCAAGGTCTGGGT
he1a	CACCATGGACATAAGAGCTTCCCTCT	TTAGCATCCATACAGCTTATTGATCCTGAGGA
cartpt	CACCATGTCAAATTTATCAATACTTGTCGTCGTGCTG	TCACAATGTCCATAAAAAGAAATGAGAGCACTTTGATCG
tmsb	CACCATGGCCGACAAACCCAACAT	TCACGGTGTGGACTCTCCTTGTCTC
fam132a	CACCGGATCCatgcgttgctgggtactagctG	CTCGAGctatacacccaacaaCATGCCCATGAA
fam132a C-tagged	/	ctcgagTACACCCAACAACATGCCCATGAAATC
fam132b	CACCGGATCCatgaagctcagatatggggcattttgggca	CTCGAGtcatactccaataaggatgccagaaaacagactgtc

Chapter 4

Discussion

Stat3 transcription factor is a key regulator of cell proliferation, differentiation, survival and migration in numerous developmental, physiological and pathological processes. Genetic inactivation of murine *Stat3* gene results in embryonic lethality at early gastrulation (Takeda et al., 1997). In zebrafish, based on morpholino oligonucleotide-mediated translation interference, Stat3 was proposed to regulate C&E gastrulation movements that shape the embryonic body (Yamashita et al., 2002). These observations imply some critical but yet undefined roles of Stat3 during vertebrate gastrulation. In this thesis work I clarified the function of Stat3 during zebrafish gastrulation; I generated mutations in zebrafish *stat3* locus to reveal its contribution to extension movements during gastrulation through positive regulation of cell proliferation before and during gastrulation. In addition, using *stat3* morpholino that is known to induce Stat3-independent severe C&E phenotypes, I identified several novel regulators of zebrafish C&E movements including Fam132a, a secreted cell contact inhibitor mediating collective cell migration during gastrulation.

4.1 Cell Proliferation – a Conserved Role of Stat3 in Animal Development

Prior to my studies, several efforts had been made towards functional analysis of Stat3 in vertebrate embryogenesis. The fact that genetic disruption of mouse *Stat3* gene leads to early embryonic lethality hinders investigations of Stat3 function during mouse embryogenesis (Takeda et al., 1997). Zebrafish studies using antisense morpholino oligomers interfering with *stat3* translation proposed that it plays a non cell-autonomous, PCP-dependent role in ML cell elongation underlying dorsal convergence movements of lateral mesoderm, and a cell-autonomous role in anterior migration of PPP cells (Miyagi et al., 2004; Yamashita et al., 2002). In contrast, my studies of zebrafish *stat3* mutants argue against a requirement for Stat3 function in convergence movements or regulation of Wnt/PCP signaling. Rather, maternal and zygotic Stat3 function contributes to axis extension during gastrulation by regulation of cell proliferation, in part through transcriptional activation of *cdc25a* gene (Chapter 2). In particular, Stat3 promotes extension of dorsal tissues by ensuring that sufficient numbers of cells are engaged in ML and radial cell intercalations that drive extension of chordamesoderm ((Glickman et al., 2003; Keller et al., 2000; Topczewski et al., 2001; Yin et al., 2008).

Cell cycle control is a well-established role of Stat3 in cancer (Carpenter and Lo, 2014). It is interesting that out of many proposed roles of Stat3 in cell migration, during zebrafish gastrulation it employs cell cycle regulation, an "old" and simple function of Stat3 signaling, as the main mechanism by which it regulates morphogenesis. In fact, some clues Stat3 regulating proliferation during animal development have been provided by previous studies. First, although *Stat3* knockout mouse embryos die by early gastrulation, when cultured *in vitro*, *stat3-/-*

blastocysts showed much less inner cell mass expansion compared to WT (Takeda et al., 1997). Second, Stat3 was shown to regulate cell cycle progression in *Xenopus* neural crest development (Nichane et al., 2010). Third, *Drosophila* Stat92E promotes epithelial cell proliferation in the second instar larval wing disc development, a function similar to vertebrate interleukin-stimulated Stat3 (Mukherjee et al., 2005). Finally, my studies also suggest a continuous requirement of Stat3 for cell proliferation throughout zebrafish development, as *stat3*-deficient animals exhibited severe growth retardation from late larval stage; although cell proliferation at these later stages needs to be experimentally addressed (Chapter 2, Figure 2.1).

Similarly, positive regulation of cell proliferation is a conserved role of Cdc25a phosphatase in development and disease (Boutros et al., 2007). Cdc25a has been shown to be a key cell cycle regulator during embryogenesis in both invertebrates and vertebrates (Bouldin and Kimelman, 2014; Dalle Nogare et al., 2009; Edgar and Datar, 1996; Edgar and O'Farrell, 1990; Kim et al., 1999). Like *Stat3* mutants, mouse *Cdc25a* mutant embryos die by early gastrulation, and *in vitro* cultured blastocysts also failed to expand their inner cell mass (Lee et al., 2009). Moreover, zebrafish *standstill*/*cdc25a* mutants lacking zygotic function show G2 arrest and morphogenetic defects at about 1 dpf (Verduzco et al., 2012). It would be interesting to characterize the potential phenotypes upon loss of both maternal and zygotic *cdc25a* function during gastrulation. Despite the well-established roles of Cdc25a in animal embryogenesis, it was not clear however, how maternal and zygotic Cdc25a function was transcriptionally activated in these animals. My study points to Stat3 as a transcriptional activator of Cdc25a during development. The same Stat3/Cdc25a pathway has also been implicated in cell cycle regulation in cancer with STAT3 directly binds to *CDC25A* promoter and activates its expression

(Barre et al., 2005). It would be worthwhile to test if Cdc25a is a direct target of Stat3 transcription factor in zebrafish development in future studies.

Together, my results support the notion of Stat3/Cdc25a pathway serving as a universal regulator of cell proliferation and morphogenesis during animal development. It will be interesting to investigate in zebrafish if such function of Stat3/Cdc25a pathway is conserved and critical for animal survival in late development.

Nevertheless, Cdc25a is likely just one of the effectors of Stat3 signaling in cell cycle regulation during zebrafish development, as several other cell cycle regulators including Cyclin D were also significantly downregulated in MZ*stat3* mutants at transcriptional level (Figure 2.13). Besides cell proliferation, zebrafish Stat3 may also regulate other processes important for gastrulation via unknown mechanisms, including cell elongation (Chapter 2). Whereas MZ*stat3* gastrula cells are rounder that their WT counterparts, it remains unclear whether this abnormal shape impairs their migration and ML intercalation behaviors during zebrafish C&E movements. One possible mechanism Stat3 could utilize to shape gastrulating cells comes from its transcription-independent role. In mouse keratinocytes and fibroblasts cytoplasmic Stat3 regulates microtubule and actin cytoskeleton through its interaction with Stathmin, a microtubule-destabilizing protein, and small Rho-GTPases, respectively (Ng et al., 2006; Teng et al., 2009). It would also be interesting to identify other downstream effectors of Stat3 in these processes by comparing gene expression profiles between WT and MZ*stat3* embryos using RNA-Seq.

4.2 Cell Proliferation Promotes Axis Extension

The causal relationship between cell proliferation and morphogenesis remains a matter of debate. Even in plant biology, where cell proliferation is closely associated with leaf morphogenesis (Laufs et al., 1998), this causal link has been questioned with evidence from studies using transgenic plants that disruption of cell division rate did not interfere with the establishment of base elements of plant structures despite reduction of total plant size (reviewed in (Fleming, 2006)).

During animal embryogenesis, cell proliferation has been generally considered dispensable or even prohibitive for gastrulation movements and morphogenesis as discussed in Chapter 2. My study, however, has provided evidence for a small but significant contribution of cell proliferation to zebrafish morphogenesis, as Stat3/Cdc25a-dependent cell proliferation promotes AP extension of both the axial and paraxial mesoderm during gastrulation (Section 2.4, Chapter 2). In accordance with plant studies, cell proliferation does not play an essential role during zebrafish gastrulation, as embryonic tissues were still able to converge and extend without Stat3 function and mutant embryos completed embryogenesis with grossly normal morphology. Instead, proliferation contributes to normal morphogenesis most likely because it provides sufficient building blocks necessary for intercalation-based extension.

4.3 Morpholino – not a Reliable Loss-of-Function Tool in Zebrafish?

Previous studies on zebrafish *stat3* in C&E gastrulation movements employed antisense morpholino oligonucleotide to interfere with its translation (Yamashita et al., 2002). That a co-injection of *stat3* RNA, a generally accepted approach for verification of morpholino specificity,

was also able to rescue *stat3* morpholino-induced C&E phenotypes, provided support for their specificity (Yamashita et al., 2002). Such severe C&E defects reported for *stat3* morphants were not confirmed by TALEN-based genetic disruption of both maternal and zygotic Stat3 function (Chapter 2), indicating the non-specificity of *stat3* morpholino and adding to the recent growing concerns about using morpholino as a reverse genetic tool.

Typically, morpholinos are synthetic 25-base nucleotide oligonucleotides with six-ring heterocycle backbone (a morpholine ring rather than deoxyribose), and are linked via nonionic phosphorodiamidate linkages rather than phosphates (Summerton and Weller, 1997). They are commonly delivered into zebrafish embryos via a microinjection at 1-cell stage and are supposed to bind specifically to the target gene to block translation or splicing (Nasevicius and Ekker, 2000). Over the past decade, people have used morpholinos as a convenient and straightforward tool for gene knockdown in the zebrafish embryos. However, there are growing concerns that morpholinos frequently induce p53-dependent apoptosis (Robu et al., 2007) and off-target effects that obscure the real phenotypes associated with target genes. Indeed, *stat3* morphants (i.e. embryos injected with 10 ng of MO1-*stat3* morpholino) in our hands displayed not only severe C&E impairment but also a general developmental delay and necrosis, and subsequently died at 1 dpf (data not shown). Further arguing that *stat3* morphant phenotypes are not specifically caused by loss of Stat3 expression, these defects could not be rescued by injecting synthetic RNA Stat3-Flag fusion protein that rescued aspects of MZstat3 mutant phenotype. A recent study compared morpholino-induced and mutant phenotypes for a large group of zebrafish genes, and found that approximately 80% of the morphant phenotypes were inconsistent with the respective mutant phenotypes, a striking result that underscores the concerns about using morpholino for zebrafish studies (Kok et al., 2015). Even more worrisome, several genes such as

megamind, the morphants of which displayed severe phenotypes and could be rescued by coinjection of synthetic RNA, turned out to be genetically dispensable for development (Ulitsky et al., 2011). Zebrafish Stat3 has been reported to function in neuronal pathfinding (Conway, 2006), hair cell regeneration (Liang et al., 2012), retina regeneration (Nelson et al., 2012), etc. We consider our zebrafish *stat3* mutant a reliable tool to verify these functions of Stat3.

4.4 All about Adhesion?

The discrepancy between *stat3* morpholino-induced and mutant phenotypes in zebrafish suggests the C&E defects in *stat3* morphants are likely due to off-target effects. In this thesis we sought for factors downregulated in *stat3* morphants during zebrafish gastrulation and report identification of several such genes and the functional characterization of one such gene, *fam132a*, in the collective migration of PPP cells (Chapter 3). Fam132a or C1qdc2, a member of the large C1q/TNF family, is a conserved and secreted molecule expressed in the dorsal midline during zebrafish gastrulation. Based on several lines of experimentation, I propose that Fam132a promotes collective cell migration by limiting cell contact and tissue cohesiveness. First, excess Fam132a expression in WT gastrulae disrupted cell contact maintenance and tissue cohesiveness, impairing persistence and coherence of PPP collective cell migration. Second, while genetic inactivation of the *fam132a* gene did not appear to affect gastrulation in WT embryos, it partially suppressed defects in cell contact, tissue cohesion and coherent migration of PPP cells in *slb/wnt11* mutant gastrulae. Cell contact maintenance and tissue cohesiveness are known to be critical for directionality and collective migration behaviors of the PPP cells (Dumortier et al., 2012; Tada and Heisenberg, 2012). Moreover, Fam132a overexpression also impaired ML planar intercalation of the notochord progenitor cells. There are several potential cellular and molecular

mechanisms by which Fam132a regulates both PPP collective migration and notochord cell ML intercalation during zebrafish C&E (Chapter 3, Section 3.4.3). Some of the potential mechanisms include that Fam132a negatively regulates cell-cell adhesion and/or promotes cell-matrix adhesion, which will be addressed in future studies. Fam132a could also indirectly regulate cell-cell adhesion through Bmp signaling. Indeed, overexpression of Fam132a dorsalization phenotype, likely via downregulation of Bmp signaling, an essential DV patterning signaling also known to regulate cell-cell adhesion (Figure 3.3)(von der Hardt et al., 2007). Future studies would address if cell adhesion is secondary effect of Fam132a through its regulation of Bmp.

Like *fam132a*, many candidate genes we identified as significantly downregulated in *stat3* morphants (Table 3.1), are directly or indirectly associated with adhesion. *cartpt*, for example, appears to be only zygotically expressed during the course of gastrulation, and is predicted to encode a secreted peptide with unknown functions during animal embryogenesis. Notably, overexpression of Cartpt caused C&E phenotypes. In particular, I observed cell dissociation and split notochord phenotypes (Figure 3.1), similar to *cdh1*/*e-cadherin*-deficient embryos (Shimizu et al., 2005b), suggesting a possible involvement of *cartpt* in cell adhesion during zebrafish gastrulation.

Indeed, adhesion has fundamental roles in both germ layer sorting and morphogenetic movements (Section 1.2.3~1.2.4, Section 3.2). Despite Wnt/PCP signaling being one of the major driving forces of zebrafish C&E gastrulation movements by regulating ML cell elongation, cell-cell adhesion under the regulation of Bmp signaling, E-cadherin and its regulator Wnt11, Snail, Gα12/13, Prostaglandin, to name a few, as well as cell-matrix adhesion mediated by FN, LM, integrin, Has2 and Efemp2 etc., are known to regulate PPP collective cell migration and ML cell intercalation of axial mesodermal cells (Babb and Marrs, 2004; Bakkers et al., 2004; Blanco

et al., 2007; Latimer and Jessen, 2010; Lin et al., 2009; Myers et al., 2002; Shimizu et al., 2005b; Speirs et al., 2010; Ulrich et al., 2005; von der Hardt et al., 2007; Yamashita et al., 2004; Zhang et al., 2014). In fact, Wnt/PCP, cell-cell adhesion and cell-matrix adhesion all cooperate with one another to govern morphogenetic movements during gastrulation. Future studies of *cartpt* and other candidate genes I identified as downregulated in *stat3* morphants may uncover additional novel regulators of adhesion and C&E movements.

4.5 Stat3 in Late Zebrafish Development

In Chapter 2 I reported that genetic disruption of zebrafish *stat3* gene led to late onset scoliosis and excessive inflammation at whole-tissue level as revealed by elevated levels of proinflammatory cytokines *il6*, *tnfα*, and *il17c*, a zebrafish Il17 homolog (Figure 4.1E), and caused lethality at juvenile stage (Figure 2.1). It is intriguing that *stat3* zebrafish mutant affords a genetic model of several human diseases including HIES and scoliosis. Scoliosis and immunodeficiency were both reported to be associated with sporadic autosomal dominant *STAT3* mutations in human HIES patients (Paulson et al., 2008). Consistent with mouse CKO studies which provided evidence that Stat3 promotes bone formation (Itoh et al., 2006b; Zhang et al., 2005), my preliminary results showed that *stat3*-deficient animals manifesting the scoliosis phenotype exhibited lower bone density (Figure 2.1). Future studies will investigate the causal relationship between bone formation and scoliosis phenotype in zebrafish *stat3* mutant animals.

In those scoliotic *stat3* mutant juveniles, I also noticed abnormal gut morphology manifested by smaller size in general and increased number of goblet cells in *stat3* mutant animals (Figure 4.1A-D). Goblet cells are cup-like secretory epithelial cells in the intestine specialized for mucin secretion, the major component of mucus. The cytoplasm of goblet cells is

filled with membrane-bound mucin granules (Birchenough et al., 2015). Despite being smaller in size, *stat3*-deficient fish gut contained an increased number of goblet cells and accumulation of excess mucus in the intestinal lumen as revealed by PAS staining (Figure 4.1C-D). Given that goblet cells are continuously renewed from gut stem cells under normal conditions (Birchenough et al., 2015), and that Stat3 function has been implicated in stem cell maintenance, particularly in gut homeostasis (Hawkins et al., 2014; Pasco et al., 2015), it is likely that normal stem cell maintenance and/or differentiation and gut homeostasis are disrupted by loss of *stat3* function in the zebrafish gut. Indeed, my preliminary results showed that two important stem cell marker, *nanog* and *pouf53*/*oct4*, were significantly downregulated in scoliotic *stat3* mutant fish (Figure 4.1F). Future studies in collaboration with Dr. John Rawls at Duke University will continue to characterize gut phenotypes and the underlying mechanisms in *stat3*-deficieint zebrafish.

Together, my thesis work has elucidated the role of Stat3-dependent cell proliferation in zebrafish gastrulation; identified Fam132a, a potential cell adhesion inhibitor and novel regulator of PPP collective cell migration; and provided a list of novel genes potentially involved in zebrafish C&E gastrulation movements. Cell proliferation and collective migration are common processes employed by cancerous cells during cancer formation and progression. Therefore, my work will provide mechanistic and therapeutic insights into human cancer. In addition, future studies of scoliosis and immunodeficiency using zebrafish *stat3* as a model will further our understanding on human idiopathic scoliosis and HIES.

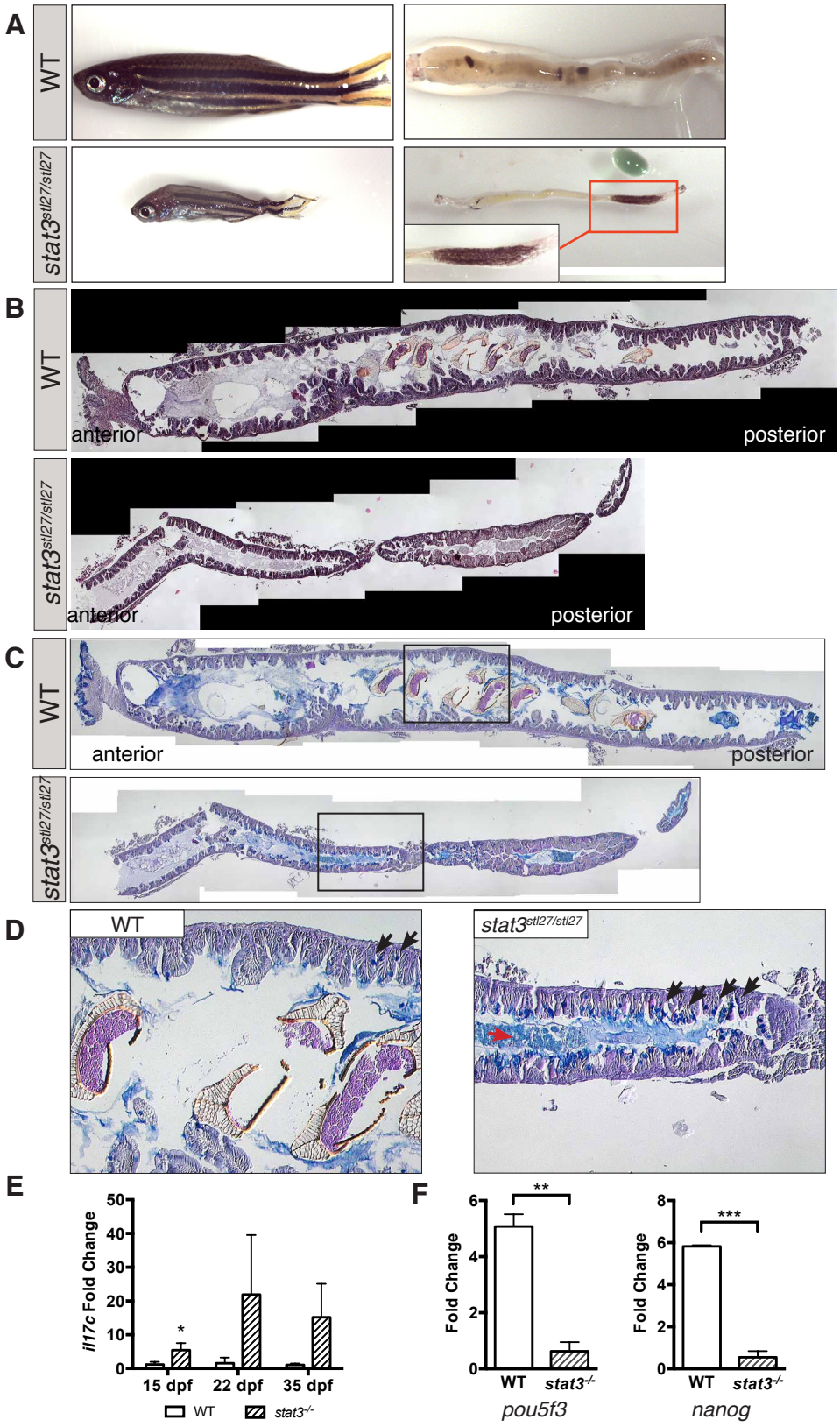

Figure 4.1 *stat3*-deficient zebrafish intestines exhibit abnormal morphology at early juvenile

stage. (A) Live images of WT and *stat3* mutant fish and dissected gut at 35 dpf (anterior to the left). (B-D) H&E (B) and PAS(C) staining of dissected WT and *stat3* mutant gut (Anterior to the left). Boxed regions in C are shown in bigger magnification in D. Black arrow, goblet cell. Red arrow, mucus. (E) *il17c* transcript level in whole animals throughout larval and juvenile stages detected by qRT-PCR. (F) *pou5f3*/*oct4* and *nanog* transcript level in 35 dpf whole animals detected by qRT-PCR. (*$p<0.05$, **$p<0.01$, ***$p<0.001$, error bars = SEM.)

References

Agathon, A., Thisse, C., and Thisse, B. (2003). The molecular nature of the zebrafish tail organizer. Nature *424*, 448-452.

Agostinis, C., Bulla, R., Tripodo, C., Gismondi, A., Stabile, H., Bossi, F., Guarnotta, C., Garlanda, C., De Seta, F., Spessotto, P.*, et al.* (2010). An alternative role of C1q in cell migration and tissue remodeling: contribution to trophoblast invasion and placental development. Journal of immunology *185*, 4420-4429.

Altschul, S.F., Gish, W., Miller, W., Myers, E.W., and Lipman, D.J. (1990). Basic local alignment search tool. Journal of molecular biology *215*, 403-410.

Angers, S., and Moon, R.T. (2009). Proximal events in Wnt signal transduction. Nature reviews Molecular cell biology *10*, 468-477.

Axelrod, J.D., and McNeill, H. (2002). Coupling planar cell polarity signaling to morphogenesis. TheScientificWorldJournal *2*, 434-454.

Babb, S.G., and Marrs, J.A. (2004). E-cadherin regulates cell movements and tissue formation in early zebrafish embryos. Developmental dynamics : an official publication of the American Association of Anatomists *230*, 263-277.

Bakkers, J., Kramer, C., Pothof, J., Quaedvlieg, N.E., Spaink, H.P., and Hammerschmidt, M. (2004). Has2 is required upstream of Rac1 to govern dorsal migration of lateral cells during zebrafish gastrulation. Development *131*, 525-537.

Barre, B., Vigneron, A., and Coqueret, O. (2005). The STAT3 transcription factor is a target for the Myc and riboblastoma proteins on the Cdc25A promoter. The Journal of biological chemistry *280*, 15673-15681.

Batlle, E., Sancho, E., Franci, C., Dominguez, D., Monfar, M., Baulida, J., and Garcia De Herreros, A. (2000). The transcription factor snail is a repressor of E-cadherin gene expression in epithelial tumour cells. Nature cell biology *2*, 84-89.

Beccari, S., Teixeira, L., and Rorth, P. (2002). The JAK/STAT pathway is required for border cell migration during Drosophila oogenesis. Mechanisms of development *111*, 115-123.

Behrndt, M., and Heisenberg, C.P. (2012). Spurred by resistance: mechanosensation in collective migration. Developmental cell *22*, 3-4.

Birchenough, G.M., Johansson, M.E., Gustafsson, J.K., Bergstrom, J.H., and Hansson, G.C. (2015). New developments in goblet cell mucus secretion and function. Mucosal immunology.

Blanco, M.J., Barrallo-Gimeno, A., Acloque, H., Reyes, A.E., Tada, M., Allende, M.L., Mayor, R., and Nieto, M.A. (2007). Snail1a and Snail1b cooperate in the anterior migration of the axial mesendoderm in the zebrafish embryo. Development *134*, 4073-4081.

Blaser, H., Eisenbeiss, S., Neumann, M., Reichman-Fried, M., Thisse, B., Thisse, C., and Raz, E. (2005). Transition from non-motile behaviour to directed migration during early PGC development in zebrafish. Journal of cell science *118*, 4027-4038.

Bolliger, M.F., Martinelli, D.C., and Sudhof, T.C. (2011). The cell-adhesion G protein-coupled receptor BAI3 is a high-affinity receptor for C1q-like proteins. Proceedings of the National Academy of Sciences of the United States of America *108*, 2534-2539.

Bordin, S., Ghebrehiwet, B., and Page, R.C. (1990). Participation of C1q and its receptor in adherence of human diploid fibroblast. Journal of immunology *145*, 2520-2526.

Bouldin, C.M., and Kimelman, D. (2014). Cdc25 and the importance of G2 control: insights from developmental biology. Cell cycle *13*, 2165-2171.

Bouldin, C.M., Snelson, C.D., Farr, G.H., 3rd, and Kimelman, D. (2014). Restricted expression of cdc25a in the tailbud is essential for formation of the zebrafish posterior body. Genes & development *28*, 384-395.

Boutros, R., Lobjois, V., and Ducommun, B. (2007). CDC25 phosphatases in cancer cells: key players? Good targets? Nature reviews Cancer *7*, 495-507.

Carland, T.M., and Gerwick, L. (2010). The C1q domain containing proteins: Where do they come from and what do they do? Developmental and comparative immunology *34*, 785-790.

Carmona-Fontaine, C., Theveneau, E., Tzekou, A., Tada, M., Woods, M., Page, K.M., Parsons, M., Lambris, J.D., and Mayor, R. (2011). Complement fragment C3a controls mutual cell attraction during collective cell migration. Developmental cell *21*, 1026-1037.

Carpenter, R.L., and Lo, H.W. (2014). STAT3 Target Genes Relevant to Human Cancers. Cancers *6*, 897-925.

Cermak, T., Doyle, E.L., Christian, M., Wang, L., Zhang, Y., Schmidt, C., Baller, J.A., Somia, N.V., Bogdanove, A.J., and Voytas, D.F. (2011). Efficient design and assembly of custom TALEN and other TAL effector-based constructs for DNA targeting. Nucleic acids research *39*, e82.

Cha, Y.I., Kim, S.H., Sepich, D., Buchanan, F.G., Solnica-Krezel, L., and DuBois, R.N. (2006). Cyclooxygenase-1-derived PGE2 promotes cell motility via the G-protein-coupled EP4 receptor during vertebrate gastrulation. Genes & development *20*, 77-86.

Chen, Y., and Schier, A.F. (2001). The zebrafish Nodal signal Squint functions as a morphogen. Nature *411*, 607-610.

Ciruna, B., Jenny, A., Lee, D., Mlodzik, M., and Schier, A.F. (2006). Planar cell polarity signalling couples cell division and morphogenesis during neurulation. Nature *439*, 220-224.

Cole, L.K., and Ross, L.S. (2001). Apoptosis in the developing zebrafish embryo. Developmental biology *240*, 123-142.

Conway, G. (2006). STAT3-dependent pathfinding and control of axonal branching and target selection. Developmental biology *296*, 119-136.

Croker, B.A., Kiu, H., and Nicholson, S.E. (2008). SOCS regulation of the JAK/STAT signalling pathway. Seminars in cell & developmental biology *19*, 414-422.

Croker, B.A., Krebs, D.L., Zhang, J.G., Wormald, S., Willson, T.A., Stanley, E.G., Robb, L., Greenhalgh, C.J., Forster, I., Clausen, B.E.*, et al.* (2003). SOCS3 negatively regulates IL-6 signaling in vivo. Nature immunology *4*, 540-545.

Dalle Nogare, D.E., Pauerstein, P.T., and Lane, M.E. (2009). G2 acquisition by transcription-independent mechanism at the zebrafish midblastula transition. Developmental biology *326*, 131-142.

Darnell, J.E., Jr. (1997). STATs and gene regulation. Science *277*, 1630-1635.

Darnell, J.E., Jr., Kerr, I.M., and Stark, G.R. (1994). Jak-STAT pathways and transcriptional activation in response to IFNs and other extracellular signaling proteins. Science *264*, 1415-1421.

Davidson, L.A., Keller, R., and DeSimone, D.W. (2004). Assembly and remodeling of the fibrillar fibronectin extracellular matrix during gastrulation and neurulation in Xenopus laevis. Developmental dynamics : an official publication of the American Association of Anatomists *231*, 888-895.

Davidson, L.A., Marsden, M., Keller, R., and Desimone, D.W. (2006). Integrin alpha5beta1 and fibronectin regulate polarized cell protrusions required for Xenopus convergence and extension. Current biology : CB *16*, 833-844.

Delvaeye, M., De Vriese, A., Zwerts, F., Betz, I., Moons, M., Autiero, M., and Conway, E.M. (2009). Role of the 2 zebrafish survivin genes in vasculo-angiogenesis, neurogenesis, cardiogenesis and hematopoiesis. BMC developmental biology *9*, 25.

Dohn, M.R., Mundell, N.A., Sawyer, L.M., Dunlap, J.A., and Jessen, J.R. (2013). Planar cell polarity proteins differentially regulate extracellular matrix organization and assembly during zebrafish gastrulation. Developmental biology *383*, 39-51.

Dumortier, J.G., Martin, S., Meyer, D., Rosa, F.M., and David, N.B. (2012). Collective mesendoderm migration relies on an intrinsic directionality signal transmitted through cell contacts. Proceedings of the National Academy of Sciences of the United States of America *109*, 16945-16950.

Dzamba, B.J., Jakab, K.R., Marsden, M., Schwartz, M.A., and DeSimone, D.W. (2009). Cadherin adhesion, tissue tension, and noncanonical Wnt signaling regulate fibronectin matrix organization. Developmental cell *16*, 421-432.

Edgar, B.A., and Datar, S.A. (1996). Zygotic degradation of two maternal Cdc25 mRNAs terminates Drosophila's early cell cycle program. Genes & development *10*, 1966-1977.

Edgar, B.A., and O'Farrell, P.H. (1990). The three postblastoderm cell cycles of Drosophila embryogenesis are regulated in G2 by string. Cell *62*, 469-480.

Emanuelsson, O., Brunak, S., von Heijne, G., and Nielsen, H. (2007). Locating proteins in the cell using TargetP, SignalP and related tools. Nature protocols *2*, 953-971.

Enomoto, T., Ohashi, K., Shibata, R., Higuchi, A., Maruyama, S., Izumiya, Y., Walsh, K., Murohara, T., and Ouchi, N. (2011). Adipolin/C1qdc2/CTRP12 protein functions as an adipokine that improves glucose metabolism. The Journal of biological chemistry *286*, 34552-34558.

Fang, Y., Gupta, V., Karra, R., Holdway, J.E., Kikuchi, K., and Poss, K.D. (2013). Translational profiling of cardiomyocytes identifies an early Jak1/Stat3 injury response required for zebrafish heart regeneration. Proceedings of the National Academy of Sciences of the United States of America *110*, 13416-13421.

Feldman, B., Gates, M.A., Egan, E.S., Dougan, S.T., Rennebeck, G., Sirotkin, H.I., Schier, A.F., and Talbot, W.S. (1998). Zebrafish organizer development and germ-layer formation require nodal-related signals. Nature *395*, 181-185.

Feng, X., Tonnesen, M.G., Peerschke, E.I., and Ghebrehiwet, B. (2002). Cooperation of C1q receptors and integrins in C1q-mediated endothelial cell adhesion and spreading. Journal of immunology *168*, 2441-2448.

Fitzgerald, J.S., Busch, S., Wengenmayer, T., Foerster, K., de la Motte, T., Poehlmann, T.G., and Markert, U.R. (2005). Signal transduction in trophoblast invasion. Chemical immunology and allergy *88*, 181-199.

Fleming, A.J. (2006). The co-ordination of cell division, differentiation and morphogenesis in the shoot apical meristem: a perspective. Journal of experimental botany *57*, 25-32.

Friedl, P., and Gilmour, D. (2009). Collective cell migration in morphogenesis, regeneration and cancer. Nature reviews Molecular cell biology *10*, 445-457.

Furthauer, M., Van Celst, J., Thisse, C., and Thisse, B. (2004). Fgf signalling controls the dorsoventral patterning of the zebrafish embryo. Development *131*, 2853-2864.

Gao, S.P., and Bromberg, J.F. (2006). Touched and moved by STAT3. Science's STKE : signal transduction knowledge environment *2006*, pe30.

Ghai, R., Waters, P., Roumenina, L.T., Gadjeva, M., Kojouharova, M.S., Reid, K.B., Sim, R.B., and Kishore, U. (2007). C1q and its growing family. Immunobiology *212*, 253-266.

Glickman, N.S., Kimmel, C.B., Jones, M.A., and Adams, R.J. (2003). Shaping the zebrafish notochord. Development *130*, 873-887.

Gray, R.S., Roszko, I., and Solnica-Krezel, L. (2011). Planar cell polarity: coordinating morphogenetic cell behaviors with embryonic polarity. Developmental cell *21*, 120-133.

Groner, B., Lucks, P., and Borghouts, C. (2008). The function of Stat3 in tumor cells and their microenvironment. Seminars in cell & developmental biology *19*, 341-350.

Grosshans, J., and Wieschaus, E. (2000). A genetic link between morphogenesis and cell division during formation of the ventral furrow in Drosophila. Cell *101*, 523-531.

Hammerschmidt, M., Serbedzija, G.N., and McMahon, A.P. (1996). Genetic analysis of dorsoventral pattern formation in the zebrafish: requirement of a BMP-like ventralizing activity and its dorsal repressor. Genes & development *10*, 2452-2461.

Hammerschmidt, M., and Wedlich, D. (2008). Regulated adhesion as a driving force of gastrulation movements. Development *135*, 3625-3641.

Harty, B.L., Krishnan, A., Sanchez, N.E., Schioth, H.B., and Monk, K.R. (2015). Defining the gene repertoire and spatiotemporal expression profiles of adhesion G protein-coupled receptors in zebrafish. BMC genomics *16*, 62.

Harvey, S.A., Sealy, I., Kettleborough, R., Fenyes, F., White, R., Stemple, D., and Smith, J.C. (2013). Identification of the zebrafish maternal and paternal transcriptomes. Development *140*, 2703-2710.

Hawkins, K., Joy, S., and McKay, T. (2014). Cell signalling pathways underlying induced pluripotent stem cell reprogramming. World journal of stem cells *6*, 620-628.

Hegedus, B., Marga, F., Jakab, K., Sharpe-Timms, K.L., and Forgacs, G. (2006). The interplay of cell-cell and cell-matrix interactions in the invasive properties of brain tumors. Biophysical journal *91*, 2708-2716.

Heisenberg, C.P., and Nusslein-Volhard, C. (1997). The function of silberblick in the positioning of the eye anlage in the zebrafish embryo. Developmental biology *184*, 85-94.

Heisenberg, C.P., Tada, M., Rauch, G.J., Saude, L., Concha, M.L., Geisler, R., Stemple, D.L., Smith, J.C., and Wilson, S.W. (2000). Silberblick/Wnt11 mediates convergent extension movements during zebrafish gastrulation. Nature *405*, 76-81.

Holland, S.M., DeLeo, F.R., Elloumi, H.Z., Hsu, A.P., Uzel, G., Brodsky, N., Freeman, A.F., Demidowich, A., Davis, J., Turner, M.L.*, et al.* (2007). STAT3 mutations in the hyper-IgE syndrome. The New England journal of medicine *357*, 1608-1619.

Hou, S.X., Zheng, Z., Chen, X., and Perrimon, N. (2002). The Jak/STAT pathway in model organisms: emerging roles in cell movement. Developmental cell *3*, 765-778.

Huelsken, J., and Behrens, J. (2002). The Wnt signalling pathway. Journal of cell science *115*, 3977-3978.

Humphries, M.J. (2001). Cell-substrate adhesion assays. Current protocols in cell biology / editorial board, Juan S Bonifacino [et al] *Chapter 9*, Unit 9 1.

Itoh, M., Murata, T., Suzuki, T., Shindoh, M., Nakajima, K., Imai, K., and Yoshida, K. (2006a). Requirement of STAT3 activation for maximal collagenase-1 (MMP-1) induction by epidermal growth factor and malignant characteristics in T24 bladder cancer cells. Oncogene *25*, 1195-1204.

Itoh, S., Udagawa, N., Takahashi, N., Yoshitake, F., Narita, H., Ebisu, S., and Ishihara, K. (2006b). A critical role for interleukin-6 family-mediated Stat3 activation in osteoblast differentiation and bone formation. Bone *39*, 505-512.

Jessen, J.R. (2015). Recent advances in the study of zebrafish extracellular matrix proteins. Developmental biology *401*, 110-121.

Jessen, J.R., Topczewski, J., Bingham, S., Sepich, D.S., Marlow, F., Chandrasekhar, A., and Solnica-Krezel, L. (2002). Zebrafish trilobite identifies new roles for Strabismus in gastrulation and neuronal movements. Nature cell biology *4*, 610-615.

Kai, M., Heisenberg, C.P., and Tada, M. (2008). Sphingosine-1-phosphate receptors regulate individual cell behaviours underlying the directed migration of prechordal plate progenitor cells during zebrafish gastrulation. Development *135*, 3043-3051.

Kane, D.A., McFarland, K.N., and Warga, R.M. (2005). Mutations in half baked/E-cadherin block cell behaviors that are necessary for teleost epiboly. Development *132*, 1105-1116.

Kane, D.A., Warga, R.M., and Kimmel, C.B. (1992). Mitotic domains in the early embryo of the zebrafish. Nature *360*, 735-737.

Keller, R. (2002). Shaping the vertebrate body plan by polarized embryonic cell movements. Science *298*, 1950-1954.

Keller, R., Davidson, L., Edlund, A., Elul, T., Ezin, M., Shook, D., and Skoglund, P. (2000). Mechanisms of convergence and extension by cell intercalation. Philosophical transactions of the Royal Society of London Series B, Biological sciences *355*, 897-922.

Kettleborough, R.N., Busch-Nentwich, E.M., Harvey, S.A., Dooley, C.M., de Bruijn, E., van Eeden, F., Sealy, I., White, R.J., Herd, C., Nijman, I.J.*, et al.* (2013). A systematic genome-wide analysis of zebrafish protein-coding gene function. Nature *496*, 494-497.

Kiehart, D.P., Galbraith, C.G., Edwards, K.A., Rickoll, W.L., and Montague, R.A. (2000). Multiple forces contribute to cell sheet morphogenesis for dorsal closure in Drosophila. The Journal of cell biology *149*, 471-490.

Kilian, B., Mansukoski, H., Barbosa, F.C., Ulrich, F., Tada, M., and Heisenberg, C.P. (2003). The role of Ppt/Wnt5 in regulating cell shape and movement during zebrafish gastrulation. Mechanisms of development *120*, 467-476.

Kim, S.H., Li, C., and Maller, J.L. (1999). A maternal form of the phosphatase Cdc25A regulates early embryonic cell cycles in Xenopus laevis. Developmental biology *212*, 381-391.

Kimmel, C.B., Ballard, W.W., Kimmel, S.R., Ullmann, B., and Schilling, T.F. (1995). Stages of embryonic development of the zebrafish. Developmental dynamics : an official publication of the American Association of Anatomists *203*, 253-310.

Kimmel, C.B., Warga, R.M., and Kane, D.A. (1994). Cell cycles and clonal strings during formation of the zebrafish central nervous system. Development *120*, 265-276.

Kimmel, C.B., Warga, R.M., and Schilling, T.F. (1990). Origin and organization of the zebrafish fate map. Development *108*, 581-594.

Kishimoto, Y., Lee, K.H., Zon, L., Hammerschmidt, M., and Schulte-Merker, S. (1997). The molecular nature of zebrafish swirl: BMP2 function is essential during early dorsoventral patterning. Development *124*, 4457-4466.

Kok, F.O., Shin, M., Ni, C.W., Gupta, A., Grosse, A.S., van Impel, A., Kirchmaier, B.C., Peterson-Maduro, J., Kourkoulis, G., Male, I.*, et al.* (2015). Reverse genetic screening reveals poor correlation between morpholino-induced and mutant phenotypes in zebrafish. Developmental cell *32*, 97-108.

Koshida, S., Kishimoto, Y., Ustumi, H., Shimizu, T., Furutani-Seiki, M., Kondoh, H., and Takada, S. (2005). Integrinalpha5-dependent fibronectin accumulation for maintenance of somite boundaries in zebrafish embryos. Developmental cell *8*, 587-598.

Krieg, M., Arboleda-Estudillo, Y., Puech, P.H., Kafer, J., Graner, F., Muller, D.J., and Heisenberg, C.P. (2008). Tensile forces govern germ-layer organization in zebrafish. Nature cell biology *10*, 429-436.

Latimer, A., and Jessen, J.R. (2010). Extracellular matrix assembly and organization during zebrafish gastrulation. Matrix biology : journal of the International Society for Matrix Biology *29*, 89-96.

Laufs, P., Grandjean, O., Jonak, C., Kieu, K., and Traas, J. (1998). Cellular parameters of the shoot apical meristem in Arabidopsis. The Plant cell *10*, 1375-1390.

Leatherman, J.L., and Dinardo, S. (2010). Germline self-renewal requires cyst stem cells and stat regulates niche adhesion in Drosophila testes. Nature cell biology *12*, 806-811.

Lee, C.H., and Gumbiner, B.M. (1995). Disruption of gastrulation movements in Xenopus by a dominant-negative mutant for C-cadherin. Developmental biology *171*, 363-373.

Lee, G., White, L.S., Hurov, K.E., Stappenbeck, T.S., and Piwnica-Worms, H. (2009). Response of small intestinal epithelial cells to acute disruption of cell division through CDC25 deletion. Proceedings of the National Academy of Sciences of the United States of America *106*, 4701-4706.

Leise, W.F., 3rd, and Mueller, P.R. (2004). Inhibition of the cell cycle is required for convergent extension of the paraxial mesoderm during Xenopus neurulation. Development *131*, 1703-1715.

Lekven, A.C., Thorpe, C.J., Waxman, J.S., and Moon, R.T. (2001). Zebrafish wnt8 encodes two wnt8 proteins on a bicistronic transcript and is required for mesoderm and neurectoderm patterning. Developmental cell *1*, 103-114.

Leptin, M. (2005). Gastrulation movements: the logic and the nuts and bolts. Developmental cell *8*, 305-320.

Levy, D.E., and Darnell, J.E., Jr. (2002). Stats: transcriptional control and biological impact. Nature reviews Molecular cell biology *3*, 651-662.

Li, X., Roszko, I., Sepich, D.S., Ni, M., Hamm, H.E., Marlow, F.L., and Solnica-Krezel, L. (2013). Gpr125 modulates Dishevelled distribution and planar cell polarity signaling. Development *140*, 3028-3039.

Liang, J., Wang, D., Renaud, G., Wolfsberg, T.G., Wilson, A.F., and Burgess, S.M. (2012). The stat3/socs3a pathway is a key regulator of hair cell regeneration in zebrafish. [corrected]. The Journal of neuroscience : the official journal of the Society for Neuroscience *32*, 10662-10673.

Lin, F., Chen, S., Sepich, D.S., Panizzi, J.R., Clendenon, S.G., Marrs, J.A., Hamm, H.E., and Solnica-Krezel, L. (2009). Galpha12/13 regulate epiboly by inhibiting E-cadherin activity and modulating the actin cytoskeleton. The Journal of cell biology *184*, 909-921.

Lin, F., Sepich, D.S., Chen, S., Topczewski, J., Yin, C., Solnica-Krezel, L., and Hamm, H. (2005). Essential roles of G{alpha}12/13 signaling in distinct cell behaviors driving zebrafish convergence and extension gastrulation movements. The Journal of cell biology *169*, 777-787.

Liongue, C., O'Sullivan, L.A., Trengove, M.C., and Ward, A.C. (2012). Evolution of JAK-STAT pathway components: mechanisms and role in immune system development. PloS one *7*, e32777.

Liu, Y., and Solnica-Krezel, L. (2015). Stat3/Cdc25a-Dependent Cell Proliferation Promotes Axis Extension during Zebrafish Gastrulation. Manuscript submitted for publication (copy on file with author).

Luo, Y., Shen, H., Liu, H.S., Yu, S.J., Reiner, D.J., Harvey, B.K., Hoffer, B.J., Yang, Y., and Wang, Y. (2013). CART peptide induces neuroregeneration in stroke rats. Journal of cerebral blood flow and metabolism : official journal of the International Society of Cerebral Blood Flow and Metabolism *33*, 300-310.

Marlow, F., Topczewski, J., Sepich, D., and Solnica-Krezel, L. (2002). Zebrafish Rho kinase 2 acts downstream of Wnt11 to mediate cell polarity and effective convergence and extension movements. Current biology : CB *12*, 876-884.

Marlow, F., Zwartkruis, F., Malicki, J., Neuhauss, S.C., Abbas, L., Weaver, M., Driever, W., and Solnica-Krezel, L. (1998). Functional interactions of genes mediating convergent extension, knypek and trilobite, during the partitioning of the eye primordium in zebrafish. Developmental biology *203*, 382-399.

Marsden, M., and DeSimone, D.W. (2001). Regulation of cell polarity, radial intercalation and epiboly in Xenopus: novel roles for integrin and fibronectin. Development *128*, 3635-3647.

Marsden, M., and DeSimone, D.W. (2003). Integrin-ECM interactions regulate cadherin-dependent cell adhesion and are required for convergent extension in Xenopus. Current biology : CB *13*, 1182-1191.

McLoughlin, R.M., Jenkins, B.J., Grail, D., Williams, A.S., Fielding, C.A., Parker, C.R., Ernst, M., Topley, N., and Jones, S.A. (2005). IL-6 trans-signaling via STAT3 directs T cell infiltration in acute inflammation. Proceedings of the National Academy of Sciences of the United States of America *102*, 9589-9594.

Miyagi, C., Yamashita, S., Ohba, Y., Yoshizaki, H., Matsuda, M., and Hirano, T. (2004). STAT3 noncell-autonomously controls planar cell polarity during zebrafish convergence and extension. The Journal of cell biology *166*, 975-981.

Mogensen, T.H. (2013). STAT3 and the Hyper-IgE syndrome: Clinical presentation, genetic origin, pathogenesis, novel findings and remaining uncertainties. Jak-Stat *2*, e23435.

Montell, D.J. (2008). Morphogenetic cell movements: diversity from modular mechanical properties. Science *322*, 1502-1505.

Montero, J.A., Carvalho, L., Wilsch-Brauninger, M., Kilian, B., Mustafa, C., and Heisenberg, C.P. (2005). Shield formation at the onset of zebrafish gastrulation. Development *132*, 1187-1198.

Montero, J.A., Kilian, B., Chan, J., Bayliss, P.E., and Heisenberg, C.P. (2003). Phosphoinositide 3-kinase is required for process outgrowth and cell polarization of gastrulating mesendodermal cells. Current biology : CB *13*, 1279-1289.

Morgan, D.O. (2007). The Cell Cycle: Principles of control. London: New Science Press Ltd.

Mukherjee, T., Hombria, J.C., and Zeidler, M.P. (2005). Opposing roles for Drosophila JAK/STAT signalling during cellular proliferation. Oncogene *24*, 2503-2511.

Mullins, M.C., Hammerschmidt, M., Kane, D.A., Odenthal, J., Brand, M., van Eeden, F.J., Furutani-Seiki, M., Granato, M., Haffter, P., Heisenberg, C.P*., et al.* (1996). Genes establishing dorsoventral pattern formation in the zebrafish embryo: the ventral specifying genes. Development *123*, 81-93.

Myers, D.C., Sepich, D.S., and Solnica-Krezel, L. (2002). Bmp activity gradient regulates convergent extension during zebrafish gastrulation. Developmental biology *243*, 81-98.

Naito, A.T., Sumida, T., Nomura, S., Liu, M.L., Higo, T., Nakagawa, A., Okada, K., Sakai, T., Hashimoto, A., Hara, Y.*, et al.* (2012). Complement C1q activates canonical Wnt signaling and promotes aging-related phenotypes. Cell *149*, 1298-1313.

Nasevicius, A., and Ekker, S.C. (2000). Effective targeted gene 'knockdown' in zebrafish. Nature genetics *26*, 216-220.

Nayak, A., Ferluga, J., Tsolaki, A.G., and Kishore, U. (2010). The non-classical functions of the classical complement pathway recognition subcomponent C1q. Immunology letters *131*, 139-150.

Nelson, C.M., Gorsuch, R.A., Bailey, T.J., Ackerman, K.M., Kassen, S.C., and Hyde, D.R. (2012). Stat3 defines three populations of Muller glia and is required for initiating maximal muller glia proliferation in the regenerating zebrafish retina. The Journal of comparative neurology *520*, 4294-4311.

Ng, D.C., Lin, B.H., Lim, C.P., Huang, G., Zhang, T., Poli, V., and Cao, X. (2006). Stat3 regulates microtubules by antagonizing the depolymerization activity of stathmin. The Journal of cell biology *172*, 245-257.

Nguyen, V.H., Schmid, B., Trout, J., Connors, S.A., Ekker, M., and Mullins, M.C. (1998). Ventral and lateral regions of the zebrafish gastrula, including the neural crest progenitors, are established by a bmp2b/swirl pathway of genes. Developmental biology *199*, 93-110.

Nichane, M., Ren, X., and Bellefroid, E.J. (2010). Self-regulation of Stat3 activity coordinates cell-cycle progression and neural crest specification. The EMBO journal *29*, 55-67.

Nishimura, T., and Takeichi, M. (2009). Remodeling of the adherens junctions during morphogenesis. Current topics in developmental biology *89*, 33-54.

Nishio, S., Gibert, Y., Bernard, L., Brunet, F., Triqueneaux, G., and Laudet, V. (2008). Adiponectin and adiponectin receptor genes are coexpressed during zebrafish embryogenesis and regulated by food deprivation. Developmental dynamics : an official publication of the American Association of Anatomists *237*, 1682-1690.

Oates, A.C., Wollberg, P., Pratt, S.J., Paw, B.H., Johnson, S.L., Ho, R.K., Postlethwait, J.H., Zon, L.I., and Wilks, A.F. (1999). Zebrafish stat3 is expressed in restricted tissues during embryogenesis and stat1 rescues cytokine signaling in a STAT1-deficient human cell line. Developmental dynamics : an official publication of the American Association of Anatomists *215*, 352-370.

Ogura, Y., Sakaue-Sawano, A., Nakagawa, M., Satoh, N., Miyawaki, A., and Sasakura, Y. (2011). Coordination of mitosis and morphogenesis: role of a prolonged G2 phase during chordate neurulation. Development *138*, 577-587.

Pasco, M.Y., Loudhaief, R., and Gallet, A. (2015). The cellular homeostasis of the gut: what the Drosophila model points out. Histology and histopathology *30*, 277-292.

Paulson, M.L., Freeman, A.F., and Holland, S.M. (2008). Hyper IgE syndrome: an update on clinical aspects and the role of signal transducer and activator of transcription 3. Current opinion in allergy and clinical immunology *8*, 527-533.

Quesada-Hernandez, E., Caneparo, L., Schneider, S., Winkler, S., Liebling, M., Fraser, S.E., and Heisenberg, C.P. (2010). Stereotypical cell division orientation controls neural rod midline formation in zebrafish. Current biology : CB *20*, 1966-1972.

Robu, M.E., Larson, J.D., Nasevicius, A., Beiraghi, S., Brenner, C., Farber, S.A., and Ekker, S.C. (2007). p53 activation by knockdown technologies. PLoS genetics *3*, e78.

Rogge, G., Jones, D., Hubert, G.W., Lin, Y., and Kuhar, M.J. (2008). CART peptides: regulators of body weight, reward and other functions. Nature reviews Neuroscience *9*, 747-758.

Roszko, I., Sawada, A., and Solnica-Krezel, L. (2009). Regulation of convergence and extension movements during vertebrate gastrulation by the Wnt/PCP pathway. Seminars in cell & developmental biology *20*, 986-997.

Rozario, T., and DeSimone, D.W. (2010). The extracellular matrix in development and morphogenesis: a dynamic view. Developmental biology *341*, 126-140.

Saka, Y., and Smith, J.C. (2001). Spatial and temporal patterns of cell division during early Xenopus embryogenesis. Developmental biology *229*, 307-318.

San Antonio, J.D., Zoeller, J.J., Habursky, K., Turner, K., Pimtong, W., Burrows, M., Choi, S., Basra, S., Bennett, J.S., DeGrado, W.F.*, et al.* (2009). A key role for the integrin alpha2beta1 in experimental and developmental angiogenesis. The American journal of pathology *175*, 1338-1347.

Sander, J.D., Cade, L., Khayter, C., Reyon, D., Peterson, R.T., Joung, J.K., and Yeh, J.R. (2011). Targeted gene disruption in somatic zebrafish cells using engineered TALENs. Nature biotechnology *29*, 697-698.

Sano, S., Itami, S., Takeda, K., Tarutani, M., Yamaguchi, Y., Miura, H., Yoshikawa, K., Akira, S., and Takeda, J. (1999). Keratinocyte-specific ablation of Stat3 exhibits impaired skin remodeling, but does not affect skin morphogenesis. The EMBO journal *18*, 4657-4668.

Saude, L., Woolley, K., Martin, P., Driever, W., and Stemple, D.L. (2000). Axis-inducing activities and cell fates of the zebrafish organizer. Development *127*, 3407-3417.

Schier, A.F. (2001). Axis formation and patterning in zebrafish. Current opinion in genetics & development *11*, 393-404.

Schier, A.F., and Talbot, W.S. (2001). Nodal signaling and the zebrafish organizer. The International journal of developmental biology *45*, 289-297.

Schier, A.F., and Talbot, W.S. (2005). Molecular genetics of axis formation in zebrafish. Annual review of genetics *39*, 561-613.

Schneider, S., Steinbeisser, H., Warga, R.M., and Hausen, P. (1996). Beta-catenin translocation into nuclei demarcates the dorsalizing centers in frog and fish embryos. Mechanisms of development *57*, 191-198.

Seldin, M.M., Peterson, J.M., Byerly, M.S., Wei, Z., and Wong, G.W. (2012). Myonectin (CTRP15), a novel myokine that links skeletal muscle to systemic lipid homeostasis. The Journal of biological chemistry *287*, 11968-11980.

Sepich, D.S., Myers, D.C., Short, R., Topczewski, J., Marlow, F., and Solnica-Krezel, L. (2000). Role of the zebrafish trilobite locus in gastrulation movements of convergence and extension. Genesis *27*, 159-173.

Shih, J., and Fraser, S.E. (1996). Characterizing the zebrafish organizer: microsurgical analysis at the early-shield stage. Development *122*, 1313-1322.

Shimizu, T., Bae, Y.K., Muraoka, O., and Hibi, M. (2005a). Interaction of Wnt and caudal-related genes in zebrafish posterior body formation. Developmental biology *279*, 125-141.

Shimizu, T., Yabe, T., Muraoka, O., Yonemura, S., Aramaki, S., Hatta, K., Bae, Y.K., Nojima, H., and Hibi, M. (2005b). E-cadherin is required for gastrulation cell movements in zebrafish. Mechanisms of development *122*, 747-763.

Shimuta, K., Nakajo, N., Uto, K., Hayano, Y., Okazaki, K., and Sagata, N. (2002). Chk1 is activated transiently and targets Cdc25A for degradation at the Xenopus midblastula transition. The EMBO journal *21*, 3694-3703.

Shin, J., Chen, J., and Solnica-Krezel, L. (2014). Efficient homologous recombination-mediated genome engineering in zebrafish using TALE nucleases. Development *141*, 3807-3818.

Silver, D.L., and Montell, D.J. (2001). Paracrine signaling through the JAK/STAT pathway activates invasive behavior of ovarian epithelial cells in Drosophila. Cell *107*, 831-841.

Silver, D.L., Naora, H., Liu, J., Cheng, W., and Montell, D.J. (2004). Activated signal transducer and activator of transcription (STAT) 3: localization in focal adhesions and function in ovarian cancer cell motility. Cancer research *64*, 3550-3558.

Solnica-Krezel, L. (2005). Conserved patterns of cell movements during vertebrate gastrulation. Current biology : CB *15*, R213-228.

Solnica-Krezel, L. (2006). Gastrulation in zebrafish -- all just about adhesion? Current opinion in genetics & development *16*, 433-441.

Solnica-Krezel, L., and Driever, W. (2001). The role of the homeodomain protein Bozozok in zebrafish axis formation. The International journal of developmental biology *45*, 299-310.

Solnica-Krezel, L., and Sepich, D.S. (2012). Gastrulation: making and shaping germ layers. Annual review of cell and developmental biology *28*, 687-717.

Song, S., Eckerle, S., Onichtchouk, D., Marrs, J.A., Nitschke, R., and Driever, W. (2013). Pou5f1-dependent EGF expression controls E-cadherin endocytosis, cell adhesion, and zebrafish epiboly movements. Developmental cell *24*, 486-501.

Speirs, C.K., Jernigan, K.K., Kim, S.H., Cha, Y.I., Lin, F., Sepich, D.S., DuBois, R.N., Lee, E., and Solnica-Krezel, L. (2010). Prostaglandin Gbetagamma signaling stimulates gastrulation movements by limiting cell adhesion through Snai1a stabilization. Development *137*, 1327-1337.

Steinberg, M.S. (1970). Does differential adhesion govern self-assembly processes in histogenesis? Equilibrium configurations and the emergence of a hierarchy among populations of embryonic cells. The Journal of experimental zoology *173*, 395-433.

Steinberg, M.S. (1975). Adhesion-guided multicellular assembly: a commentary upon the postulates, real and imagined, of the differential adhesion hypothesis, with special attention to computer simulations of cell sorting. Journal of theoretical biology *55*, 431-443.

Steinberg, M.S. (2007). Differential adhesion in morphogenesis: a modern view. Current opinion in genetics & development *17*, 281-286.

Steward-Tharp, S.M., Laurence, A., Kanno, Y., Kotlyar, A., Villarino, A.V., Sciume, G., Kuchen, S., Resch, W., Wohlfert, E.A., Jiang, K.*, et al.* (2014). A mouse model of HIES reveals pro- and anti-inflammatory functions of STAT3. Blood *123*, 2978-2987.

Strutt, H., and Strutt, D. (2009). Asymmetric localisation of planar polarity proteins: Mechanisms and consequences. Seminars in cell & developmental biology *20*, 957-963.

Summerton, J., and Weller, D. (1997). Morpholino antisense oligomers: design, preparation, and properties. Antisense & nucleic acid drug development *7*, 187-195.

Swanhart, L.M., Takahashi, N., Jackson, R.L., Gibson, G.A., Watkins, S.C., Dawid, I.B., and Hukriede, N.A. (2010). Characterization of an lhx1a transgenic reporter in zebrafish. The International journal of developmental biology *54*, 731-736.

Tada, M., and Heisenberg, C.P. (2012). Convergent extension: using collective cell migration and cell intercalation to shape embryos. Development *139*, 3897-3904.

Takeda, K., Noguchi, K., Shi, W., Tanaka, T., Matsumoto, M., Yoshida, N., Kishimoto, T., and Akira, S. (1997). Targeted disruption of the mouse Stat3 gene leads to early embryonic lethality. Proceedings of the National Academy of Sciences of the United States of America *94*, 3801-3804.

Takeichi, M. (1988). The cadherins: cell-cell adhesion molecules controlling animal morphogenesis. Development *102*, 639-655.

Tam, P.P., and Loebel, D.A. (2007). Gene function in mouse embryogenesis: get set for gastrulation. Nature reviews Genetics *8*, 368-381.

Teng, T.S., Lin, B., Manser, E., Ng, D.C., and Cao, X. (2009). Stat3 promotes directional cell migration by regulating Rac1 activity via its activator betaPIX. Journal of cell science *122*, 4150-4159.

Theveneau, E., and Mayor, R. (2013). Collective cell migration of epithelial and mesenchymal cells. Cellular and molecular life sciences : CMLS *70*, 3481-3492.

Thisse, C., and Thisse, B. (2008). High-resolution in situ hybridization to whole-mount zebrafish embryos. Nature protocols *3*, 59-69.

Thisse, C., Thisse, B., Schilling, T.F., and Postlethwait, J.H. (1993). Structure of the zebrafish snail1 gene and its expression in wild-type, spadetail and no tail mutant embryos. Development *119*, 1203-1215.

Topczewski, J., Sepich, D.S., Myers, D.C., Walker, C., Amores, A., Lele, Z., Hammerschmidt, M., Postlethwait, J., and Solnica-Krezel, L. (2001). The zebrafish glypican knypek controls cell polarity during gastrulation movements of convergent extension. Developmental cell *1*, 251-264.

Tsai, T.Y., Theriot, J.A., and Ferrell, J.E., Jr. (2014). Changes in oscillatory dynamics in the cell cycle of early Xenopus laevis embryos. PLoS biology *12*, e1001788.

Ulitsky, I., Shkumatava, A., Jan, C.H., Sive, H., and Bartel, D.P. (2011). Conserved function of lincRNAs in vertebrate embryonic development despite rapid sequence evolution. Cell *147*, 1537-1550.

Ulrich, F., Concha, M.L., Heid, P.J., Voss, E., Witzel, S., Roehl, H., Tada, M., Wilson, S.W., Adams, R.J., Soll, D.R.*, et al.* (2003). Slb/Wnt11 controls hypoblast cell migration and morphogenesis at the onset of zebrafish gastrulation. Development *130*, 5375-5384.

Ulrich, F., Krieg, M., Schotz, E.M., Link, V., Castanon, I., Schnabel, V., Taubenberger, A., Mueller, D., Puech, P.H., and Heisenberg, C.P. (2005). Wnt11 functions in gastrulation by controlling cell cohesion through Rab5c and E-cadherin. Developmental cell *9*, 555-564.

Verduzco, D., Dovey, J.S., Shukla, A.A., Kodym, E., Skaug, B.A., and Amatruda, J.F. (2012). Multiple isoforms of CDC25 oppose ATM activity to maintain cell proliferation during vertebrate development. Molecular cancer research : MCR *10*, 1451-1461.

von der Hardt, S., Bakkers, J., Inbal, A., Carvalho, L., Solnica-Krezel, L., Heisenberg, C.P., and Hammerschmidt, M. (2007). The Bmp gradient of the zebrafish gastrula guides migrating lateral cells by regulating cell-cell adhesion. Current biology : CB *17*, 475-487.

Wang, X., Li, L., and Liu, D. (2014). Expression analysis of integrin beta1 isoforms during zebrafish embryonic development. Gene expression patterns : GEP *16*, 86-92.

Ward, A.C., Touw, I., and Yoshimura, A. (2000). The Jak-Stat pathway in normal and perturbed hematopoiesis. Blood *95*, 19-29.

Warga, R.M., and Kane, D.A. (2007). A role for N-cadherin in mesodermal morphogenesis during gastrulation. Developmental biology *310*, 211-225.

Warga, R.M., and Kimmel, C.B. (1990). Cell movements during epiboly and gastrulation in zebrafish. Development *108*, 569-580.

Weber, G.F., Bjerke, M.A., and DeSimone, D.W. (2012). A mechanoresponsive cadherin-keratin complex directs polarized protrusive behavior and collective cell migration. Developmental cell *22*, 104-115.

Wei, Z., Lei, X., Seldin, M.M., and Wong, G.W. (2012a). Endopeptidase cleavage generates a functionally distinct isoform of C1q/tumor necrosis factor-related protein-12 (CTRP12) with an altered oligomeric state and signaling specificity. The Journal of biological chemistry *287*, 35804-35814.

Wei, Z., Peterson, J.M., Lei, X., Cebotaru, L., Wolfgang, M.J., Baldeviano, G.C., and Wong, G.W. (2012b). C1q/TNF-related protein-12 (CTRP12), a novel adipokine that improves insulin sensitivity and glycemic control in mouse models of obesity and diabetes. The Journal of biological chemistry *287*, 10301-10315.

Weijer, C.J. (2009). Collective cell migration in development. Journal of cell science *122*, 3215-3223.

Welte, T., Zhang, S.S., Wang, T., Zhang, Z., Hesslein, D.G., Yin, Z., Kano, A., Iwamoto, Y., Li, E., Craft, J.E.*, et al.* (2003). STAT3 deletion during hematopoiesis causes Crohn's disease-like pathogenesis and lethality: a critical role of STAT3 in innate immunity. Proceedings of the National Academy of Sciences of the United States of America *100*, 1879-1884.

Wienholds, E., van Eeden, F., Kosters, M., Mudde, J., Plasterk, R.H., and Cuppen, E. (2003). Efficient target-selected mutagenesis in zebrafish. Genome research *13*, 2700-2707.

Witzel, S., Zimyanin, V., Carreira-Barbosa, F., Tada, M., and Heisenberg, C.P. (2006). Wnt11 controls cell contact persistence by local accumulation of Frizzled 7 at the plasma membrane. The Journal of cell biology *175*, 791-802.

Woo, K., and Fraser, S.E. (1997). Specification of the zebrafish nervous system by nonaxial signals. Science *277*, 254-257.

Yamashita, S., Miyagi, C., Carmany-Rampey, A., Shimizu, T., Fujii, R., Schier, A.F., and Hirano, T. (2002). Stat3 Controls Cell Movements during Zebrafish Gastrulation. Developmental cell *2*, 363-375.

Yamashita, S., Miyagi, C., Fukada, T., Kagara, N., Che, Y.S., and Hirano, T. (2004). Zinc transporter LIVI controls epithelial-mesenchymal transition in zebrafish gastrula organizer. Nature *429*, 298-302.

Yin, C., Ciruna, B., and Solnica-Krezel, L. (2009). Convergence and extension movements during vertebrate gastrulation. Current topics in developmental biology *89*, 163-192.

Yin, C., Kiskowski, M., Pouille, P.A., Farge, E., and Solnica-Krezel, L. (2008). Cooperation of polarized cell intercalations drives convergence and extension of presomitic mesoderm during zebrafish gastrulation. The Journal of cell biology *180*, 221-232.

Yu, H., Lee, H., Herrmann, A., Buettner, R., and Jove, R. (2014). Revisiting STAT3 signalling in cancer: new and unexpected biological functions. Nature reviews Cancer *14*, 736-746.

Zallen, J.A. (2007). Planar polarity and tissue morphogenesis. Cell *129*, 1051-1063.

Zeidler, M.P., Perrimon, N., and Strutt, D.I. (1999). Polarity determination in the Drosophila eye: a novel role for unpaired and JAK/STAT signaling. Genes & development *13*, 1342-1353.

Zhang, L., Kendrick, C., Julich, D., and Holley, S.A. (2008). Cell cycle progression is required for zebrafish somite morphogenesis but not segmentation clock function. Development *135*, 2065-2070.

Zhang, T., Yin, C., Qiao, L., Jing, L., Li, H., Xiao, C., Luo, N., Lei, S., Meng, W., Zhu, H*., et al.* (2014). Stat3-Efemp2a modulates the fibrillar matrix for cohesive movement of prechordal plate progenitors. Development *141*, 4332-4342.

Zhang, Z., Welte, T., Troiano, N., Maher, S.E., Fu, X.Y., and Bothwell, A.L. (2005). Osteoporosis with increased osteoclastogenesis in hematopoietic cell-specific STAT3-deficient mice. Biochemical and biophysical research communications *328*, 800-807.

Zhong, Y., Brieher, W.M., and Gumbiner, B.M. (1999). Analysis of C-cadherin regulation during tissue morphogenesis with an activating antibody. The Journal of cell biology *144*, 351-359.

Zutter, M.M., and Edelson, B.T. (2007). The alpha2beta1 integrin: a novel collectin/C1q receptor. Immunobiology *212*, 343-353.